Probabilistic Safety Assessment using Detailed Groundwater Flow and Transport Models

NWMO TR-2013-09 **April 2013**

John Avis and Nicholas Sgro

Geofirma Engineering Ltd.

nwmo

NUCLEAR WASTE MANAGEMENT ORGANIZATION

SOCIÉTÉ DE GESTION DES DÉCHETS NUCLÉAIRES

Nuclear Waste Management Organization
22 St. Clair Avenue East, 6th Floor
Toronto, Ontario
M4T 2S3
Canada

Tel: 416-934-9814
Web: www.nwmo.ca

Probabilistic Safety Assessment using Detailed Groundwater Flow and Transport Models

NWMO TR-2013-09

April 2013

John Avis and Nicholas Sgro
Geofirma Engineering Ltd.

Document History

Title:	Probabilistic Safety Assessment using Detailed Groundwater Flow and Transport Models		
Report Number:	NWMO TR-2013-09		
Revision:	R000	Date:	April 2013
Geofirma Engineering Ltd.			
Authored by:	J. Avis and N. Sgro		
Verified by:	R. Walsh		
Approved by:	J. Avis		
Nuclear Waste Management Organization			
Reviewed by:	M. Gobien		
Accepted by:	N. Hunt		

ABSTRACT

Title: **Probabilistic Safety Assessment using Detailed Groundwater Flow and Transport Models**
Report No.: **NWMO TR-2013-09**
Author(s): John Avis and Nicholas Sgro
Company: Geofirma Engineering Ltd.
Date: April 2013

Abstract
This work program demonstrates the application of a probabilistic safety assessment (PSA) methodology to computationally intense three-dimensional (3D) numerical simulations of the transport of radionuclides from a hypothetical repository in a fractured granite geosphere.

Previous safety assessments conducted by the NWMO have used two modelling approaches: probabilistic safety assessments have been conducted using simplified geosphere and repository transport models, while very detailed deterministic finite-element models have been used to simulate flow and transport for a limited number of cases and a limited number of nuclides. This report describes a proof-of-concept approach to conducting probabilistic simulations using detailed 3D numeric models. Existing numeric models used in the Fourth Case Study (4CS) Assessment (NWMO, 2012) have been simplified and the modelling workflow automated to allow complete simulations to be executed under the control of a probabilistic sampling executive.

The basic scenario includes a water-supply well intersecting a fracture that extends to repository depth. A defective container located within a placement room adjacent to the fracture supplies the radionuclide source-term. A single radionuclide, I-129, is used in the simulations. Parameters describing geosphere, fracture, engineered barrier system (EBS) and placement room excavation and thermal damage zone (EDZ) are defined in terms of probability distributions, which are sampled under the control of an executive code. Flow and transport simulations are conducted for each realization and model results extracted. Results are analyzed using graphical and regression approaches.

An initial assessment based on transport times indicated by Mean Life Expectancy (MLE) was conducted to validate the 4CS well placement. Subsequently a full transport assessment determined the parameters with the most significant impact on transport related safety assessment metrics. This assessment showed that geosphere properties are the primary controls on radionuclide transport. Additional assessments fixed geosphere variables at median values and focussed on repository components (EBS and EDZ) to determine the relative importance of parameters describing these sub-systems.

After proof of concept was demonstrated on a local cluster computer, the assessments were duplicated using cloud based computing resources from Amazon Web Services (AWS). The AWS implementation demonstrates that complex numeric PSA does not require dedicated local hardware and can be conducted using readily available commercial facilities. AWS is also a scalable resource, allowing complex simulations with many thousands of realizations to be conducted, albeit at not insignificant cost.

The approach demonstrated here is ideally suited to the particular attributes of the 4CS geosphere and the single defective container radionuclide transport reference case scenario. However, it could be extended to other scenarios such as multiple container failure and to other models such as TOUGH2.

TABLE OF CONTENTS

LIST OF TABLES

Page

LIST OF FIGURES

Page

1. INTRODUCTION

The NWMO is undertaking postclosure safety assessments of Adaptive Phased Management (APM) deep geological repositories (DGR) for used nuclear fuel. The recently completed Fourth Case Study (4CS) (NWMO, 2012) considers a repository hosted in crystalline rock.

The 4CS safety assessment used two modelling approaches: a probabilistic safety assessment (PSA) conducted using simplified geosphere and repository transport models, and very detailed deterministic finite-element models used to simulate flow and transport for a limited number of cases and a limited number of nuclides. The detailed results have been used to inform and verify the probabilistic results.

The probabilistic model used, SYVAC-CC4, samples selected parameters and calculates the dose impact to a critical group. SYVAC3-CC4 uses simplified representations of the vault and geosphere to model radionuclide transport, which allows computationally tractable analyses to be performed for a large suite of radionuclides and transport parameters. However these simplifications reduce the transparency of the analyses, particularly as to the impact of variation in geosphere and engineered barrier parameters.

The primary restriction preventing probabilistic assessments using detailed 3D flow and transport models has been computational power. However, with the advent of relatively cheap processing power and cluster or parallel computing, running detailed models probabilistically is becoming more feasible. FRAC3DVS-OPG v1.3 is the reference detailed flow and transport code used in the 4CS project. This project explores the ability to run FRAC3DVS-OPG within a probabilistic sampling framework and to analyze the results. For the purposes of this report, the methodology and approach developed shall be referred to as “3D PSA” to distinguish it from the geometrically simplified SYVAC-CC4 PSA. The report is structured in the following sections:

- Section 2 – Approach – A description of the general 3D PSA approach to be used including selected software and simplifications to the 4CS deterministic models.

- Section 3 – Flow and Mean Life Expectancy Model – The first step in the 4CS modelling approach determined the source location that provides the fastest transport time to a well. The 4CS flow model is revised and verified against the 4CS Reference Case model. Geosphere parameter distributions are developed and Mean Life Expectancy (MLE) simulations conducted in a probabilistic framework to assess sensitivity of the fastest transport source location to geosphere parameters.

- Section 4 – Radionuclide Transport Model – An appropriately simplified transport model is developed and verified against 4CS RC transport results. Engineered Barrier System (EBS) and Excavation Damaged Zone (EDZ) parameter distributions are described and probabilistic simulations conducted.

- Section 5 – Probabilistic Simulations and Results – Graphical and numeric sensitivity analyses are performed on the probabilistic results. Additional simulations are performed with certain groups of parameters set to median values to assess areas of variability.

- Section 6 – Cloud Implementation – Probabilistic simulations in Sections 3 through 5 were executed on a local cluster computer. Proof-of-concept simulations were

performed using a virtual cluster implemented with Amazon Web Services. Costs and scalability are compared to the local cluster approach
.

- Section 7 – Expansions and Limitations – A description of additional modelling capabilities that could be incorporated within the 3D PSA approach to expand coverage of 4CS model attributes, and a summary of potential limitations applying the 3D PSA approach to other numeric models, geologic settings, and alternate safety assessment scenarios.

- Section 8 – Conclusions and Recommendations – A summary of the 3D PSA application to the 4CS system, and discussion of significant findings in the assessment results.

2. 3D PSA APPROACH

2.1 MODELLING FRAMEWORK

The 4CS deterministic flow and transport models provide the starting point for the 3D PSA framework. Three scales of detailed flow and transport models were used:

1. Sub-regional flow (SRF) – consists of the flow domain within the watershed encompassing the repository but not including repository features. The model is based on a constant 50m grid discretization, oriented coincident with the local mapping coordinate system. A hypothetical fracture system has been defined as a series of triangles representing 3D fractures. These fracture surfaces were mapped to SRF model elements and equivalent porous media (EPM) element properties calculated. Steady state flow and MLE calculations were performed to determine discharge to surface times within the repository footprint. A water-supply well was placed in a fracture located within the repository footprint.

2. Site-scale transport – includes a portion of the flow domain surrounding the repository. Repository features, including EBS and inner EDZ, were represented in some detail. Various simplifications to sealing systems were made, and placement rooms were modeled as rectangular rather than elliptically shaped. In-floor containers were not represented in the model. A source term was placed at the defective container location closest to the fracture with the water-supply well. Simulation results include radionuclide concentrations in the geosphere and EBS and radionuclide activity transport rates (denoted “transport” in this report) at the water-supply well and over defined surface discharge areas. This is the main transport model from which most reference and sensitivity case results were extracted.

3. Repository-scale transport – a very detailed model that includes the semi-elliptical source placement room, the defective container, several adjacent rooms, and the main fracture. The geosphere extents were limited to several hundred metres above and below the source room. Inner and outer EDZ were included. In-floor containers were included and the EBS was entirely congruent with the engineering design. The source term is a pinhole leak from a single container. Simulation results include geosphere and EBS concentrations, and transport from the EBS enclosing the container into the surrounding geosphere.

Figure 2.1 illustrates the spatial relationship between the three models. The SRF vertical boundaries were zero flow at the watershed limits and fixed head at ground surface. The site scale vertical boundaries were fixed heads extracted directly from the SRF model with fixed heads at ground surface, while all sides of the vault scale were set at fixed heads extracted from the site-scale model. The transport leaving the container EBS in the repository-scale model was defined as the source term for the site scale model.

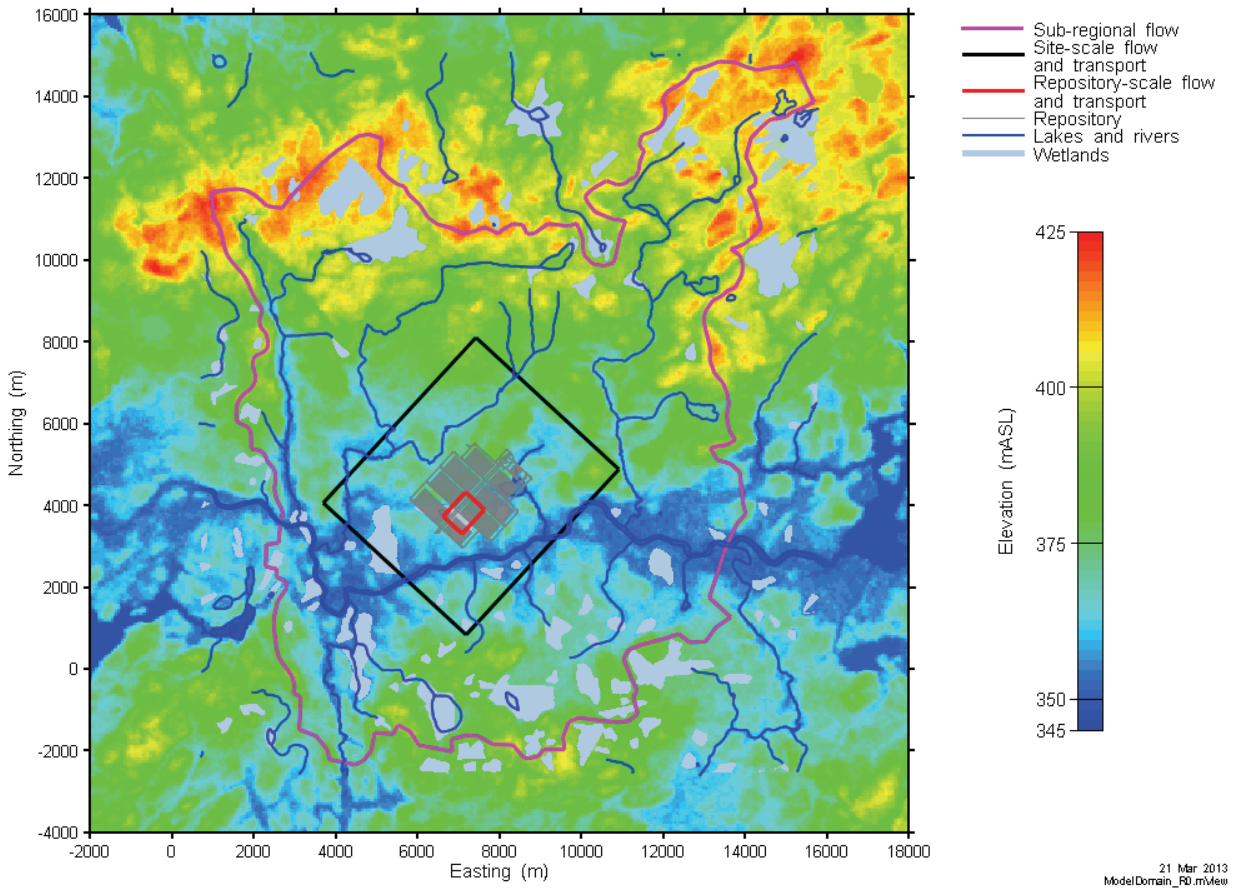

Figure 2.1: Fourth Case Study Model Domains

The multiple model scales were required to address the wide range in spatial scales describing the overall system attributes. For example, it would not be possible to represent the detailed source room features (see Figure 2.2) as well as watershed scale fractures within a single numeric model that would execute in a reasonable time frame on available computation platforms. FRAC3DVS-OPG is a single processor code, so cluster solutions are not available to allow larger models with reduced execution times. Even using a multi-scale approach, all models required several million elements (SRF: 3.2M active nodes, Site-scale 8.9M, Vault-scale: 9.75M) with transport simulations requiring several days execution time.

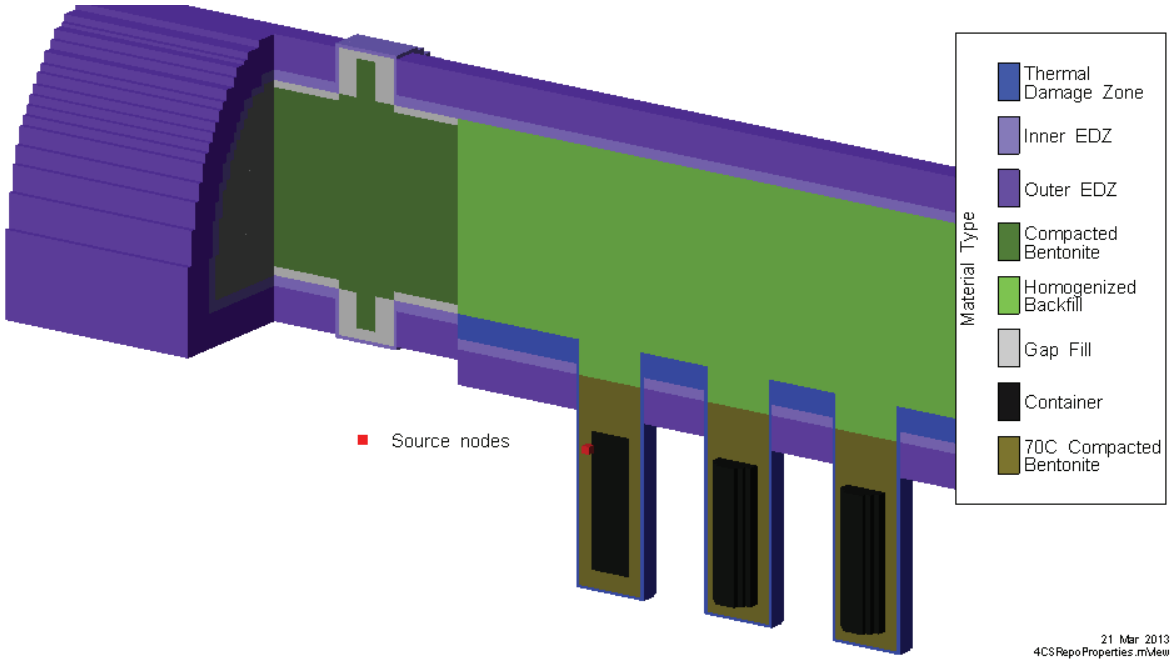

Figure 2.2: Fourth Case Study Vault Scale Model Property Details

For the 3D PSA it was necessary to simplify the framework to reduce execution time and model workflow complexity. The first simplification was to include only two models: an SRF and a transport model at smaller than repository scale. The SRF is used for repository scale MLE calculations and transport model head boundary calculations. The transport model was further simplified by including only a single placement room and ignoring other repository features such as adjacent room and tunnels. However, the transport model did extend to surface and did include the water supply well. Results from 4CS sensitivity assessments showed that the surrounding repository features (i.e. other rooms, access drifts and tunnels, shafts) had virtually no impact on transport at the water supply well.

Further model simplification, particularly reducing the number of elements in the grid by increasing element size, was required to reduce execution time and memory footprint by a sufficient amount to allow reasonable run times for probabilistic simulations. The 4CS site- and vault- scale transport models have a combined average run time of 7.7 days (1 hour SRF, 1.1 days site, 6.6 days vault) and a peak memory requirement of 15GB. As a target for tractability, a goal of 12 hour average run time and 3 GB peak memory is appropriate. The reference hardware platform for these simulations was a locally available cluster machine consisting of five Intel Xeon server boards, each with 48 GB of RAM and 16 hyper-threaded cores. The target memory footprint would allow up to 15 realizations to be executed simultaneously on each available server. Model domain, discretization, property assignment and verification for revised SRF and transport model scales are described in Sections 3 and 4 respectively.

For the remainder of this document, the revised SRF model is referred to as the “PSA Flow” model, while the transport model is referred to as the “PSA Transport” model.

2.2 WORKFLOW

The 3D PSA workflow can be described as follows:

1. Setup – the tasks that form the foundation of the assessment. These include grid definition and property zone assignment for the numeric models, deterministic variable assignment (those values that are not subject to probabilistic assessment), specification of probabilistic variable parameter distributions, and definition of the sampling regime (e.g. Monte-Carlo or Latin Hypercube Sampling (LHS)) and number of realizations.

2. Sample – a single sample realization includes values for all defined probabilistic variables. These values are made available for external model use in a formatted text file with values and variable identifiers.

3. Model pre-processing – the sampled variable property values are transferred to the numeric model. Elements of this step may be simple (i.e. variable substitution in text files) or more complex (calculations based on sampled values, further pre-processing), or may include a combination of approaches.

4. Model Execution – the numeric model is executed. The ability to terminate the model after a specified time interval is useful to prevent poorly-conditioned simulations from dominating overall assessment run-time.

5. Model post-processing – results from the simulations are acquired in a form that will support analyses. In general, numerical models produce gigabytes of output which cannot be completely retained for every realization. Extraction involves a reduction of model output to the minimal set required for results assessment. Typically values, tables, or time-series associated with specific model metrics (e.g. water-supply-well transport) are extracted as are execution time statistics.

Steps 2 through 5 are repeated for each sample realization.

6. Output – all extracted results and execution statistics are written to an output file.

7. Results Post-processing – the results from one or more probabilistic simulations are assessed and compared. Graphical (i.e. scatter plot, horsetail plot) and numerical (regression analyses, partial correlation coefficient) analysis methods allow determination of the most significant variables and the relative contribution of significant variables to overall variability.

This basic workflow is used in the assessments presented in this report.

2.3 CODES USED

2.3.1 FRAC3DVS-OPG

FRAC3DVS-OPG Version 1.30 is the numeric code used for all flow and transport simulations.

2.3.2 paCalc

The proprietary Geofirma Engineering code paCalc Version 1.7 is the sampling executive code. paCalc is a Windows application that was originally developed for the Yucca Mountain Project to provide a framework for developing a simplified Performance Assessment (PA) model. It has subsequently been used in assessing site characterization data requirements at the Nevada Test Site (Deschler et. al, 2005). paCalc consists of a sampling core that provides Monte-Carlo Sampling (MCS) or Latin Hypercube sampling (LHS) approaches, a GUI to define variables and correlations, and internal transport calculations. paCalc also has the ability to export sampled variables and to execute external models. The sampling methodology used in paCalc was originally developed at Sandia National Laboratories (Iman and Shortencarier, 1984). Variables are assigned distributions (normal, truncated normal, uniform, triangular, log-normal, truncated log-normal, log-uniform, log-triangular, exponential, Poisson, Weibull, Beta, T, user CDF, tabulated) and distributions are parameterized. For LHS sampling, variable correlations can be specified. paCalc Version 1.5 was qualified to DOE standards in support of the Nevada Test Site analyses. A limited amount of code enhancements have been performed since that qualification. These enhancements have been tested and verified as required by Geofirma's ISO 9001:2008 Quality Management system.

With LHS, each variable's distribution is sliced into ***n*** equally sized intervals, and a single random sample is selected from each interval. For MCS, the entire CDF is taken as a single interval and randomly sampled ***n*** times. In general, LHS requires a reduced number of realizations compared to MCS to adequately cover the domain of each variable. However, the number of realizations required to ensure complete statistical coverage of all variables is a function of the number of model variables and the system being simulated. Models with more variables, more complexity, and more non-linearity require a greater number of samples. Benedetti et al (2011) provide a useful discussion of different a priori estimates and describe an approach to confirming coverage based on stability of output metrics. They reference Iman and Helton (1985) as suggesting 4/3 times the number of uncertain parameters. In the past we have used 10 times the number of parameters as a rule of thumb defining minimum number of realizations. In general, as many realizations as practical are executed, with computation time being the primary constraint. Results from Benedetti et al's (2011) analyses of their highly nonlinear wastewater treatment model indicated that 40 to 150 times the number of uncertain parameters was required. In this report we assess adequate coverage by examining stability of output metric measures and statistics (see Section 3.7.1 for example).

The paCalc sampler executes one or more models sequentially, and subsequently extracts and compiles metrics from individual realizations. paCalc was used to define all assessments presented in this report.

2.3.3 mView

Model pre- and post-processing are performed using the proprietary Geofirma Engineering code mView, Version 4.2. mView is a Windows based numerical model pre- and post-processor that provides a high level of support for FRAC3DVS modelling, being capable of generating all complex input files and post-processing all model results. mViewX is a command line version of mView which can be invoked from within a paCalc configuration. mViewX is compiled from the same source code as mView with the Windows GUI and plotting functionality removed.

mViewX reads mView configuration files previously created with mView to prepare model input files, post-process results and extract metrics. This allows mViewX to be used within batch files or to be called by another program (paCalc in this case) to perform automated model pre- and post-processing.

2.3.4 paView/STEPWISE

Graphics presented in this report are prepared with mView and paView. paView Version 1.7 is a companion code to paCalc that is similar in design to mView with capabilities optimized to read, post-process and visualize paCalc output files.

paView contains an implementation of the Sandia code STEPWISE (WIPP-PA, 1995a) which performs a wide range of statistical analyses on PSA results including backwards, stepwise, and forward regression. Some discussion of STEPWISE is warranted as it is used extensively within this report to assess significance of PSA results. STEPWISE was originally developed as a basic regression code developed by K.E. Kemp, at the Statistics Department of Kansas State University. The code was further developed by Iman et al. (1980) and subsequently served as the main regression-analysis code used within Sandia National Laboratories on performance assessments of the Waste Isolation Pilot Plant (WIPP). The FORTRAN code was converted to C++ and implemented as an mView/paView object during paCalc development for Yucca Mountain. Correct porting of the code was verified in preliminary paCalc testing and mView qualification.

In one-dimension, linear regression analysis is the process of determining the best fit line to the points describing a dependent variable response (Y) to an independent variable (X). In this case best-fit is defined as the line that minimizes the sum of squared errors (SSE) or differences between the line and the dependent variable values. Standardized regression analysis removes dimensionality from the linear regression by centring the variables on the means and normalizing by the sample's standard deviation. The analyses can be extended to **n** dimensions, where **n** is the number of independent variables. The coefficients of the standardized regression line/surface are the standardized regression coefficients (SRC). As noted in WIPP-PA (1995a): "They are more useful for sensitivity studies than ordinary regression coefficients in that they are dimensionless, and they vary over roughly the same range of numerical values. Therefore, they can be compared one to another to provide a direct quantitative measure of the relative importance of the various input variables ... Thus, if b_3* (the SRC for variable 3, or X_3) is numerically greater than b_4*, then Y (the dependent variable) is more sensitive to variations in X_3 than it is to variations in X_4."

For the stepwise regression analysis implemented in STEPWISE a sequence of regression models are constructed starting with a single selected input parameter, and including one additional input variable at each successive step until all significant input variables have been included in the model.

Output from the STEPWISE model includes the coefficient of determination (R^2) for each independent variable included in the regression. R^2 provides a quantitative measure of the adequacy of a regression model to account for the variability in the model results. It varies between 0 and 1 and measures the fraction of the variation in Y attributable to regression on the variable. If it is near one, the regression model is accounting for most of the output variability. If it is near zero, the regression model is failing to represent output variability well.

In the STEPWISE output R^2 is presented in a cumulative fashion with the total R^2 for all included ("R^2 Included") variables representing the overall significance of the combined linear models. The change in total R^2 for each included variable indicates the incremental reduction in output variability due to the variable. STEPWISE also outputs "R^2 Deleted" for each variable

which indicates the overall significance of the model if the variable is **not** included in the analysis.

All regression analyses performed in this report are based on variable ranks, rather than variable values. This is appropriate for complex models and eliminates the requirement to perform log transforms on variables with log-uniform sampling distributions prior to performing the regression analyses. Assuming that the sampled distributions are reasonable approximations of the physical ranges and distributions of each variable, a ranked regression will give a meaningful assessment of variable importance.

2.4 MULTIPROCESSOR IMPLEMENTATION

A multiprocessor command line version of paCalc (called paCalcX) supports execution of multiple concurrent sample realizations. paCalcX bears the same relationship to paCalc as mViewX does to mView; all Windows GUI and plotting capabilities are removed, however the calculation source code is identical.

paCalcX uses a master/slave operation mode to support simultaneous processing of multiple sample realizations on multiple processors. Code based on a message passing interface (MPI) is used to support communication between different instances. The MPI is third party software that supports communication between processes running in different address spaces, either on the same or on different hardware. There are a number of different MPIs available. paCalcX uses MPICH2 (the acronym refers to MPI over CHameleon, where Chameleon is a now defunct system) which is an MPI implementation originally developed at Argonne National Laboratories. paCalcX currently uses MPICH2 version 1.1.

Sampling problems like MCS and LHS are a member of a class of problems known as "embarrassingly parallel" as they are exceeding easy to run in parallel on multiple processors, as there is very little inter-process communication required. When paCalcX is started it is invoked on a specified number of processors (**m**). Each instance reads the previously prepared paCalc configuration file which describes Steps 2 to 5 in the workflow presented above. The first instance started (instance 0) becomes the master program, while instances 1 to **m**-1 are designated as slaves. The master provides each slave with the index of the next realization to be simulated. The slave informs the master when each simulation is complete. After all simulations are complete, the master collects output files from each slave and creates a full simulation output file. paCalcX was used to conduct all assessments presented in this report.

FRAC3DVS-OPG uses and generates a number of input, internal and output files. The mView based pre- and post-processing tasks also creates numerous files, both for FRAC3DVS input and to extract simulation results. A critical issue with a multiprocessor implementation is ensuring that all files associated with a particular sample realization are kept distinct and separate from identical files associated with concurrent sample realizations. With paCalcX and mViewX, this is accomplished using the concept of a processor instance directory structure. Within the base paCalc and mView configurations, files that will be realization specific are placed in directories structures that include a "/00/" subdirectory. Additionally, the file is denoted as an MPI run-time file in the paCalc and mView object GUI. For example, the directory "D:\Projects\NWMO-PSA\Runs\Transport\00" contains all the FRAC3DVS-OPG and mView files for the PSA Transport simulation. At runtime, the '00' string is replaced by '**mm**' where **mm** is the index of the processor running the simulation such '01', '04', '12' etc. The processor index is known to paCalcX as the MPI rank of the process, which is an integer variable unique to each processor instance provided by the MPICH2 system. The master simulation will have a rank of 0, while each slave will have a rank within the range 1 to **m**-1. paCalcX passes this information to mViewX as a command line parameter. mViewX has identical support for runtime directory renaming. The directory structures must be created and populated with required run-

independent files prior to the start of the simulation. This approach offers a simple and efficient method of segregating realization independent files.

3. FLOW AND MEAN LIFE EXPECTANCY MODEL

The PSA Flow model was developed first. In addition to providing a less complex test case compared to the transport model, this model could also be used to provide additional validation of 4CS assumptions regarding well and source container location. The assessment is performed in two steps. First, the MLE at nodes within the placement room is calculated in a probabilistic simulation with no water-supply well. The results of this simulation are used to guide selection of water-supply well locations; the well(s) are located within the nearest fracture to the placement room nodes with the shortest MLE. Secondly, additional probabilistic simulations are conducted with wells included, and the shortest MLE node location verified. The placement room container location closest to the most-likely minimum MLE node is assumed to be the most conservative source term placement.

3.1 DISCRETIZATION AND PROPERTY ASSIGNMENT

As discussed in Section 2.1 the 4CS SRF model had the smallest memory footprint and shortest execution time of the three 4CS models. Consequently, it was not necessary to significantly reduce the model size in order to meet PSA Flow model requirements. Instead, the model discretization was optimized to provide better head resolution within the repository footprint while maintaining execution and memory limits. The model was revised to use a variable finite element length and width, ranging from 25m within the repository footprint to 125m at the far extents of the domain (Figure 3.1). The coordinate system was rotated clockwise 47.3 degrees and the origin reset to the intersection of the repository access drift and main perimeter drifts. This lined up element discretization with placement room orientation. EPM fracture element locations were determined based on the 4CS reference case fracture triangulation.

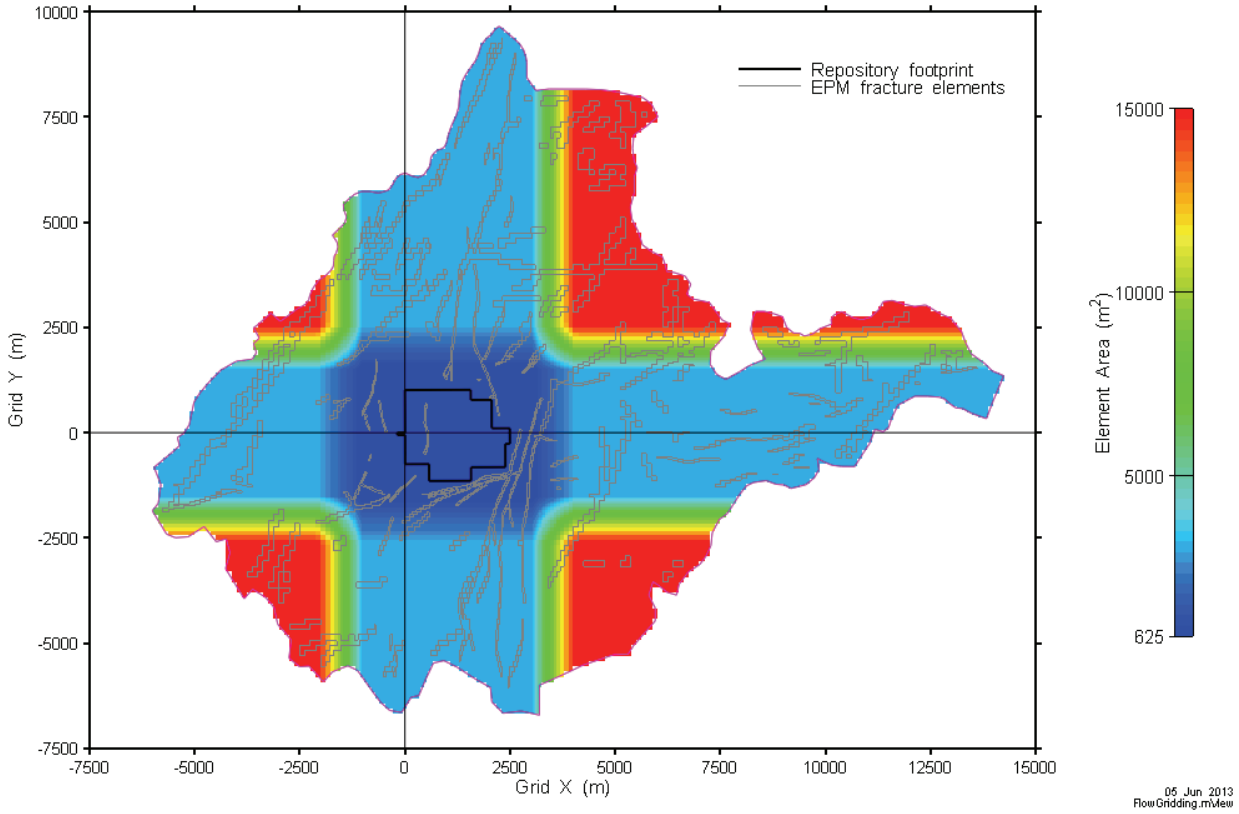

Figure 3.1: PSA Flow Model Plan Discretization

Property groups were assigned based on depth below ground surface as shown in Figure 3.2. The complete discretization included 2.9M nodes in 51 layers, compared to 3.2M active nodes in 52 layers for the 4CS SRF model. The base property groups shallow overburden (SH_OVR), shallow bedrock (SH_ROCK), intermediate bedrock (INT_ROCK), and deep bedrock (DEEP_ROCK) are shown on the figure. EPM fracture elements are outlined.

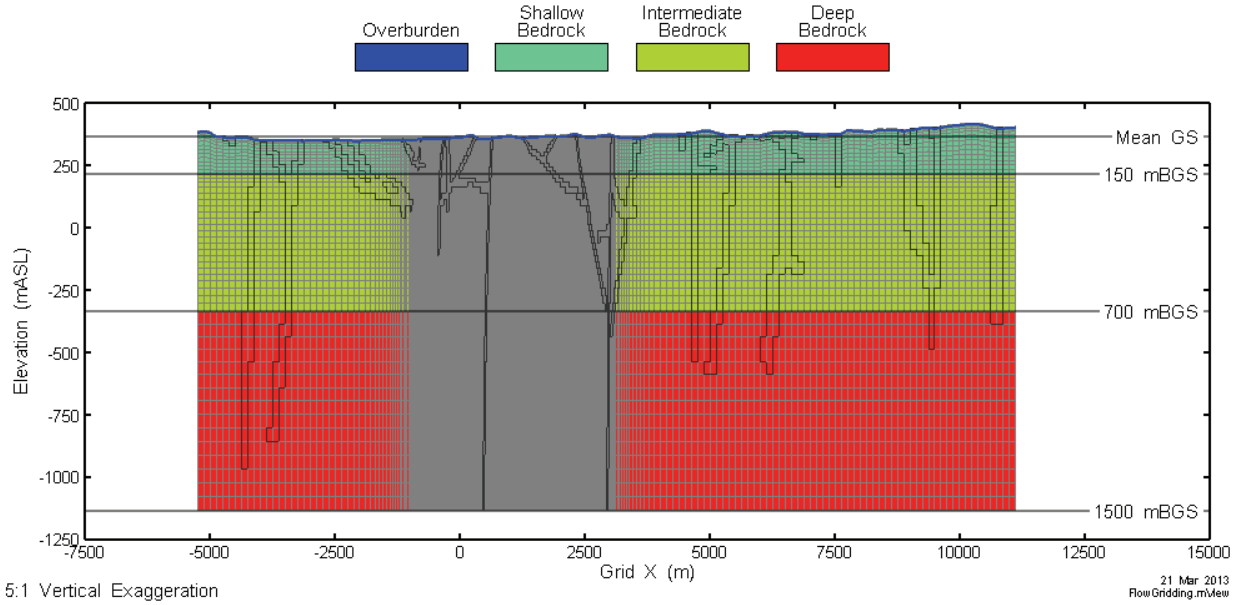

Figure 3.2: PSA Flow Model Vertical Slice Discretization and Property Assignment

3.2 BOUNDARY CONDITIONS

The elevation of the top surface of the model is used to define fixed head boundaries where topography is the principal driver of flow. All other model surfaces (bottom and vertical sides) are zero flow.

3.3 SIMULATION METRICS

Results from probabilistic simulations are generally limited to the most useful subset of output as it is not feasible to store all simulation results. For the PSA Flow simulations, results of most interest are MLE at nodes within the repository placement room footprint at the repository elevation, as shown in Figure 3.3. These are all nodes in the grid layer at the repository elevation that are located within 25m of a placement room. As such they broadly represent the domain of potential releases from a defective container.

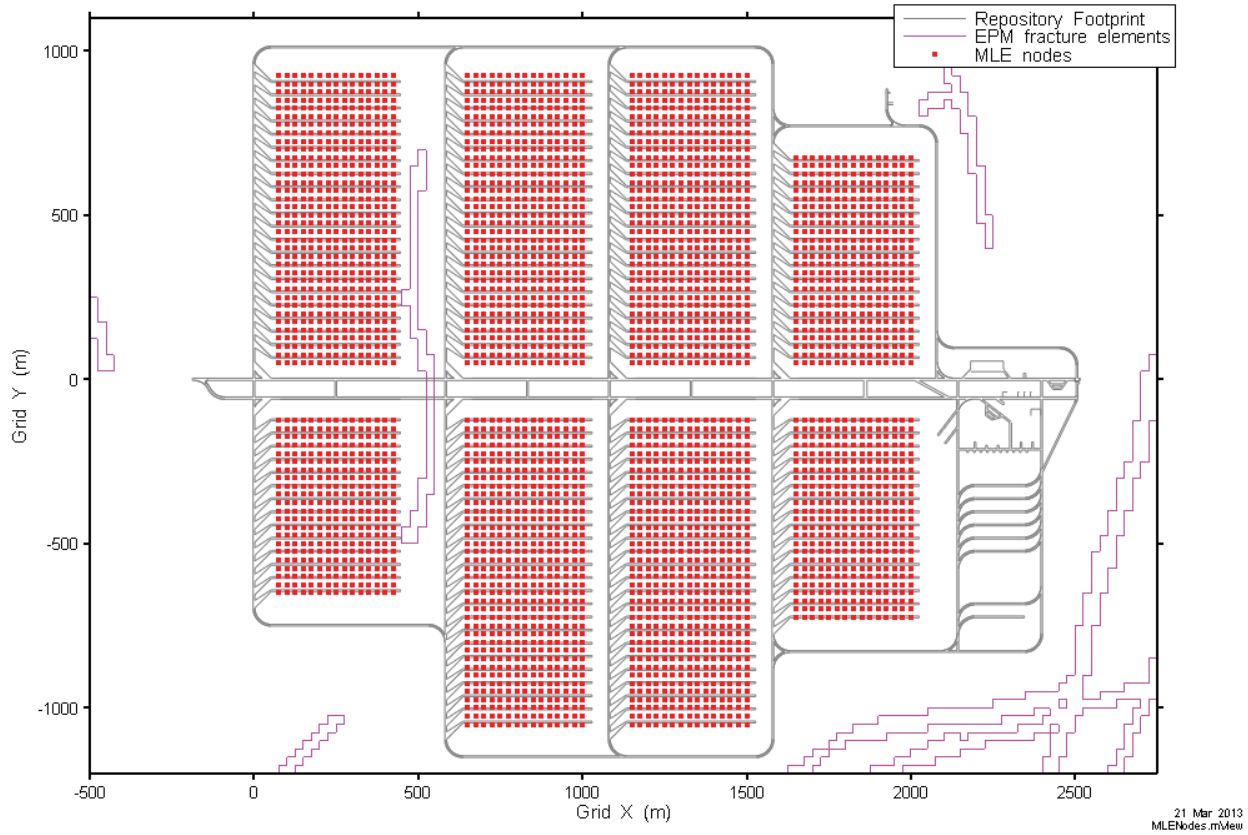

Figure 3.3: PSA Flow Model MLE Node Location

For simulations with pumping wells, it is useful to determine if the pumping rate is physically compatible with the geosphere properties. To this end, simulated head at the pumping well location is extracted from each simulation. Well head is then calculated as the difference between simulation head and the elevation of the lowest well node. If well head is positive, the discretized geosphere is able to provide sufficient water to meet well pumping rate requirements. If the well head is less than zero, in colloquial terms the well has been sucked dry. The simulation will complete, but MLE or transport results may be misleading as they are representative of a flow-field that is numerically possible, but may not be physically possible. Parameters verifying correct numeric implementation such as flow solution and MLE iteration count are also useful, as are general simulation performance measures such as execution time.

3.4 DETERMINISTIC VERIFICATION

A single deterministic simulation was performed using the PSA Flow model with 4CS Reference Case parameter values. Head and MLE results at the repository elevation are visually compared to the analogous 4CS Reference Case Sub-Regional Flow results in Figure 3.4 and Figure 3.5. Both comparisons show a very good match between the two discretizations.

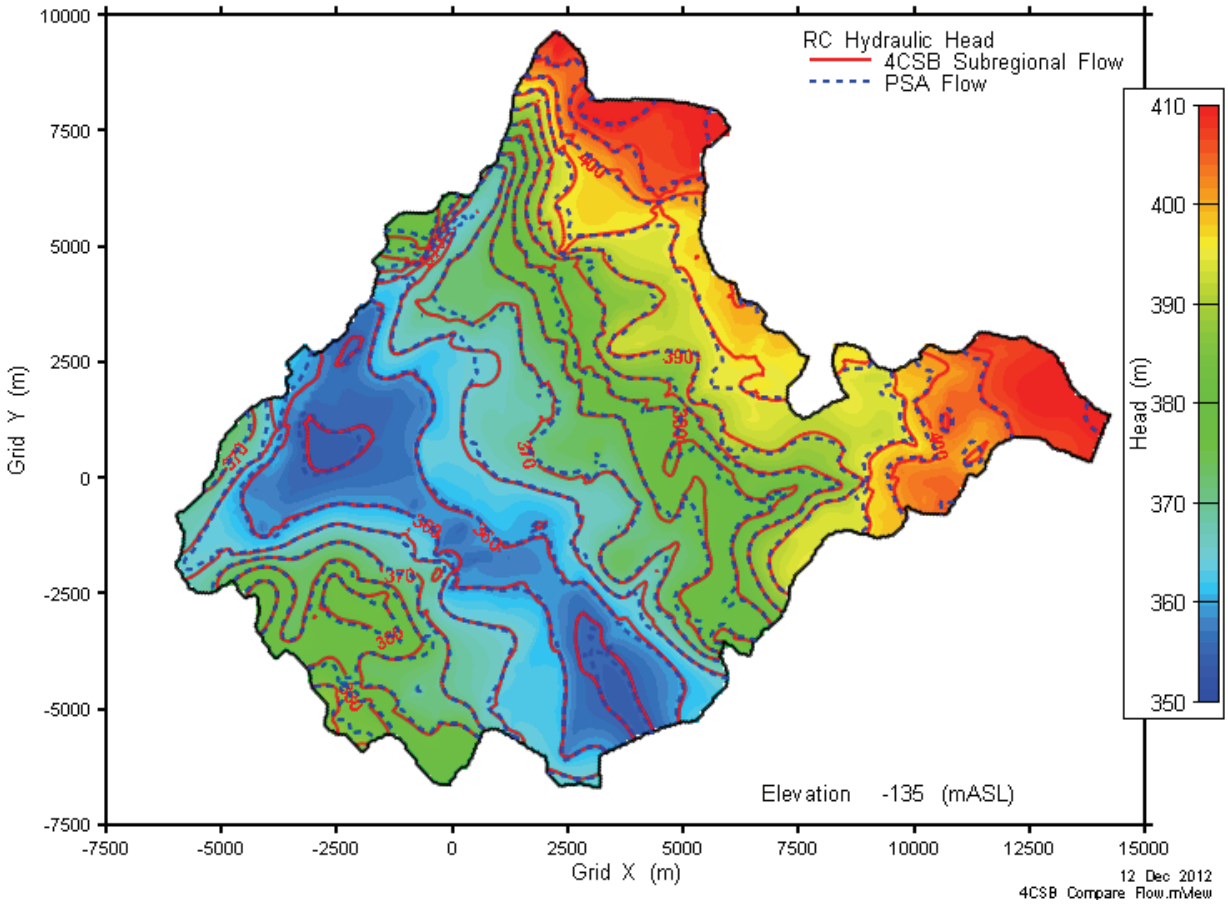

Figure 3.4: PSA Flow Model Verification – Head Comparison

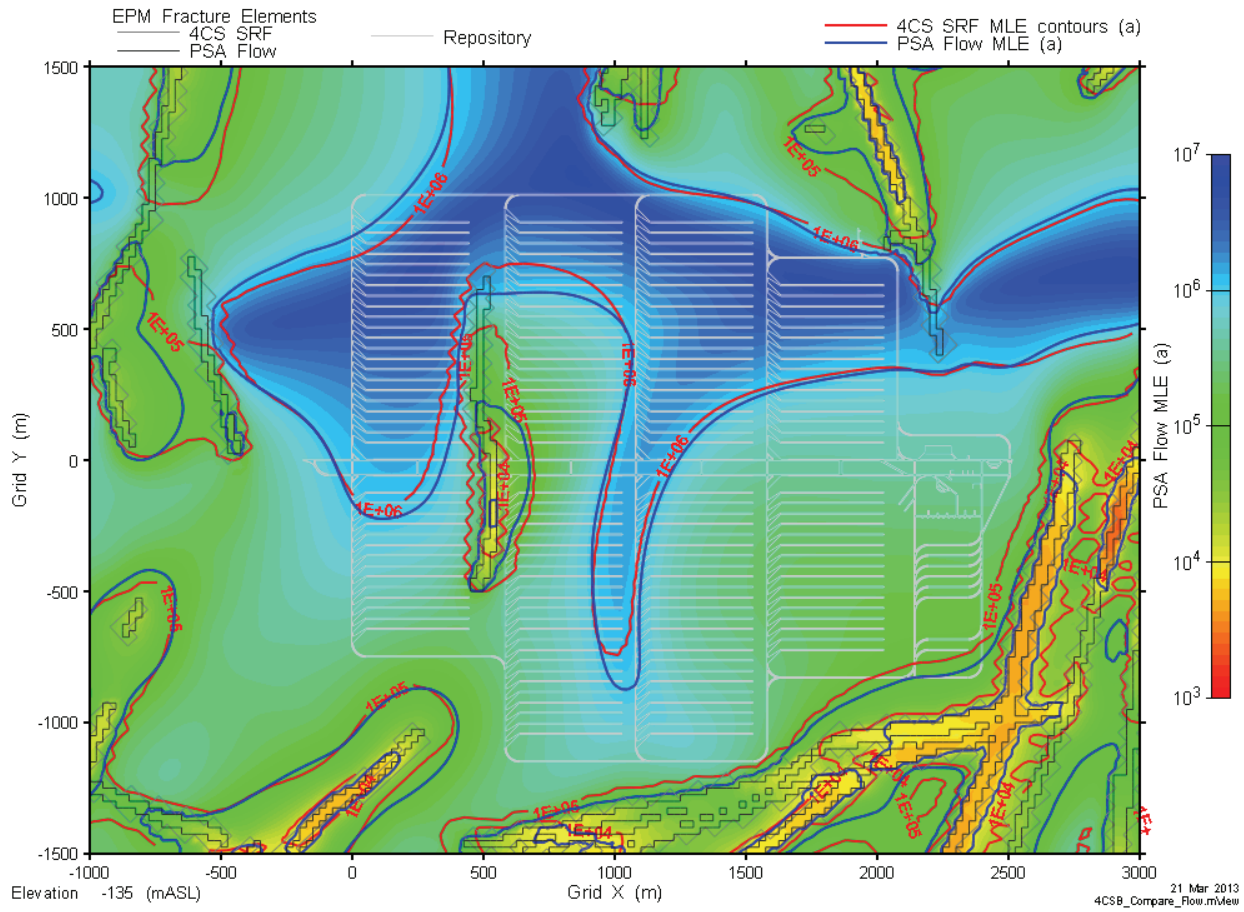

Figure 3.5: PSA Flow Model Verification – Detailed MLE Comparison at Repository Elevation

The impact of the refined repository area discretization is shown on the MLE results, where greater differences in contours are apparent near the EPM fracture zones. Nonetheless, the otherwise close correspondence of the contours shows that the flow systems are very similar, with good matching of flow directions and magnitudes. The ratio of MLEs at the repository horizon is shown in Figure 3.6, with a CDF of the ratios within the placement room footprint presented in Figure 3.7. Ratios are close to one for most of the footprint, with the exception of areas around the fracture where effects of the different discretization size are most apparent.

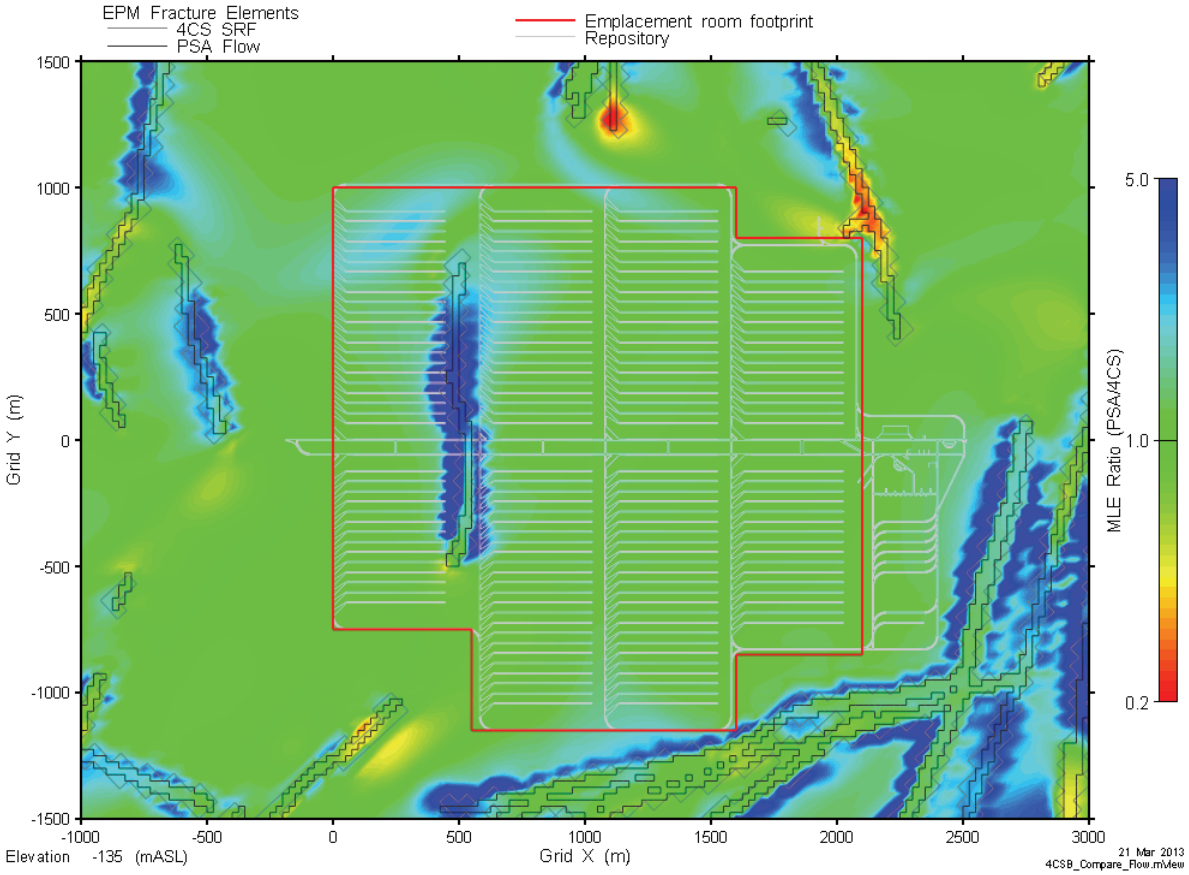

Figure 3.6: PSA Flow Model Verification – MLE Ratio (PSA MLE / 4CS MLE) Comparison at Repository Elevation

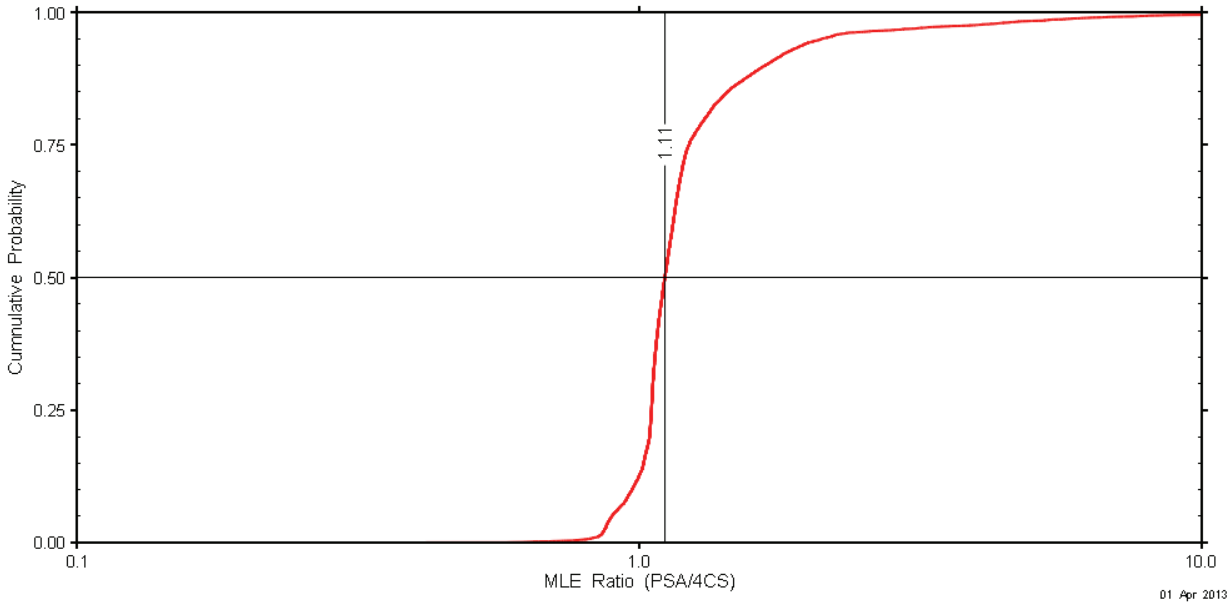

Figure 3.7: PSA Flow Model Verification – CDF of ratios within repository room footprint Head Differences over model domain

3.5 PROPERTY PARAMETERIZATION

Property value assignments for each geosphere property group are based on fixed and sampled variables. Sampled variables are represented by probability distributions. With the LHS methodology, each distribution is sampled **n** times, where n is the number of realizations specified for each specific assessment, and is independent of the actual distributions.

One feature of the 4CS geological conceptual model is that hydraulic conductivity decreases with depth. The shallow bedrock (SH_ROCK) is higher conductivity than the intermediate bedrock (INT_ROCK), which is higher conductivity than the deep bedrock (DEEP_ROCK). Two possible approaches to honoring this constraint within the variable sampling scheme are: 1) sample the permeability from different non-overlapping distributions and force correlations to keep relative contrasts, or 2) sample a base permeability, and calculate other permeabilities from a sampled multiplier variable. The second approach has been selected for use in this assessment as regression analyses will be able to provide an indication of the importance of this attribute. The INT_ROCK property group is viewed as the “base”, with hydraulic conductivities of deep and shallow bedrock calculated based on multipliers. The same approach is used for porosity.

For conductivity, deep rock multipliers range from 0.01 to 0.5, and shallow rock multipliers range from 2 to 100. The 4CS Reference Case ratios are 0.25 and 50, respectively. This ensures that shallow bedrock conductivity is always greater than intermediate bedrock conductivity, which in turn is always greater than deep bedrock conductivity.

In the current assessment, intact rock porosity and fracture system conductivity also vary with depth in a piecewise fashion similar to hydraulic conductivity. This is in contrast to the 4CS conceptual model, which assumes a single constant porosity for all bedrock, and constant fracture hydraulic conductivity. In general, fracture conductivity and porosity are expected to decrease with depth due to increasing rock stress fields. However, there are few data on these properties at depth, so the 4CS conceptual model assumed constant properties. The current assessment allows uncertainties to be incorporated so reasonable estimates of property variation are included. In the 4CS Reference Case, bedrock porosity is 0.003. In the PSA Flow model, porosity will change but the range multipliers have a lower limit of one for shallow bedrock and an upper limit of one for deep bedrock, to allow deep and shallow porosity to be close to the intermediate bedrock porosity value in some realizations. Fracture conductivity multipliers are set similarly, although as for the intact rock conductivity, with a log-uniform distribution to reflect the general attributes of conductivity distributions.

Initial sampled variables and distributions are given in Table 3.1. The parameter distributions specified encompass the 4CS parameter space, but median values do not necessarily represent 4CS Reference Case values. In particular, the Intermediate Bedrock Hydraulic Conductivity distribution ranges from 1E-08 m/s to 1E-12 m/s and is biased slightly higher than the 4CS Reference Case and permeability sensitivities, which encompassed a range from 4E-10 m/s (Sensitivity 1) to 4E-13 m/s (Sensitivity 3). The high end of the sampled distribution represents bedrock properties that are probably inappropriate for a DGR. They are included within the range so as to examine the possible performance of such unlikely settings. The median value (1E-10 m/s) is a factor of 2.5 higher than the 4CS Reference Case (4E-11 m/s).

Table 3.1: PSA Flow Model Parameters and Distributions

Group	Parameter	4CS Reference Case Value	Distribution
Shallow Overburden	all		All fixed at 4CS values
Shallow Bedrock	Hydraulic Conductivity	2E-09 m/s	Multiplier on intermediate bedrock value, Log-uniform, Min 2, Max 100
	Porosity	0.003	Multiplier on intermediate bedrock value, uniform, Min 1, Max 5
	Fracture Hydraulic Conductivity	1E-06 m/s	Multiplier on intermediate bedrock value, Log-uniform, Min 1, Max 10
Intermediate Bedrock	Hydraulic Conductivity	4E-11 m/s	Log-uniform, Min 1E-12, Max 1E-08
	Porosity	0.003	Uniform, Min 0.001, Max 0.005
	Fracture Hydraulic Conductivity	1E-06 m/s	Log-uniform, Min 1E-07, Max 1E-05
Deep Bedrock	Hydraulic Conductivity	1E-11 m/s	Multiplier on intermediate bedrock value, Log-uniform, Min 0.001, Max 0.5
	Porosity	0.003	Multiplier on intermediate bedrock value, uniform, Min 0.1, Max 1
	Fracture Hydraulic Conductivity	1E-06 m/s	Multiplier on intermediate bedrock value, :Log-uniform, Min 0.01, Max 1
All	Effective Diffusion	3.6E-13 m^2/s (I129 for intermediate and deep bedrock)	Log-uniform, Min 1.0E-13, Max 1.0E-11
	Longitudinal Dispersivity	80 m	Uniform, Min 50m, Max 100 m
	Transverse Dispersivity	8 m	Calculated, 10% of longitudinal
	Fracture Porosity	0.10	Uniform, Min 0.05, Max 0.15
	Well Rate	911 m^3/a	Uniform , Min 0, Max 2500 (used for second assessment)

3.6 PROBABILISTIC IMPLEMENTATION

Table 3.2 describes the various sub-steps that are used to implement that basic assessment workflow described in Section 2.2. With the exception of sample and model execution, most sub-steps are implemented with mViewX configurations.

Table 3.2: PSA Flow Model Workflow

Workflow Step	Configuration	Description
Sample	n/a	Write variable file sample.var in the processor instance directory. Sample.var contains a list of variable values and names, one per line. Variable names include property group identifier and name. For example: 1.085627631138E-09 INT*K 3.000000000000E-03 INT*Porosity 2.149757685421E-06 INT*FRAC_K
Pre-Process	UpdateBaseProps	Reads sample.var and substitutes variable values into mView property structure. Calculates multiplier properties. Writes mView case property file and FRAC3DVS material property file.
	EPM_FracSetup	Reads mView case property file and sample.var. Performs EPM calculations. Writes FRAC3DVS element K and porosity files for all fracture elements in processor instance directory.
	SetWellRate	Reads sample.var and template file to perform variable substitution on well rate. Writes well.include file in processor instance directory.
Execute	pref3d_130.exe	Execute FRAC3DVS preprocessor.
	f3dopg_130.exe	Execute FRAC3DVS simulator. Flow simulation is set to use a maximum of 9999 matrix solver iterations.
Post-Process	Convert	Read FRAC3DVS output in processor instance directory Convert head, MLE, and processor execution stats (iteration count for flow and MLE solution) to mView format.
	Process	Reads mView results file. Converts MLE from seconds to years and extracts nodal MLE associated with repository rooms (see Figure 3.3). Extracts heads at well node locations. Calculates well head. Writes text file tables with MLE coordinates and values, well data.
	Save results	Reads processed tables. Processes MLE table. Calculates location and value of shortest MLE, add to MLE results table. Calculates CDF of MLE table, adds this to output time series. Adds processor instance and execution times to results table.

3.7 RESULTS

3.7.1 No-Well Case

The “No-well” assessment was conducted with 1000 realizations, simulated using 10 cores on each of two server boards. The MLE simulations must be executed in full finite-element mode with FRAC3DVS-OPG which leads to a relatively large memory footprint (4.6GB peak, 3.9GB average). This allowed a maximum of 10 concurrent simulations to execute with allowances for occasional concurrent peaks on 2 processors. As one of the 20 cores is the designated master instance, which does not perform computation, the 1000 realizations were effectively simulated on 19 cores. Total elapsed real time was 1.2 days, with total processor time of 516 processor hours. Individual realization execution time ranged from 603 seconds to 28430 seconds. Execution time is primarily a function of the number of matrix iterations required to solve the steady-state flow equations. This is significantly affected by permeability contrasts and magnitudes. Lower permeabilities and greater ratios between intact rock and fracture permeabilities require more iterations to reach specified solution convergence criteria. Overall execution time could likely be reduced without loss of MLE accuracy by increasing the convergence factor; however such an assessment has not been performed.

Figure 3.8 shows results in terms of the minimum MLE of all placement room nodes (previously shown as red symbols in Figure 3.3 and shaded grey in Figure 3.8). Two distinct clusters are present, denoted “West Group” and “East Group” in the figure. Of the 1000 simulations, 604 had shortest MLE in West Group, with 322 in East Group. The remaining 74 simulations, all with shortest MLE greater than 100,000 years, are near the repository fracture adjacent to the West Group, and are designated as “Other”. Grouping is determined by bedrock conductivity and its impact on the flow regime, as further described below.

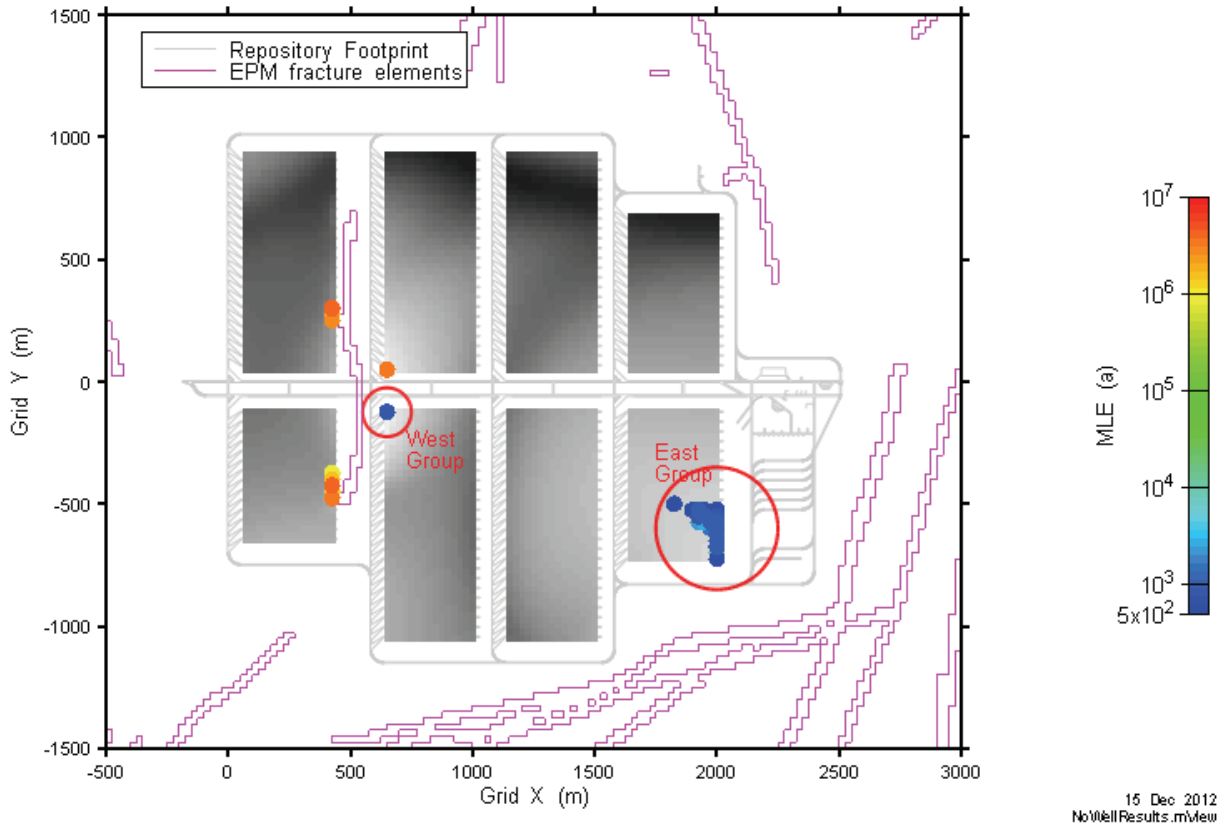

Figure 3.8: PSA Flow "No Well" – Minimum MLE Node Location

A regression analysis was performed using STEPWISE (see Section 2.3.4) to determine the relative significance of the sampled variables. Sampled variables form the independent variables in the assessment, while minimum MLE is the dependent variable. Results (Table 3.3) show that the regression model captured system performance at a very high level of significance (R^2 = 0.98757) and that intermediate bedrock hydraulic conductivity (INT*K) was by far the most important variable, accounting for 95.4% of the variance in the results. Intermediate bedrock porosity (INT*Porosity) was the second most important, accounting for a further 2.7% of variance (calculated as difference in R^2 from INT*Rock). No other variable accounted for more than 1% of the model variability.

Table 3.3: PSA Flow "No well" – MLE Ranked Stepwise Regression Results

Model significance (R^2)			0.98757
Variable	**R^2 Included**	**R^2 Deleted**	**Regression Coefficient**
INT*K	0.9544752	0.02666	-0.98705
INT*Porosity	0.9817981	0.960456	0.165657
INT*FRAC_K	0.986246	0.982947	-0.06837
ROCK*Dispersivity	0.9866189	0.987189	0.019675
SHALL*K_Mult	0.9869463	0.987247	-0.0181
DEEP*K_Mult	0.9871434	0.987386	-0.01368
ROCK*Diffusion	0.9872824	0.98743	0.011943
DEEP*FRAC_K_Mult	0.9874033	0.987449	-0.01109
DEEP*Porosity_Mult	0.9875158	0.987449	0.011136
SHALL*FRAC_K_Mult	0.9875714	0.987516	-0.00751

Scatter plots of the two most significant variables are shown in Figure 3.9 and Figure 3.10, respectively. The plots show variable values (X axis) and MLE values (Y axis) while also indicating the node location group (groups were defined in Figure 3.8). Three realizations where the flow solution failed to converge in 10000 iterations are also indicated. Figure 3.9 shows the very strong relationship between MLE and hydraulic conductivity. The figure also shows that East Group and "Other" minimum MLE locations are associated with higher and lower extremes of the hydraulic conductivity distribution, respectively, and that the failed simulations are associated with very low hydraulic conductivities.

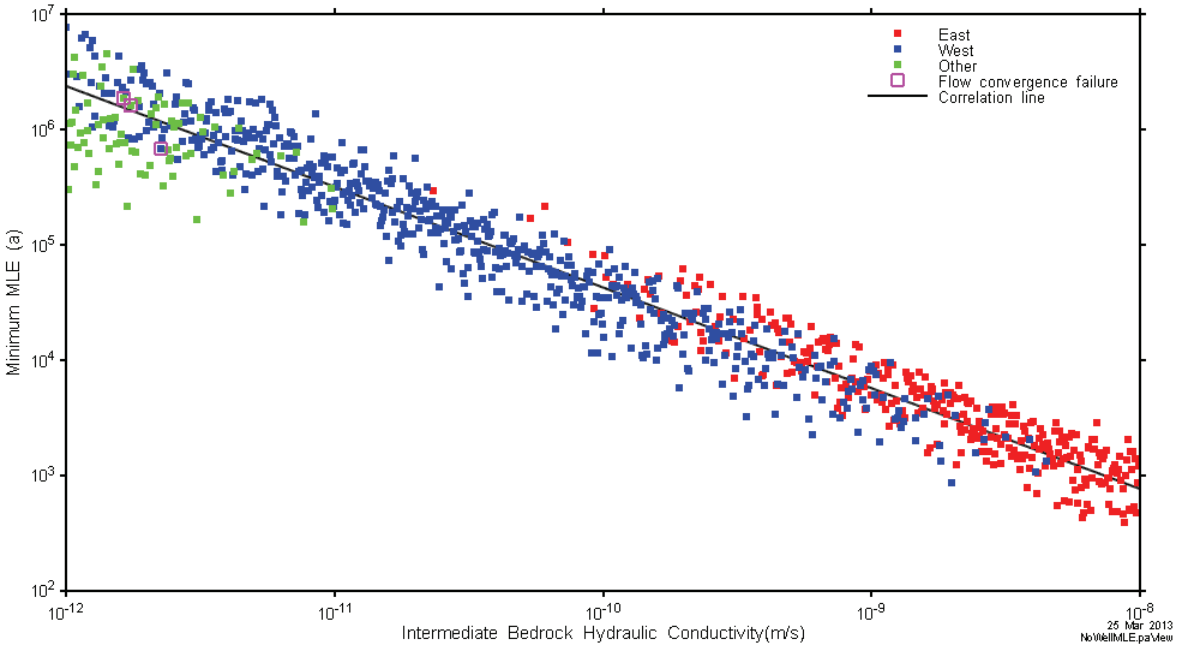

Figure 3.9: PSA Flow "No Well" Minimum MLE Scatterplot versus Intermediate Bedrock Hydraulic Conductivity

By contrast, even though intermediate bedrock porosity is the second most significant variable, there are no clear correlations with node location grouping or failed realizations in Figure 3.10. A slight general trend to increased MLE with increased porosity is evident, and is physically realistic given that advective velocity (the primary driver of MLE in this system) is inversely proportional to porosity.

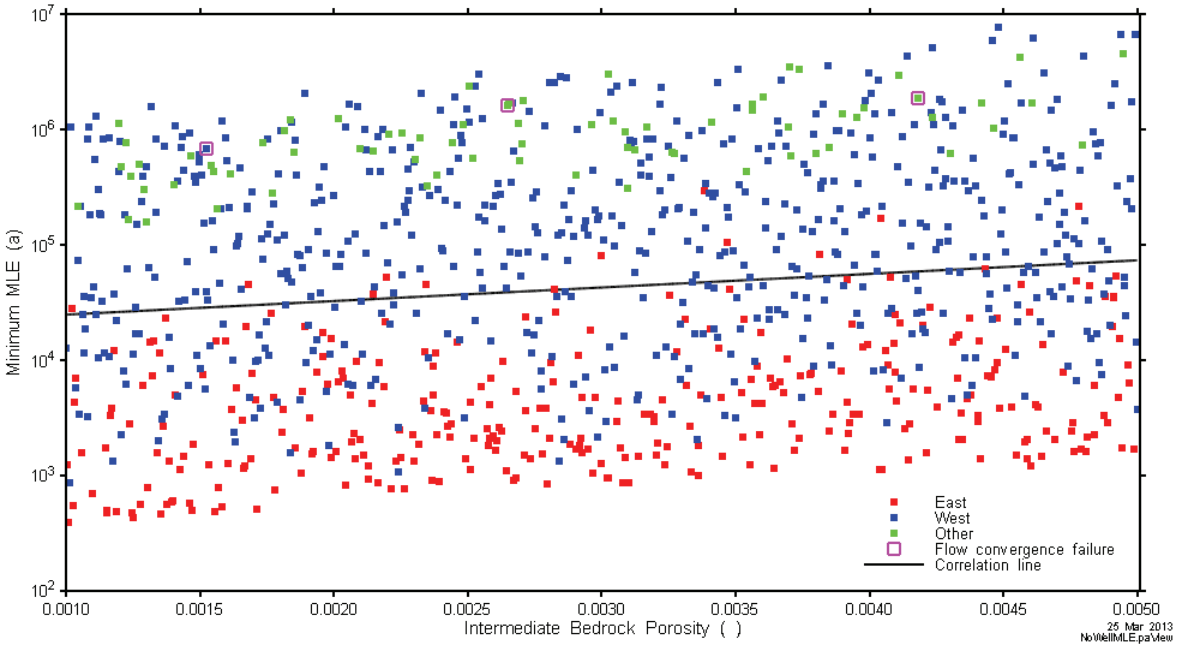

Figure 3.10: PSA Flow "No Well" Minimum MLE Location versus Intermediate Bedrock Porosity Scatterplot

The "No-Well" model sampled 13 variables with 1000 realizations, or approximately 77 samples per variable. Additional simulations were performed as part of the cloud computing test (details provided in Section 6.2) with 125, 500, and 2500 realizations to test convergence and determine the adequacy of sampling. Figure 3.11 compares the CDF of minimum MLE for each simulation. It is clear that the 125 realization case is slightly different, while the other cases are more difficult to visually distinguish. Sample medians are within a 0.1 percent range (log time) for 500, 1000, and 2500 cases (39,905 a, 39,698 a, 37,994 a), while the 125 realization case median times are approximately 1.5% different (33,661 a).

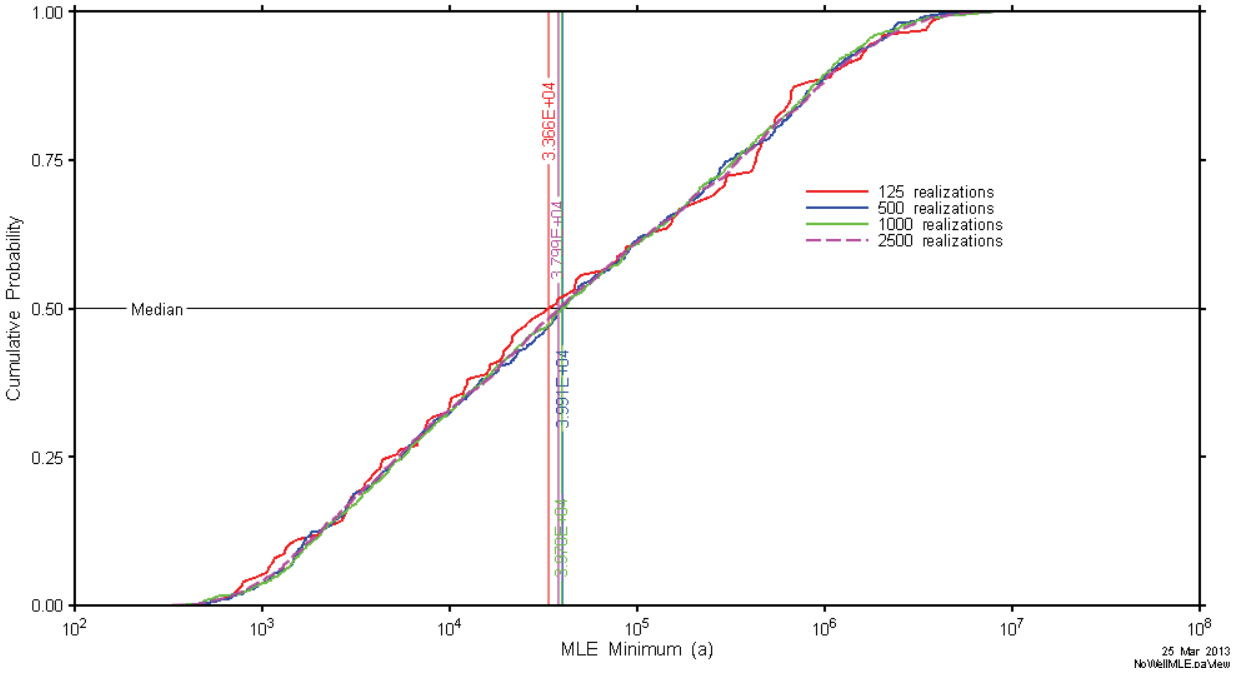

Figure 3.11: CDF of Minimum MLE for Different Sampling Densities

An alternate measure of convergence is the stability of the regression coefficients. Table 3.4 shows calculated regression coefficients and percentage of the 1000 run coefficients for the three most important parameters.

Table 3.4: PSA Flow "No well" –Regression Coefficient Convergence

Variable	Regression Coefficient				% of 1000 Realization Coefficient			
	125	500	1000	2500	125	500	1000	2500
INT*K	-0.9609	-0.9846	-0.9870	-0.9720	97.4%	99.8%	100.0%	98.5%
INT*Porosity	0.1583	0.1625	0.1657	0.1653	95.6%	98.1%	100.0%	99.8%
INT*FRAC_K	-0.0687	-0.0782	-0.0684	-0.0721	100.4%	114.4%	100.0%	105.4%

Considering the overwhelming importance of the intermediate bedrock conductivity, even the 125 realization CDF would be adequate as a representation of system performance. A log-uniform distribution calculated from the 1000 realization 0.1 and 0.9 CDF values provides a good visual fit to all but the tails of the CDF. This reflects the log-uniform distribution assigned to the intermediate bedrock conductivity. If there were multiple parameters which influenced the MLE with a similar significance, rather than one predominant parameter, the MLE distribution would take the form of a hybrid of the significant input distributions.

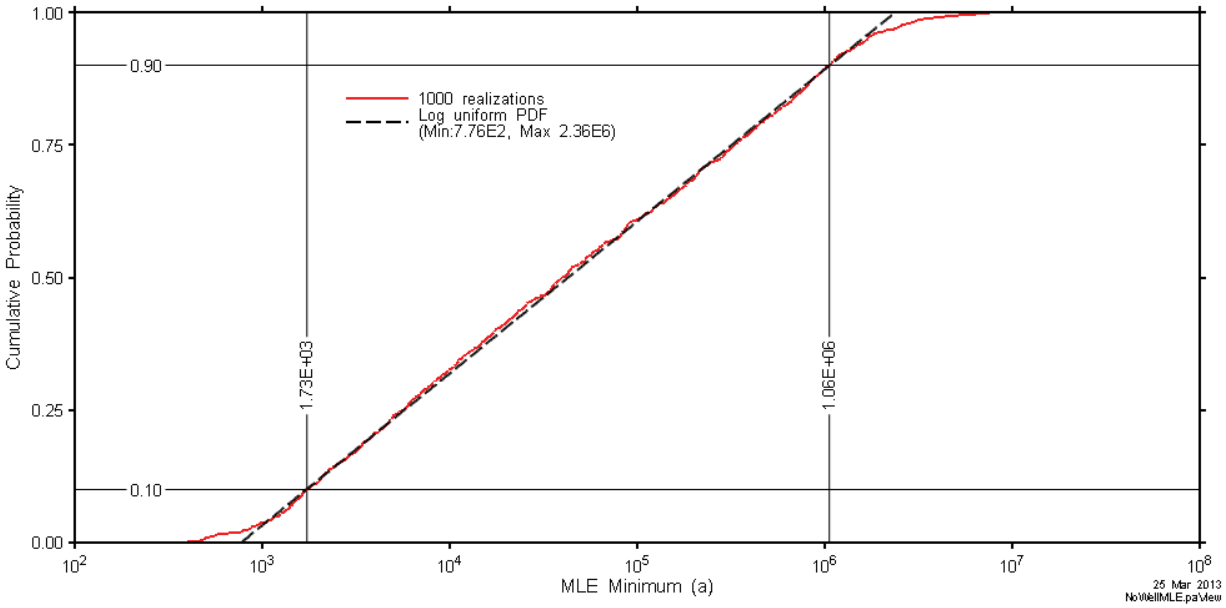

Figure 3.12: Comparison of Actual and Fitted Distributions

3.7.2 Well Case

Two well locations were specified based on the clear spatial distinction between the main groups (Figure 3.13). The West Well is adjacent to the West Group and is located similarly to the 4CS reference well. The East Well is located in the fracture system closest to the East Group. As in the 4CS, both wells are located at a depth of approximately 100 mBGS with the well pumping nodes intersecting the fracture system.

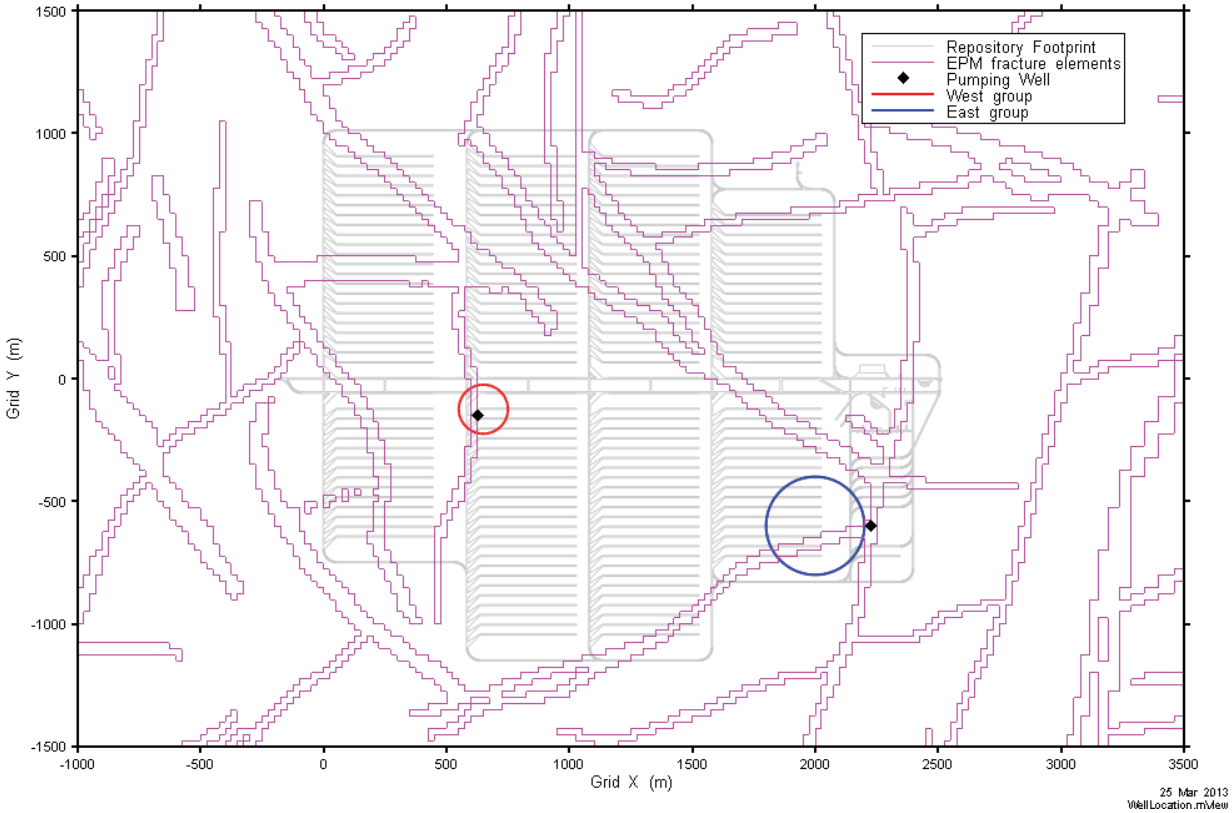

Figure 3.13: PSA Flow with Well – Water-Supply Well Location at Well Screen Elevation (100 mBGS, or 260 mASL)

The selection of which well to use in a particular simulation could be problematic. A straightforward approach would be to perform a no-well simulation, determine the spatial group of the minimum MLE location, and then rerun the simulation with the corresponding well turned on. This is computationally expensive, requiring two flow and MLE simulations per realization. The wells are sufficiently distant from each other so that their radii of influence do not overlap, at least within the range of pumping rates described in Table 3.1. Consequently, both wells are included in each simulation.

A 1000 realization assessment of the well case on the same hardware configuration resulted in very similar results to the no-well case. There were slight changes in allocation, with 679 simulations in West group, 253 in East group, and 68 in Other. Figure 3.14 shows the spatial distribution. Execution time statistics were similar: total elapsed real time was 1.25 days, and total processor time of 547 processor hours. Individual realization execution time ranged from 635 seconds to 28977 seconds. Of the processor hours, 537 hours were spent within the FRAC3DVS simulator and pre-processor.

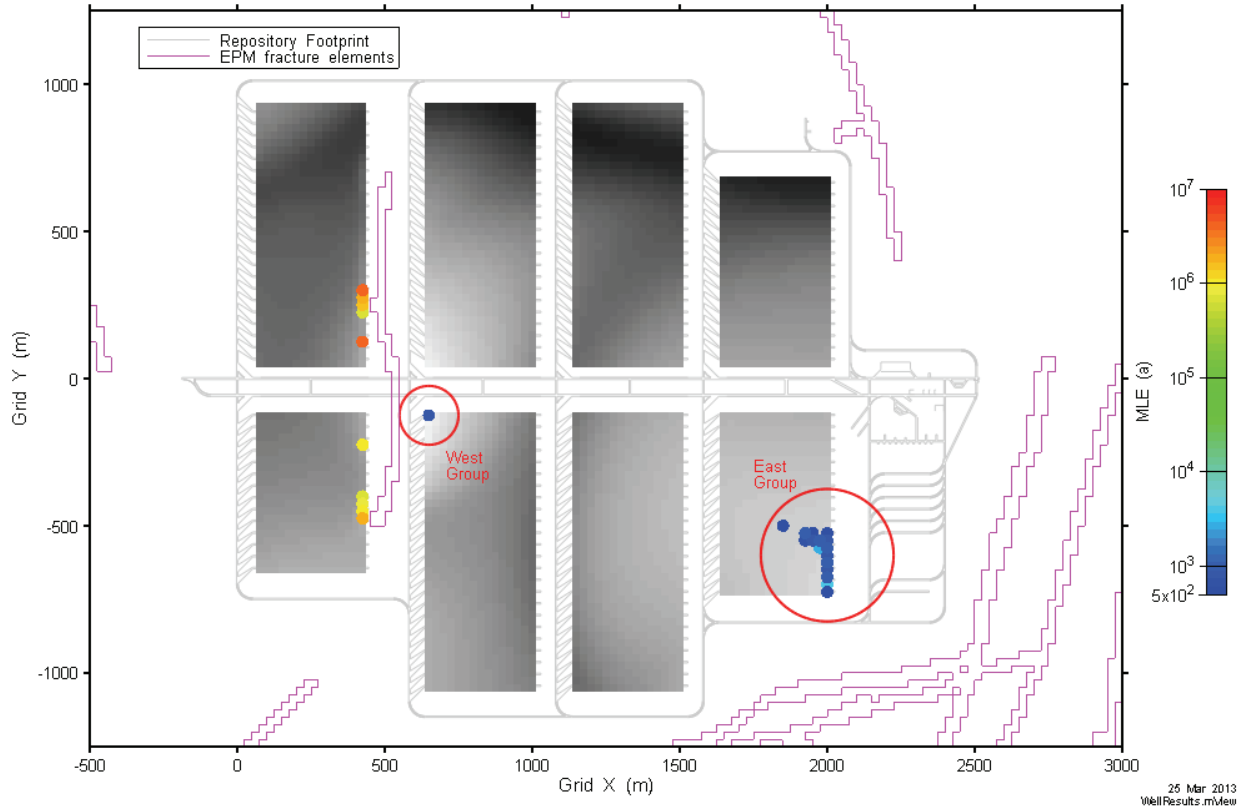

Figure 3.14: PSA Flow with Well – Minimum MLE Node Location

With wells included in the simulation, there is a possibility of non-physical results. As described in Section 3.3, these occur when the pumping rate at the well is greater than the ability of the formation to supply water, and can be identified when the calculated well head is less than zero. Figure 3.15 and Figure 3.16 are scatter plots of minimum MLE versus intermediate bedrock and well rate versus fracture conductivity respectively, with location grouping, numeric failure, and well failure cases identified.

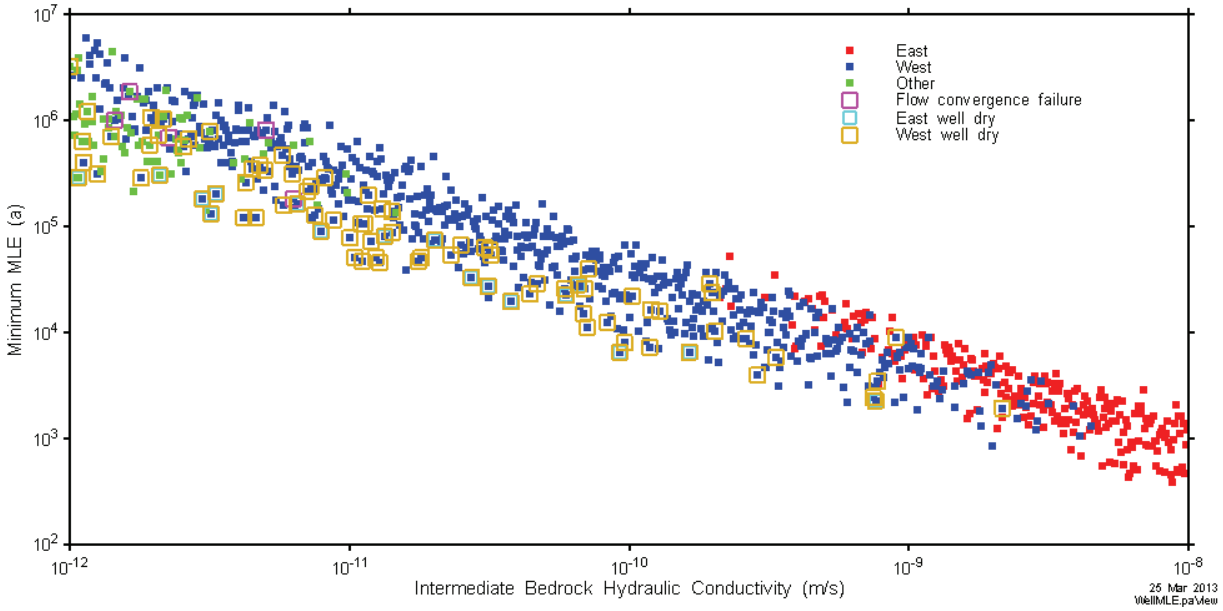

Figure 3.15: PSA Flow with Well - Minimum MLE vs Intermediate Bedrock Hydraulic Conductivity with Numeric Failure Cases

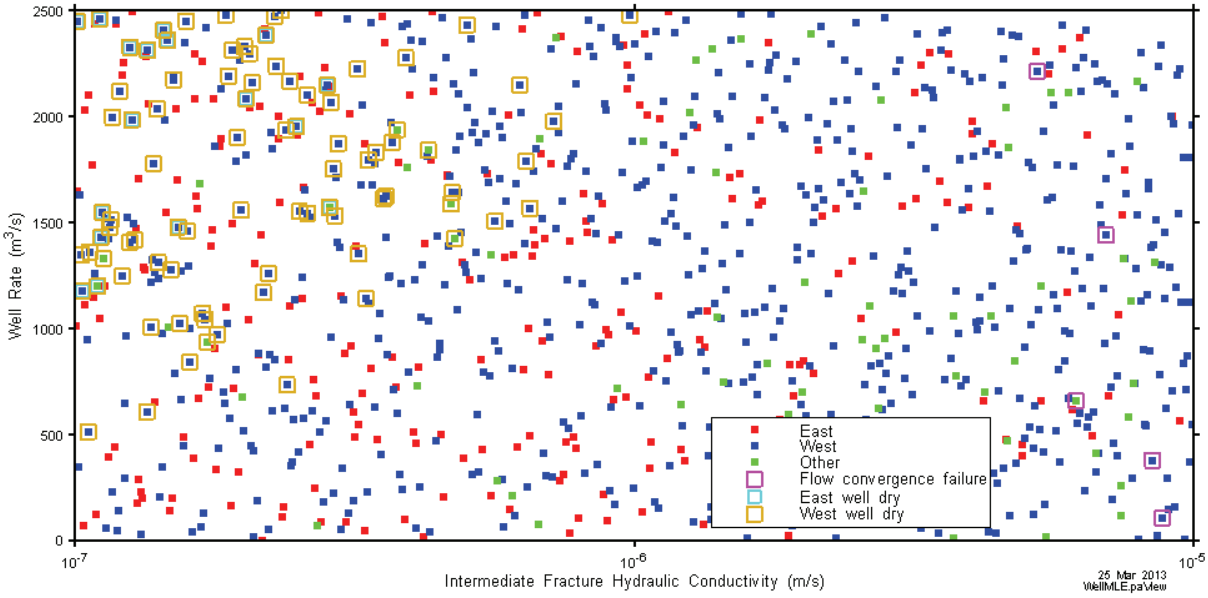

Figure 3.16: PSA Flow with Well – Well Rate vs Intermediate Fracture Hydraulic Conductivity Scatterplot with Numeric Failure Cases

There were five flow convergence failures, all of which are correlated with combinations of high fracture conductivities and low intact rock conductivity. Approximately 9% of realizations had excessive pumping in the West Well, which is clearly correlated with low fracture conductivities and higher well pumping rates. A regression analysis on western well head (Table 3.5) shows that intermediate fracture conductivity, well pumping rate and intermediate bedrock conductivity are the most important variables contributing to the metric.

Table 3.5: PSA Flow "No well" – West Well Head Ranked Stepwise Regression Results

Model significance (R^2)			0.76089
Variable	**R^2 Included**	**R^2 Deleted**	**Regression Coefficient**
INT*FRAC_K	0.33419	0.43034	0.57731
ROCK*WellRate	0.51874	0.55612	-0.45455
INT*K	0.67548	0.60440	0.39606
SHALL*FRAC_K_Mult	0.72272	0.71830	0.20686
SHALL*K_Mult	0.75991	0.72401	0.19298
DEEP*FRAC_K_Mult	0.76089	0.75991	-0.03133

Cumulative distributions of well head are plotted in Figure 3.17, with negative well heads to the left of the "Well Dry" line. Correlating well pumping rate with fracture hydraulic conductivity may be a possible approach to eliminate or reduce this problem. From a physical perspective, this is reasonable; well production is limited by geosphere capabilities. This is also reasonable from an SA perspective. Although the critical group activities do determine the water demand, any requirement in excess of what the well can physically supply will be drawn from surface water features. However, in this report we have left fracture conductivity and well rate independent, and modified assessment results to eliminate realizations with negative well heads and/or other numeric problems.

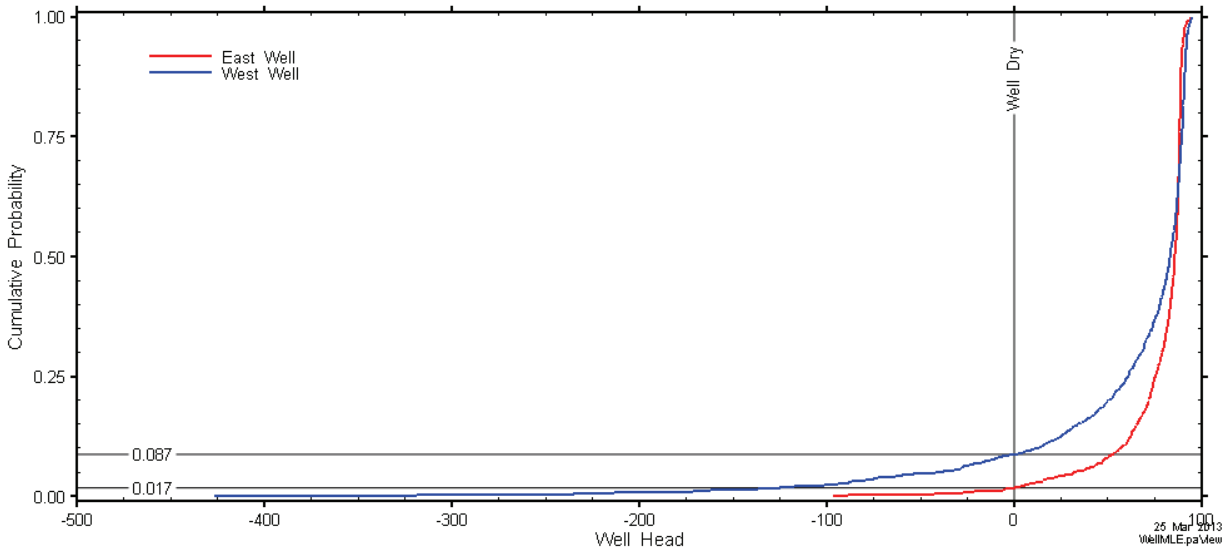

Figure 3.17: PSA Flow with Well – Well Head Cumulative Distribution Function

Related realizations can be extracted from the full data sets and their characteristics examined. Figure 3.18 presents minimum MLE CDFs for the full data set and the following subsets: all results with errors (convergence or negative well head) removed, errors only, east well group, west well group, and other group. East and Other well groups are characteristically outliers at the short and long MLE extremes, which is not unexpected given their associated conductivity distribution (Figure 3.15). The West well group is the most similar to the overall CDF, offering a nearly complete coverage of the range of values. The "Errors only" group is similar to the West

well group, which again is expected given the predominance of negative well heads in those realizations.

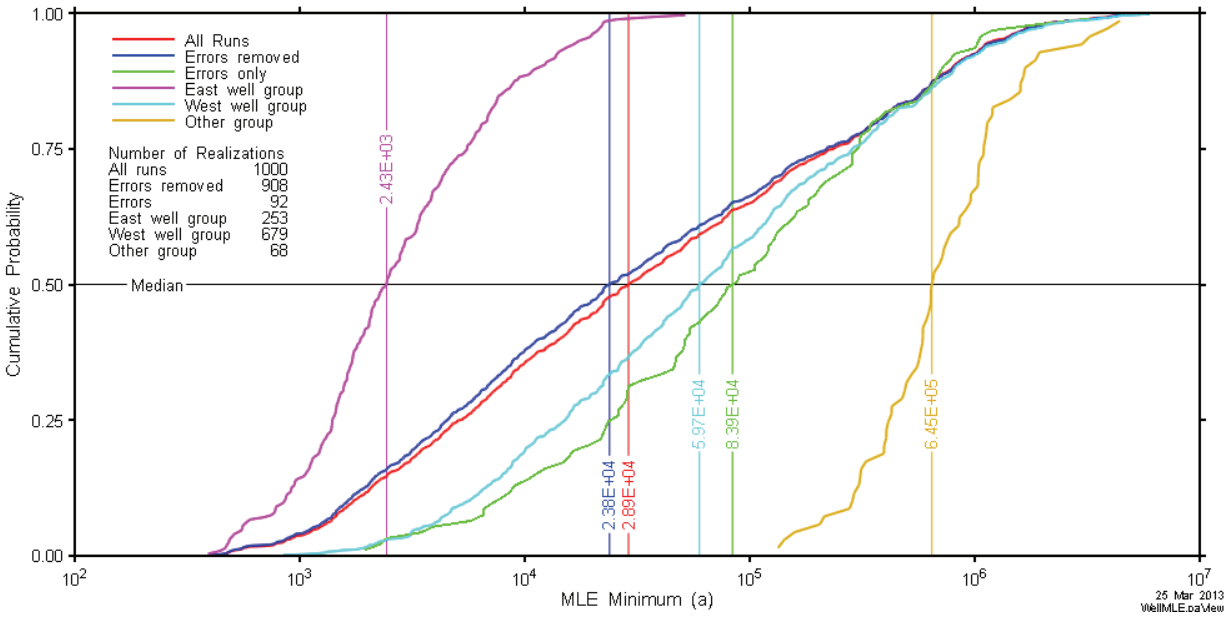

Figure 3.18: PSA Flow with Well – MLE Minimum Cumulative Distribution Function for Data Subsets

These results show that the West well group source location is dominant (in terms of number of realizations) and covers the probabilistic parameter space, which validates the assumptions that led to a near identical location being selected for the 4CS transport model. Although the East well group has the shortest MLE, they are only valid for a limited number of very high permeabilities that represent bedrock properties which would likely be considered inappropriate for a DGR.

Separate ranked regression analyses of minimum MLE against sampled variables with flow convergence failures removed for East and West well groups lead to slightly different results. Intermediate bedrock hydraulic conductivity remains the most important variable, with porosity second. However, for west wells, rock diffusion coefficient is the third most important variable while for east wells fracture hydraulic conductivity is third. This is again consistent with the associated conductivity distribution (Figure 3.15), with west well minimum MLE associated with lower conductivity rock, where diffusion is of increased importance.

Table 3.6: PSA Flow "Well" – MLE West Well with Errors Removed (596 Samples) Ranked Stepwise Regression Results

Model significance (R^2)			0.98536
Variable	**R^2 Included**	**R^2 Deleted**	**Regression Coefficient**
INT*K	0.93806	0.06889	-0.97504
INT*Porosity	0.97861	0.94452	0.20327
ROCK*Diffusion	0.98143	0.98255	0.05366
ROCK*WellRate	0.98339	0.98336	-0.04539
SHALL*FRAC_K_Mult	0.98436	0.98431	0.03275
ROCK*Dispersivity	0.98477	0.98496	0.02029
DEEP*K_Mult	0.98502	0.98513	-0.01520
SHALL*K_Mult	0.98524	0.98514	-0.01475
SHALL*Porosity_Mult	0.98536	0.98524	0.01103

Table 3.7: PSA Flow "Well" – MLE East Well (No Errors) (253 Samples) Ranked Stepwise Regression Results

Model significance (R^2)			0.96685
Variable	**R^2 Included**	**R^2 Deleted**	**Regression Coefficient**
INT*K	0.79090	0.36167	-0.84220
INT*Porosity	0.95524	0.81041	0.40118
INT*FRAC_K	0.96063	0.96142	-0.07930
DEEP*K_Mult	0.96280	0.96520	-0.04160
ROCK*FRAC_Porosity	0.96444	0.96564	0.03537
ROCK*Dispersivity	0.96571	0.96567	0.03513
SHALL*FRAC_K_Mult	0.96631	0.96625	-0.02502
SHALL*K_Mult	0.96685	0.96631	0.02352

Figure 3.19 presents the full data set for 500, 1000, and 2500 realization runs. All curves are very similar indicating that CDF stability has been achieved, and providing confidence in the adequacy of the simulation results to represent the range of variable values within the sampling domain. Median results vary over a very limited range (27,659 a for 500; 28,918 a for 1000; 27,338 a for 2500).

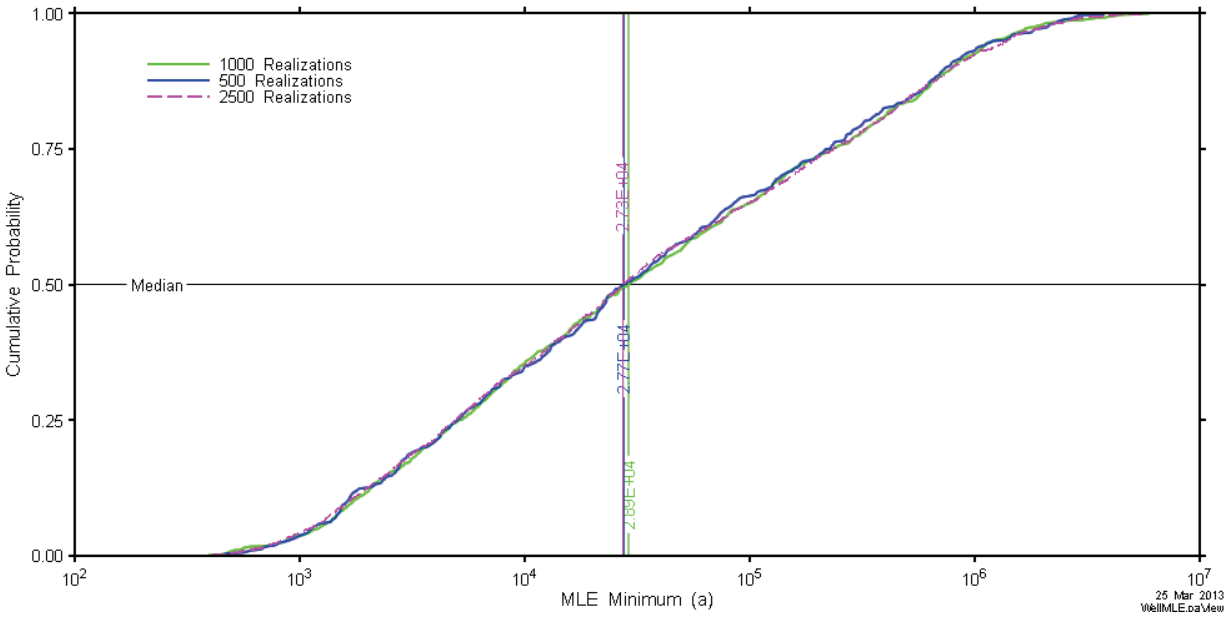

Figure 3.19: PSA Flow with Well – CDF Stability - MLE Minimum Cumulative Distribution Function for Different Number of Realizations

4. TRANSPORT MODEL

The PSA Transport model was developed based on the west well source location. As described in Section 2.1, the transport model is a hybrid of the 4CS Site- and Repository-scale models; like the 4CS Site model it includes a water supply well and a limited surface discharge area, but, consistent with the 4CS Repository model, also includes a detailed representation of a single placement room with a defective container. The model domain is shown in Figure 4.1. Model setup is described in this section; assessment results and interpretation are given in Section 5.

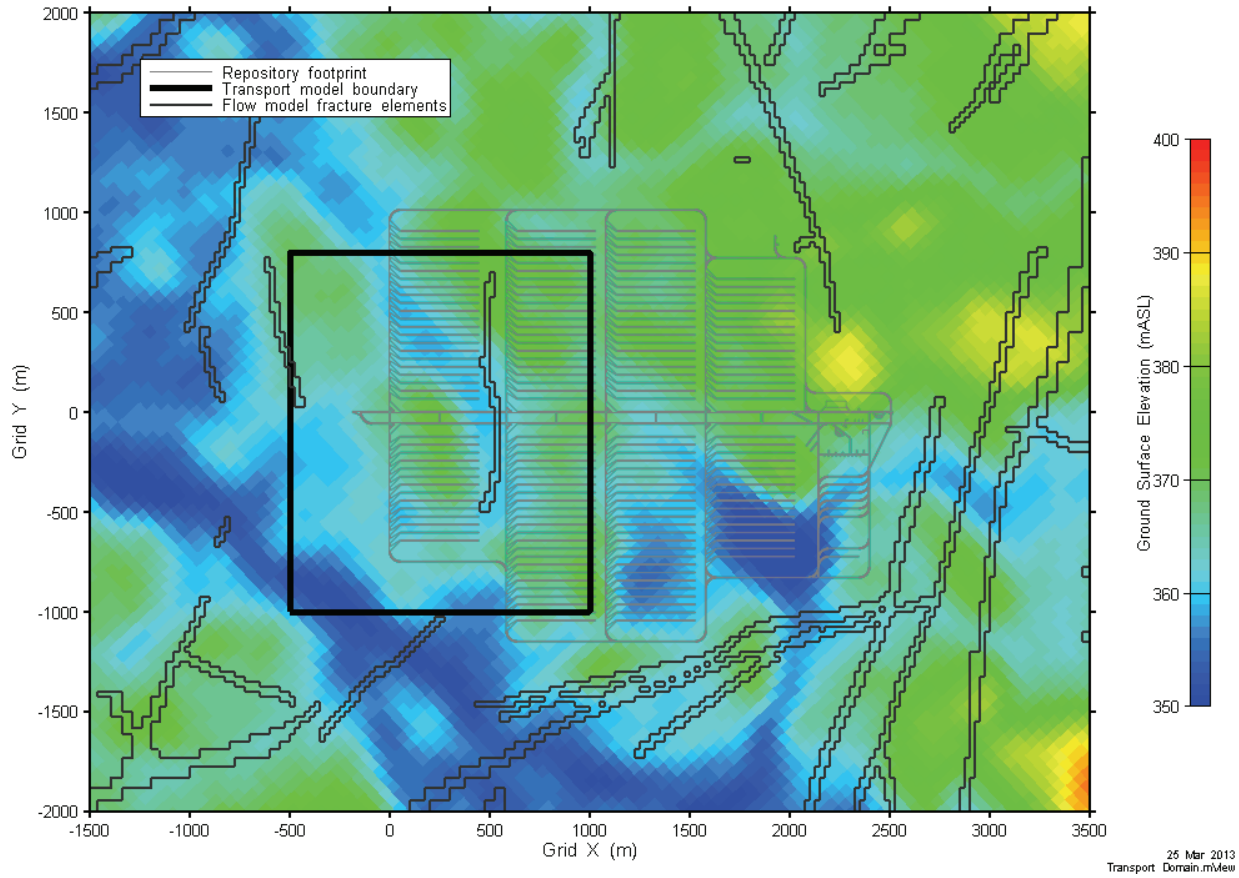

Figure 4.1: PSA Transport – Model Domain

4.1 DISCRETIZATION AND PROPERTY ASSIGNMENT

The model discretization includes a single room with backfill, bulkhead, seal, and used fuel canister (UFC) emplacement boreholes set in a geosphere extending from depth to surface, including the main repository fracture and the West well. Note that the property assignments are not modified by the PSA process; only property parameters are changed. For example EDZ thickness remains identical for all realizations, although EDZ hydraulic conductivity and porosity may change. Figure 4.2 through Figure 4.4 illustrate the discretization at increasing levels of detail. Comparing Figure 4.4 and Figure 2.2 shows that the transport model contains features at the same level of detail as the 4CS repository-scale model.

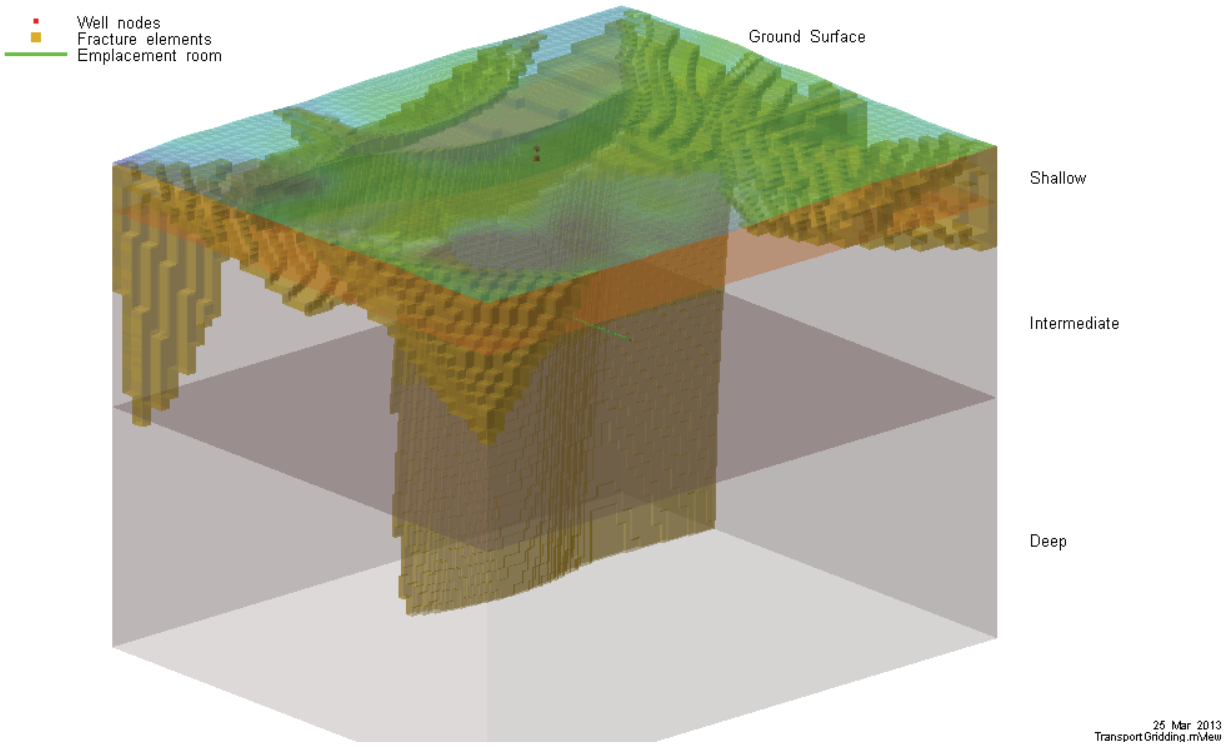

Figure 4.2: PSA Transport Grid – Full Grid Extents, Fracture System and Well

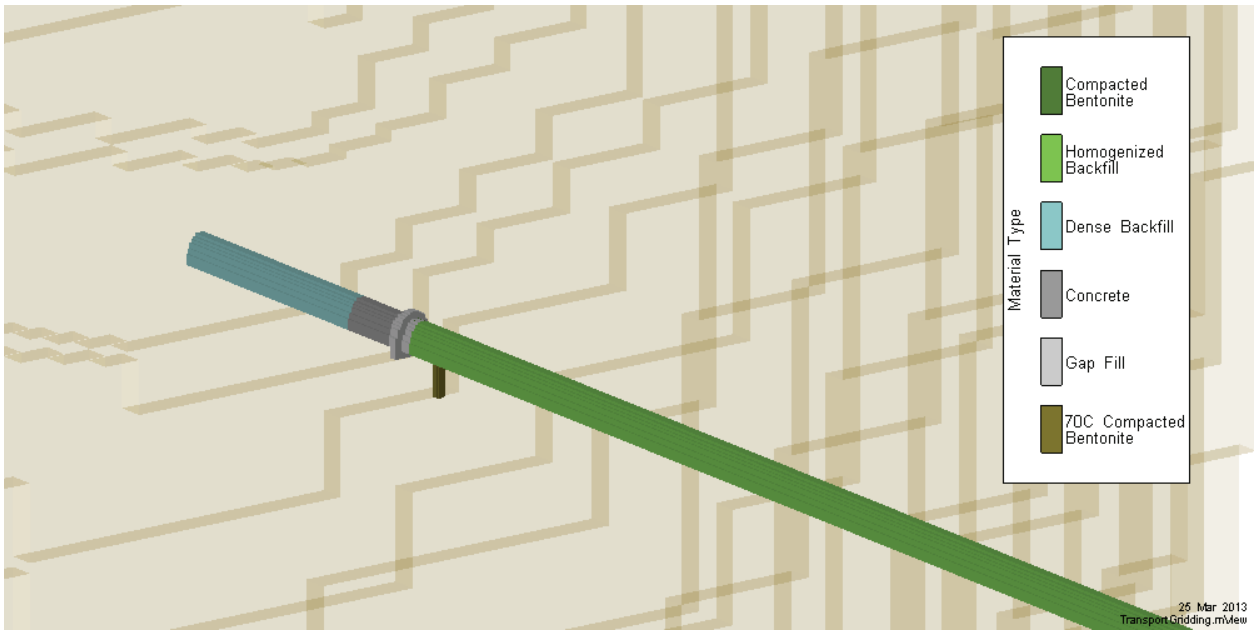

Figure 4.3: PSA Transport Grid – Room, Source Container, Seal, Bulkhead and Fracture

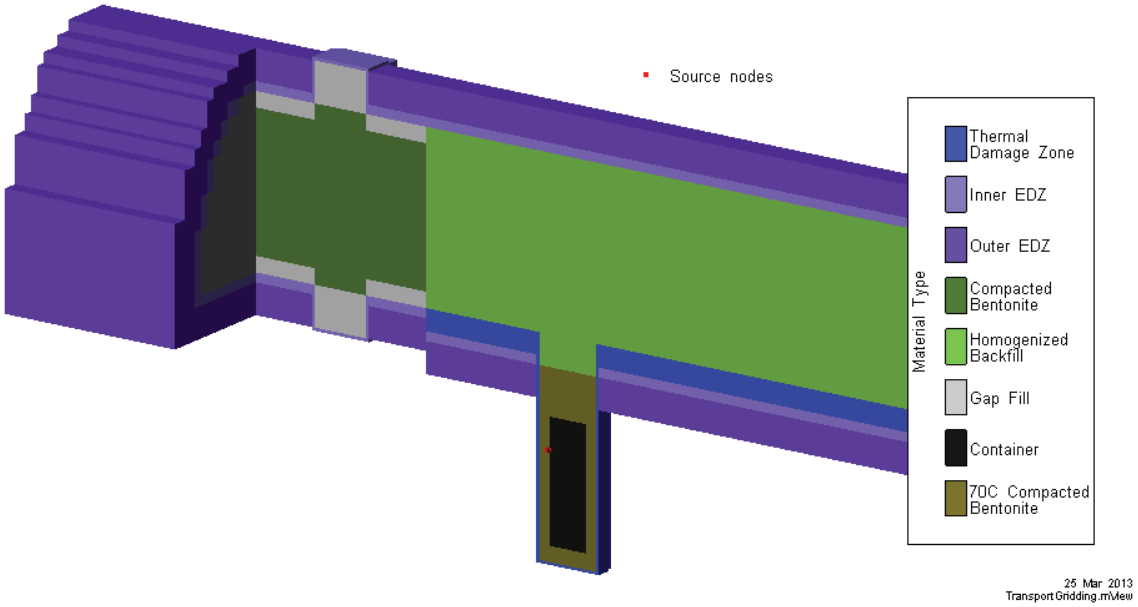

Figure 4.4: PSA Transport Grid – Source Container, EBS and EDZ Detail

Figure 4.5 illustrates the element discretization in the vicinity of the source. The transport model coordinate system has been set so that the origin is located at the intersection of the crosscut and source room centrelines. Only that portion of the cross-cut drift coincident with the placement room profile is included in the model (first 5m of dense backfill shown in Figure 4.3).

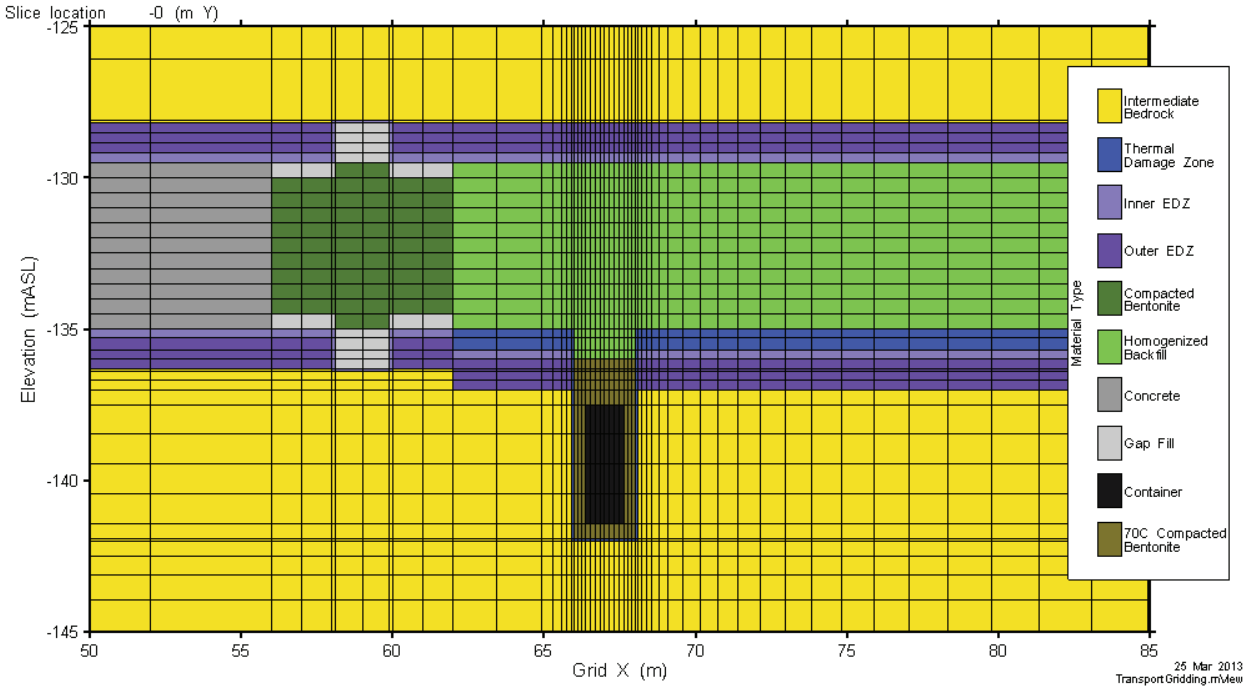

Figure 4.5: PSA Transport Grid – Discretization Detail

4.2 BOUNDARY CONDITIONS

The top surface of the model is specified as a fixed head at elevation boundary and the bottom boundary as zero flow. The side boundaries are specified head, where the values are extracted directly from the PSA Flow model. This ensures that the flow system is accurately reproduced.

Third-type transport boundary conditions are applied at all model faces. This ensures that any counter-gradient diffusive or dispersive radionuclide flux reaching the boundary does not cause erroneous mass generation.

The specified well rate is applied at nodes coincident with the water-supply well nodes in the PSA Flow model.

4.3 SOURCE TERM

The 4CS Iodine-129 container source term from the 4CS model was also used in the PSA transport model. This was defined as the release from a pinhole in a defective container. Releases from three defective containers were combined and released from a single location. The same source term was used for all simulations; there are no probabilistic variables associated with source magnitude or release rates. If a probabilistic source term model was required it could be implemented within paCalc or could be implemented as a random table selection (i.e. select a time series from a suite of equally likely time series).

4.4 SIMULATION METRICS

The primary metrics for the PSA Transport model are transport versus time at points or through various surfaces within the system, defined as follows:

1. Container — radionuclides leaving the EBS surrounding the defective container and entering the EDZ or the EBS within the placement room (Figure 4.6).
2. Room — leaving the EBS and entering the geosphere (Figure 4.7).
3. Well — captured in the water-supply well (well nodes in Figure 4.2)
4. Surface — discharge through the top layer of the model (ground surface in Figure 4.2).

Well heads described in Section 3.3 were also collected for the PSA transport model, as were numeric performance measures for both flow and transport components. MLE calculations were not performed.

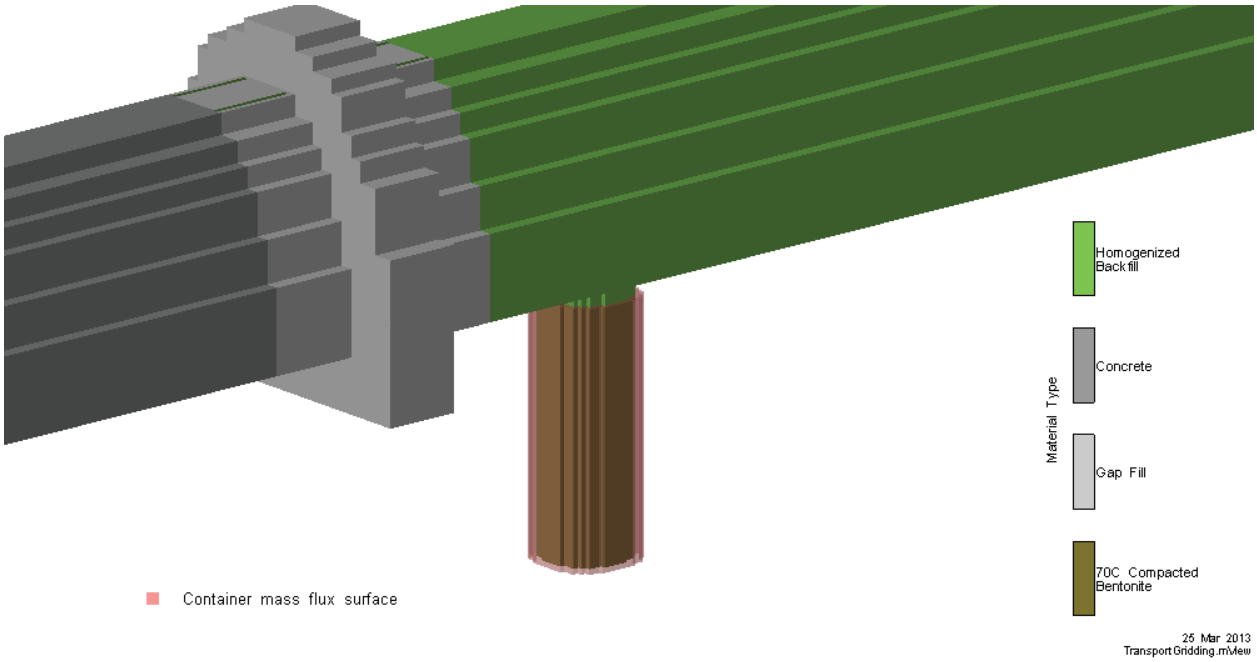

Figure 4.6: PSA Transport Grid –Container Mass Flux Metric Surface

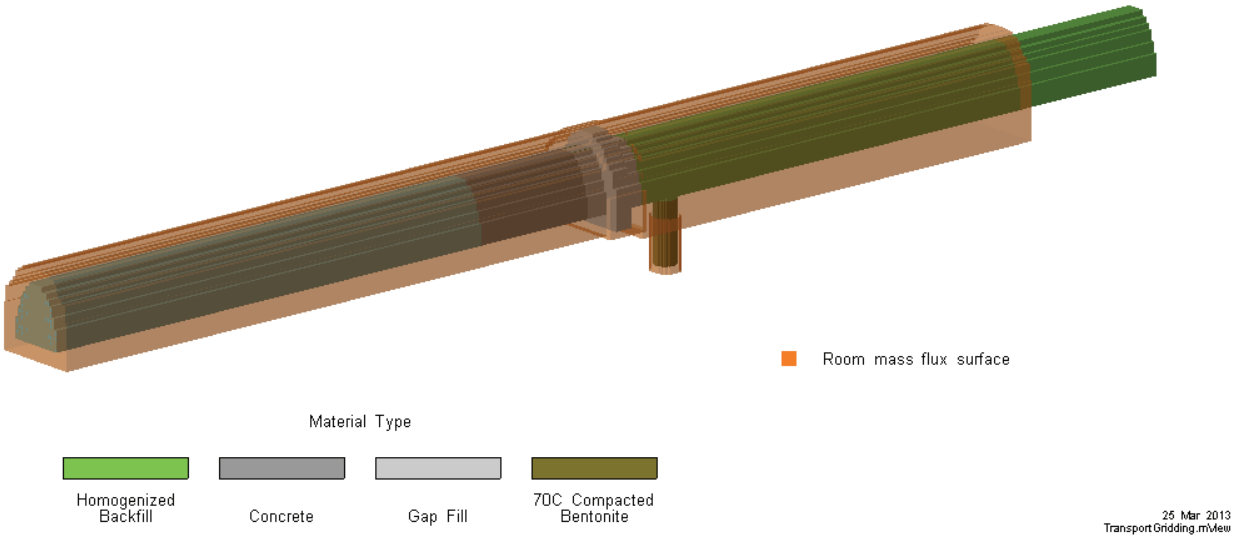

Figure 4.7: PSA Transport Grid –Room Mass Flux Metric Surface

4.5 DETERMINISTIC VERIFICATION

The PSA Transport model was verified using a single deterministic simulation with all parameters set equivalent to the 4CS Reference Case model. Head boundaries were extracted from the flow model deterministic verification simulation. Figure 4.8 compares simulated heads from the 4CS site-scale model and the PSA Transport model. Although the impacts of repository features present in the 4CS model (access and cross-cut drifts, and additional rooms) are apparent, the overall gradient is very similar.

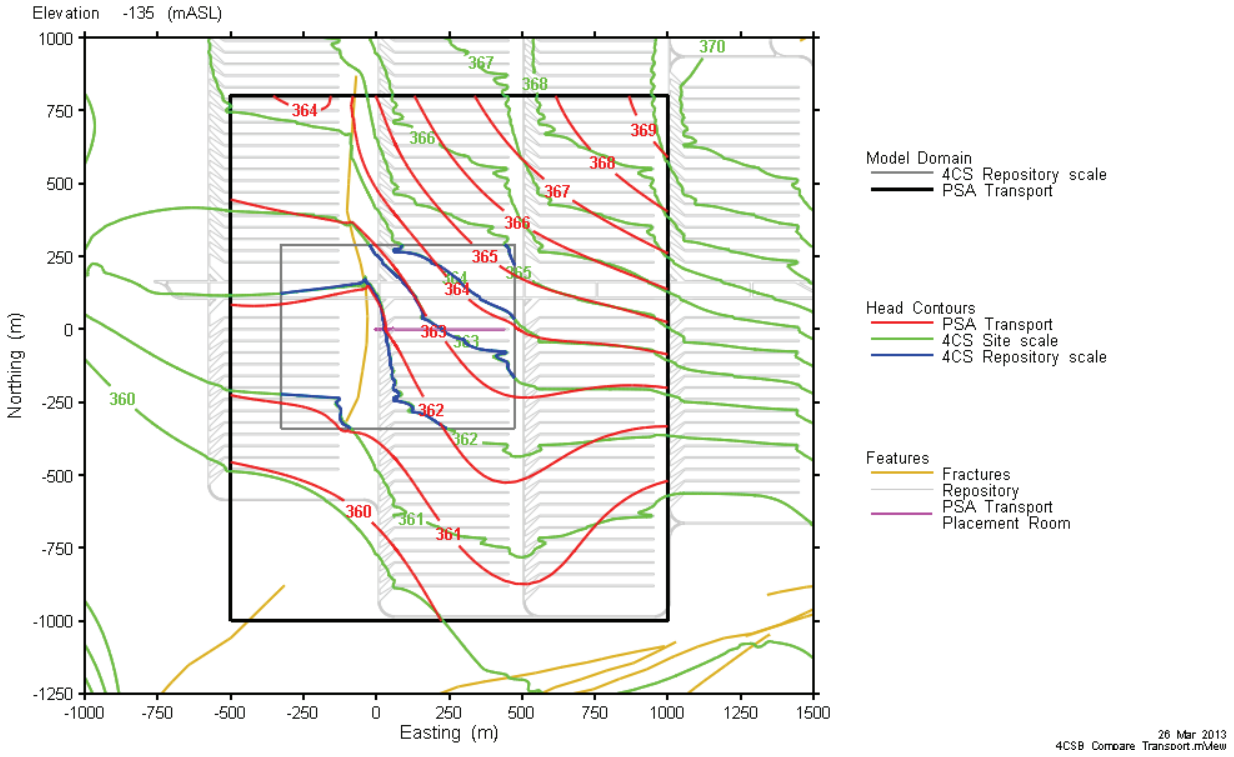

Figure 4.8: PSA Transport Model –Head Comparison

Transport results at 100,000 years from three model scales (4CS Site, 4CS Repository and PSA Transport) are compared in Figure 4.9 and Figure 4.10. As was seen for the head comparison, the effects of the repository features included in the 4CS models are apparent. However, results are very similar for all models in the main transport region between the defective container and the fracture, and within the fracture vertically up to the well.

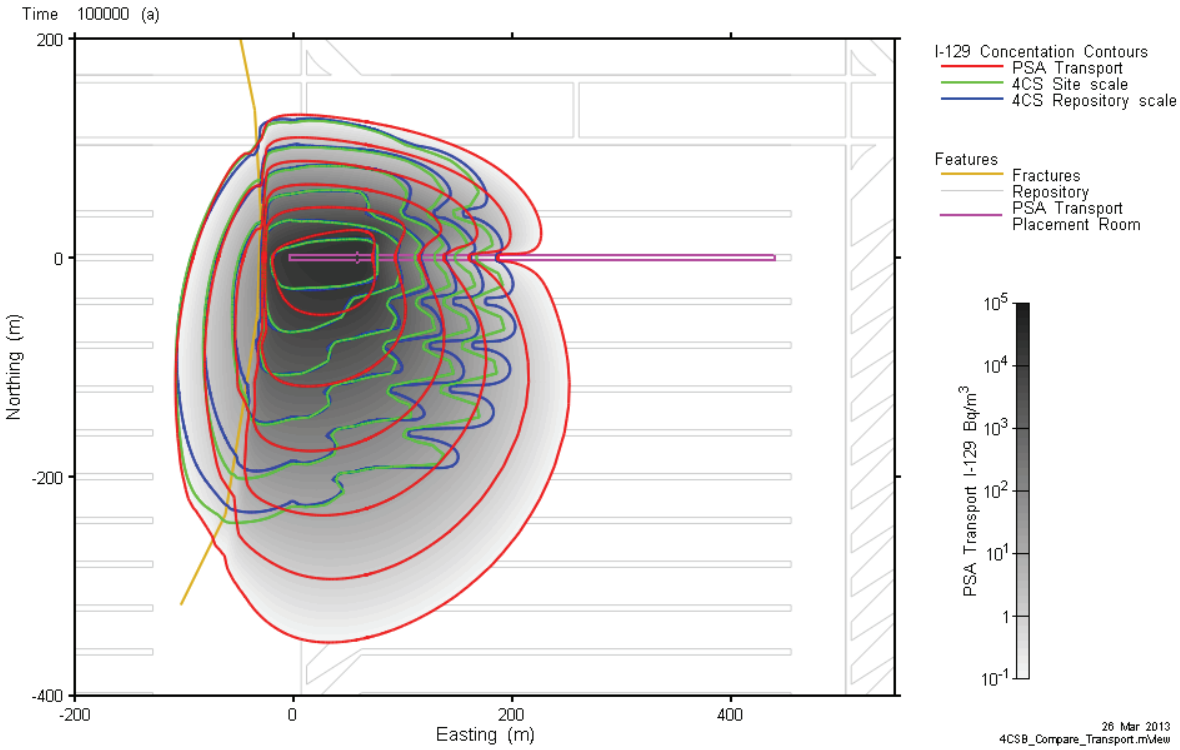

Figure 4.9: PSA Transport Model – I-129 Comparison – Plan View

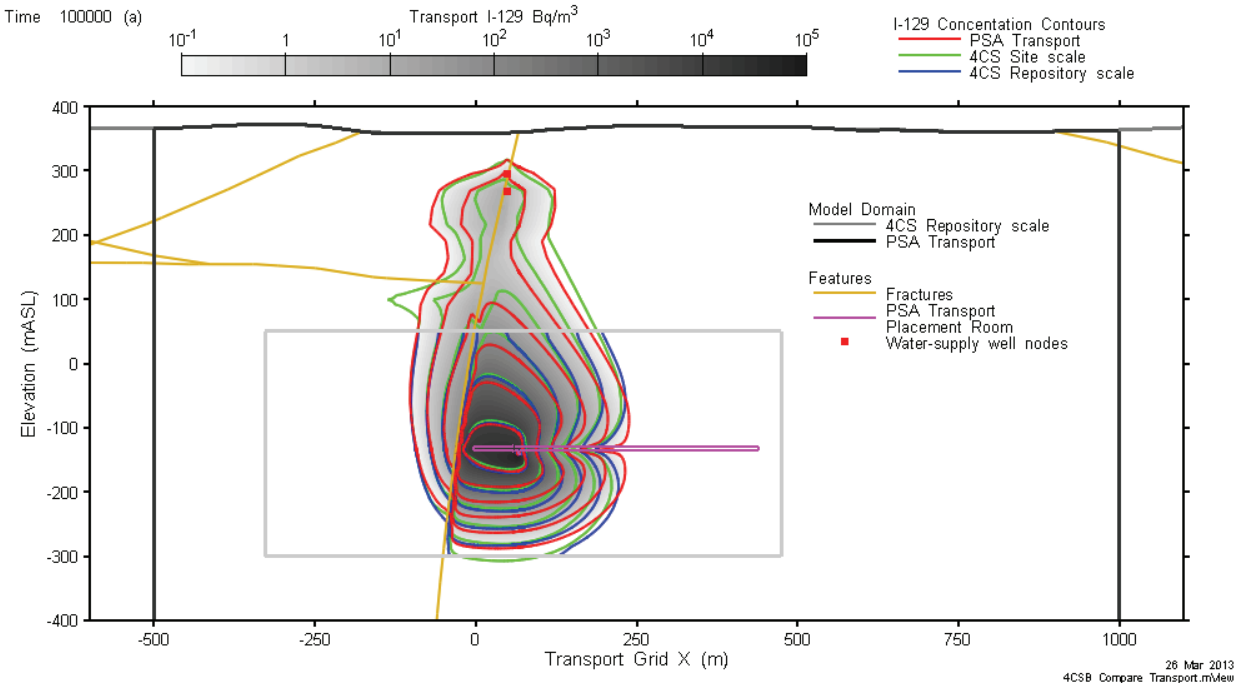

Figure 4.10: PSA Transport Model – I-129 Comparison – Vertical Cross-Section View

Transport at the system metric points (Figure 4.2, Figure 4.6, and Figure 4.7) are compared in Figure 4.11. Results compare very well at all points except for surface discharge, where the PSA Transport model predicts a slightly earlier arrival time. The PSA Transport model captures slightly less transport at the well (peak 1540 Bq/a at 107 ka) than the site scale model (peak

1674 Bq/a at 102.5 ka). The portion of the plume not captured by the well continues on to the surface, which may account for the differences in surface transport between 100 ka and 300 ka. Additionally, the surface discharge zones for the site scale model include areas outside the PSA transport model domain which show transport at late times (the peak at 600 ka and elevated beyond). Corresponding PSA model transport is not accounted for in the figure as it exits the model through the vertical boundaries.

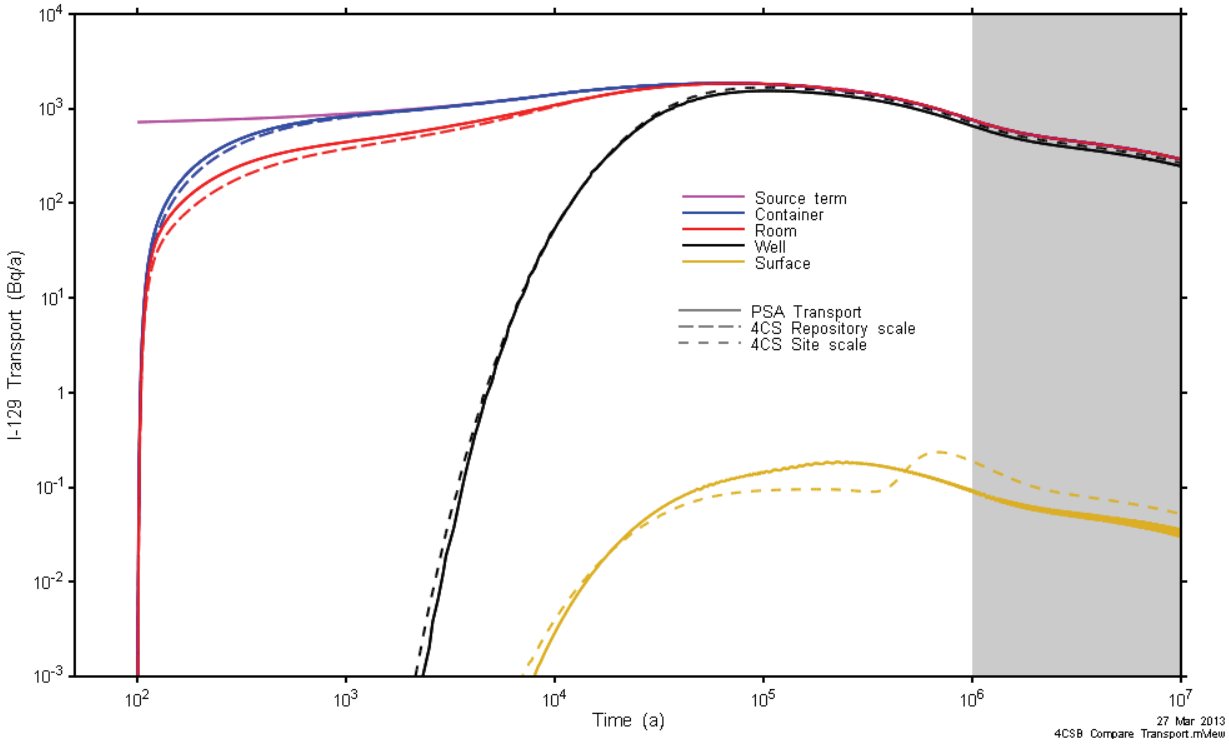

Figure 4.11: PSA Transport Model – I-129 Transport Comparison

The deterministic results indicate that the single PSA Transport model effectively combines the important attributes of the 4CS Site-scale and Repository-scale transport models.

4.6 PROBABILISTIC PARAMETERIZATION

The probabilistic parameterization for the PSA Transport model follows an approach consistent with that described for the PSA Flow model. With one exception, parameters common to both models (bedrock and fracture hydraulic conductivity and porosity) are implemented identically and are not further described in this section. The distribution for intermediate bedrock hydraulic conductivity was shifted by a factor of 10 to reflect the lower permeabilities required for the west well to be the shortest path, and to also better reflect the likely properties an actual candidate site. The minimum and maximum for the log uniform distribution were set to 1E-13 m/s and 1E-09 m/s respectively. Additional parameters for the PSA Transport model consist of those required to describe repository EDZ and EBS, which are not included in the PSA Flow model, and I-129 transport parameters for the intact rock.

There are three EDZ zones: the inner and outer EDZ surrounding the drift and placement room and the thermal (or highly) damaged zone (HDZ) which is limited to a zone below the placement room floor and surrounding the container EBS (see Figure 4.4). EDZ zone hydraulic conductivities are defined by multipliers of the intact bedrock conductivity. Inner EDZ and HDZ

porosities are also specified using multipliers. Outer EDZ porosity is the same as the intact rock. All EDZ D_e are initially set to sampled intact rock D_e but are then adjusted by the porosity multiplier for inner EDZ and HDZ. There are six EBS components (see Figure 4.4 and Figure 4.3):

1. Compacted bentonite (CB) blocks used in the room seal
2. Homogenized backfill (HBF) bentonite used in room backfill
3. Concrete (CONC) concrete bulkhead providing mechanical integrity to seal
4. Gap fill (GF) used to seal zone between CB and tunnel wall
5. 70C Compacted Bentonite (CB70) – compacted bentonite surrounding container, properties assumed to be modified by container heat.
6. Dense backfill (DBF) bentonite sand mixture used to seal tunnels and access drifts

Isotropic hydraulic conductivities for each EBS material are sampled. Porosities are fixed at 4CS reference case values. Diffusion coefficients are set to property specific 4CS Reference Case D_e, but are then adjusted with a sampled multiplier common to all EBS materials. Dispersivities for EDZ and EBS are sampled separately from intact rock dispersivities to account for the potentially shorter direct transport path from defective container to water-supply well. A common sampled dispersivity is used for all EDZ and EBS properties. Sampled EDZ and EBS parameters are given in Table 4.1. All geosphere flow parameters remain as described in Table 3.1.

Table 4.1: PSA Transport Model Additional Parameters and Distributions

Group	Parameter	4CS RC Value	Distribution
Outer EDZ	Hydraulic Conductivity	4E-10 m/s	Multiplier on intermediate bedrock value, Log-uniform, Min 2, Max 20
Inner EDZ	Hydraulic Conductivity	2E-09 m/s	Multiplier on intermediate bedrock value, Log-uniform, Min 20, Max 1000
	Porosity	0.006	Multiplier on intermediate bedrock value, Uniform, Min 1, Max 4
HDZ	Hydraulic Conductivity	4E-07 m/s	Multiplier on intermediate bedrock value, Log-uniform, Min 1000, Max 100000
	Porosity	0.006	Same multiplier as Inner EDZ
CB	Hydraulic Conductivity	1.3E-13 m/s	Log-uniform, Min 1E-14, Max 1E-12
HBF	Hydraulic Conductivity	1.8E-11 m/s	Log-uniform, Min 1E-13, Max 1E-10
CONC	Hydraulic Conductivity	1.0E-10 m/s	Log-uniform, Min 1E-12, Max 1E-08
GF	Hydraulic Conductivity	3.7E-13 m/s	Log-uniform, Min 1E-14, Max 1E-11
CB70	Hydraulic Conductivity	3.4E-13 m/s	Log-uniform, Min 1E-14, Max 1E-12
DBF	Hydraulic Conductivity	8.8E-11 m/s	Log-uniform, Min 1E-12, Max 1E-09
Rock	Longitudinal Dispersivity	20 m	Uniform, Min 20m, Max 40 m
	Transverse Dispersivity	2 m	Calculated, 10% of longitudinal

Group	Parameter	4CS RC Value	Distribution
	D_e	4E-13 m^2/s	Log-uniform, Min 1E-13, Max 1E-11
EBS and EDZ	Longitudinal Dispersivity	10 m	Uniform, Min 10m, Max 20 m
	Transverse Dispersivity	1 m	Calculated, 10% of longitudinal
EBS	D_e Multiplier	n/a	Log-uniform, Min 0.1, max 10

4.7 PROBABILISTIC IMPLEMENTATION

The 3D PSA workflow is similar to that described in Section 3.6 for the PSA Flow model, with additional steps for the PSA Transport model, as described in Table 4.2. As stated previously, flow model MLE calculations are not performed.

Table 4.2: PSA Transport Model Workflow

Workflow Step	Configuration	Description
Sample	n/a	Write variable file sample.var in the processor instance directory.
Pre-Process PSA Flow	UpdateBaseProps	Reads sample.var and substitutes variable values into mView property structure. Calculates multiplier properties. Writes mView case property file and FRAC3DVS material property file in flow model processor instance directory.
	EPM_FracSetup	Reads mView case property file and sample.var. Performs EPM calculations. Writes FRAC3DVS element K and porosity files for all fracture elements in flow model processor instance directory.
	SetWellRate	Reads sample.var and template file to perform variable substitution on well rate. Write well.include file in processor instance directory.
Execute PSA Flow	pref3d_130.exe	Execute FRAC3DVS preprocessor
	f3dopg_130.exe	Execute FRAC3DVS simulator (maximum 9999 flow solver iterations)
Post-Process PSA Flow	Convert	Reads FRAC3DVS output in processor instance directory Converts head to mView format Extracts processor execution stats (iteration count for flow) table
	Process	Reads mView results file Extracts heads at well node locations, Calculates well head Writes text file table.
	Import results	Reads well head tables and flow model iteration data
Pre-Process PSA Transport	UpdateBaseProps	Reads sample.var and substitutes variable values into mView property structure. Calculates multiplier properties. Writes mView case property file and FRAC3DVS material property file in transport model processor instance

Workflow Step	Configuration	Description
		directory.
	EPM_FracSetup	Reads mView case property file and sample.var. Performs EPM calculations. Writes FRAC3DVS element K and porosity files for all fracture elements in processor instance directory.
	SetWellRate	Reads sample.var and template file to perform variable substitution on well rate. Writes well.include file in transport model processor instance directory. Note: the same sampled well rate is used for PSA Flow and PSA Transport models to ensure flow field consistency.
	SetHeadBC	Reads PSA Flow model heads and interpolates on to vertical boundary of PSA Transport model
Execute PSA Transport	pref3d_130.exe	Execute FRAC3DVS preprocessor
	f3dopg_130.exe	Execute FRAC3DVS simulator. Flow matrix solution is limited to 9999 iterations. Simulation execution time is limited to a 24 hour maximum.
Post-Process PSA Transport	Convert	Converts well concentration and mass transport rates results to transport metric tables, assuming unit well flow rate. Converts head to mView format. Converts processor execution stats (iteration count for flow and transport).
	Process	Reads mView head file, Calculates well head. Reads well activity table and multiplies by sampled well rate to create well transport table. Writes text file tables with well head and well transport.
	Save results	Reads zone transport, well transport, well head and iteration count data Adds Flow and Transport processor instance and execution times to realization result table Adds Flow and Transport well head results to realization results table Extracts peak well transport time and value, transport at 1E4 and 1E5 a, and adds to results table Adds well and zone transport time series to realization time series output

5. PROBABILISTIC SIMULATIONS AND ASSESSMENT

Three separate PSA simulations were performed:

1. Full Probabilistic – 500 realizations of the PSA transport model with all parameters sampled according to the distributions in Table 3.1 and Table 4.1. These simulations allow for a full assessment of system response.

2. Median Geosphere – 250 realizations with geosphere parameters and well rate set fixed to median values. These simulations removed geosphere variability and allowed for determination of the impact of repository related variables.

3. Median Geosphere and EDZ – 250 realizations with geosphere, well rate, and EDZ parameters set to median values. The simulations are used to assess EBS related variables.

In addition to scatter plots, visual presentations of results include horsetail plots of transport. Horsetail plot results are compared to the PSA Median Input Case, a single deterministic run with all sampled variables set to median values. Table 5.1 compares 4CS Reference Case and PSA Median Input Case parameter values. The PSA Median Input Case results are less conservative than the 4CS Reference Case variable simulations as shown in Figure 5.1.

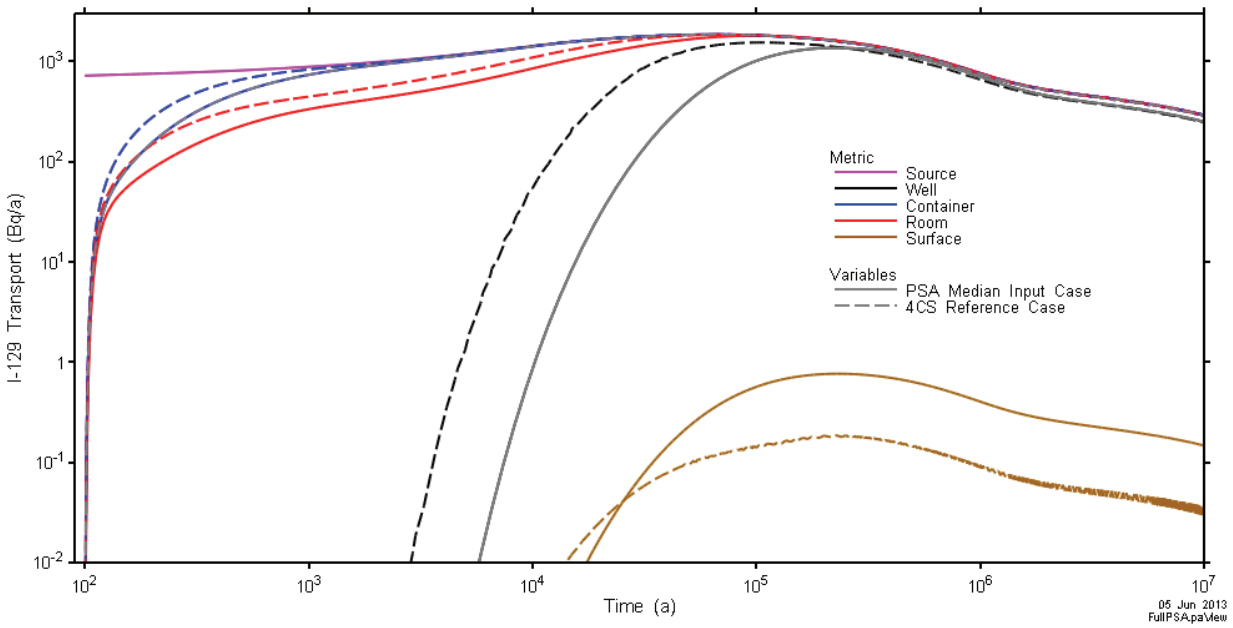

Figure 5.1: PSA Transport Model – 4CS Reference Case vs PSA Median Input Case I-129 Transport Comparison

The peak well and surface transport and the time of peak are single valued metrics that are used as dependent variables in regression analyses. Graphical results for these metrics are also presented in terms of CDFs and scatter plots.

Table 5.1: PSA Model Parameters – Comparison of Reference 4CS Case and Median Input Case Values

Group	Parameter	4CS Reference Case Value	PSA Median Input Case Values
Shallow Bedrock	Hydraulic Conductivity (m/s)	2.00E-09	1.41E-10
	Porosity(-)	3.00E-03	9.00E-03
	Fracture Hydraulic Conductivity (m/s)	1.00E-06	3.16E-06
	D_e (m^2/s)	6.00E-12	3.00E-12
Intermediate Bedrock	Hydraulic Conductivity	4.00E-11	1E-11 m/s
	Porosity (-)	3.00E-03	3.00E-03
	Fracture Hydraulic Conductivity (m/s)	1.00E-06	1E-06
	D_e (m^2/s)	3.59E-13	1.00E-12
Deep Bedrock	Hydraulic Conductivity (m/s)	1.00E-11	7.07E-13
	Porosity (-)	3.00E-03	1.65E-03
	Fracture Hydraulic Conductivity (m/s)	1.00E-06	1.00E-07
	D_e (m^2/s)	3.59E-13	5.50E-13
All Bedrock	Fracture Porosity (-)	0.10	0.10
	Well Rate (m^3/a)	911	1250
	Longitudinal Dispersivity (m)	20	30
	Transverse Dispersivity (m)	2	3
Outer EDZ	Hydraulic Conductivity (m/s)	4.00E-10	6.32E-11
Inner EDZ	Hydraulic Conductivity (m/s)	2.00E-09	1.41E-09
	Porosity (-)	6.00E-03	7.50E-03
HDZ	Hydraulic Conductivity (m/s)	4.00E-07	1.00E-07
	Porosity (-)	6.00E-03	7.50E-03
CB	Hydraulic Conductivity (m/s)	1.30E-13	1.00E-13
	D_e (m^2/s)	1.10E-11	1.10E-11
HBF	Hydraulic Conductivity (m/s)	1.80E-11	3.16E-12
	D_e (m^2/s)	4.20E-12	4.20E-12
CONC	Hydraulic Conductivity (m/s)	1.00E-10	1.00E-10
	D_e (m^2/s)	1.25E-10	1.25E-10
GF	Hydraulic Conductivity (m/s)	3.70E-13	3.16E-13
	D_e (m^2/s)	1.10E-11	1.10E-11
CB70	Hydraulic Conductivity (m/s)	3.40E-13	1.00E-13
	D_e (m^2/s)	3.00E-11	3.00E-11
DBF	Hydraulic Conductivity (m/s)	8.80E-11	3.16E-11
	D_e (m^2/s)	4.20E-12	4.20E-12
EBS and EDZ	Longitudinal Dispersivity (m)	10	15
	Transverse Dispersivity (m)	1	1.5

5.1 FULL PROBABILISTIC SIMULATIONS

The “Full” assessment was conducted with 500 realizations, simulated using a total of 46 cores on three server boards. Fifteen cores on each machine were involved in active computation, while a sixteenth core on one board serviced the paCalcX master.

Transport simulations were executed in finite-difference mode with FRAC3DVS-OPG. This reduced the memory footprint significantly, to a maximum of 3.43 GB for a short period during the operation of the pre-processor with 2.6 GB required on average. By delaying the initial start times of consecutive simulations by 30 seconds a full 15 cores could be used per server board. Total elapsed real time was 4.9 days, with total processor time of 4915 processor hours. Individual realization execution time ranged from 5.16 hours to 26.4 hours, with an average time of 9.83 hours. Execution of the PSA Transport model (Execute PSA Transport/f3dopg_130.exe in Table 4.2) dominated total realization time (Figure 5.2). The longest times include four cases that were terminated after the transport simulation had been executing for 24 hours. Model execution times are at least partially affected by the transport matrix convergence criteria. Values used in this assessment (1E-16) were in the mid range of those determined suitable in 4CS numeric sensitivity assessments. Increasing convergence factor to the upper end of the 4CS range (1E-12) may reduce overall execution time at the possible expense of increased oscillations in surface transport.

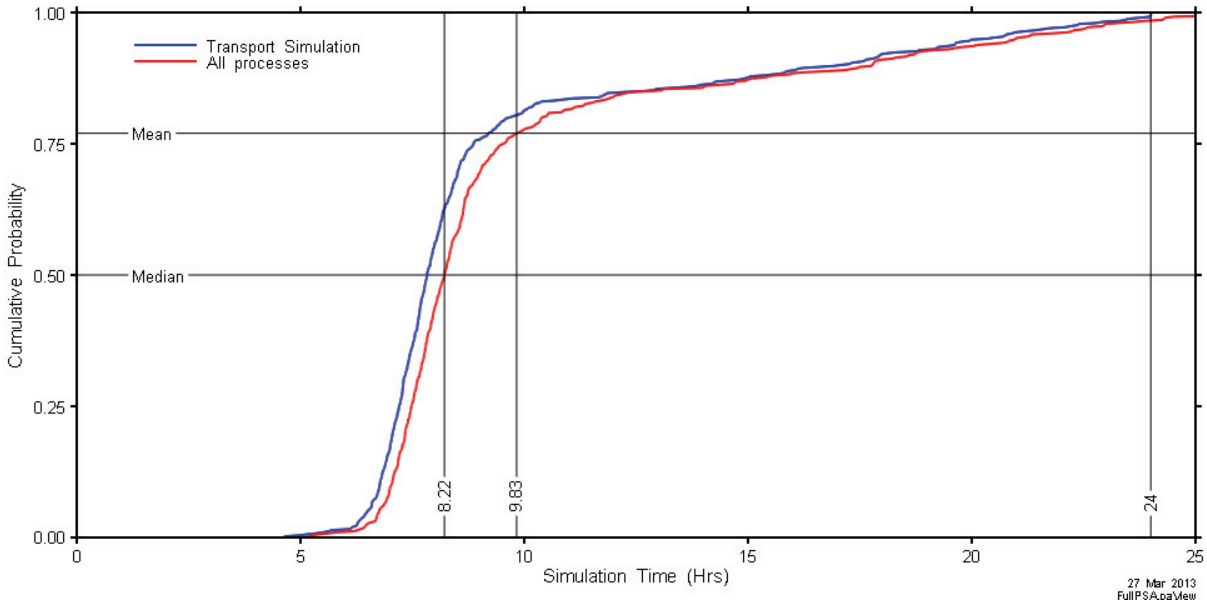

Figure 5.2: Full PSA – Execution Time CDF

5.1.1 Realization Selection

The initial 500 realizations were reduced to remove four cases of flow convergence failure in the transport model, 21 cases with negative well head in the transport model, and an additional four cases with oscillations in the surface mass flux response as indicated on Figure 5.3.

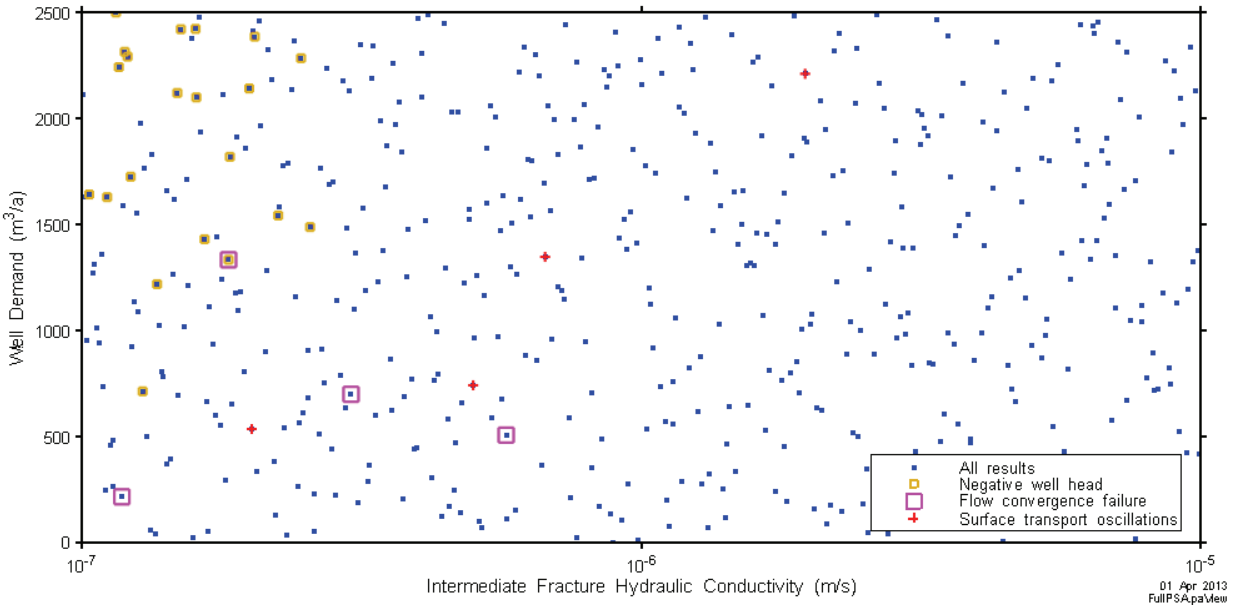

Figure 5.3: Full PSA– Well Rate vs Intermediate Rock Fracture Hydraulic Conductivity Scatter plot with Numeric Failure Cases

Interestingly, there were no flow convergence failures in the associated PSA Flow model simulations. This is probably due to the use of the finite-difference solution approach, which, in our previous experience, has generally been more robust numerically than full finite-element mode. The PSA Flow and PSA Transport models also showed some variance in well head calculations (Figure 5.4), with the PSA Transport model generally predicting slightly lower draw down in the water supply well. This is due to the reduced fracture element grid size in the PSA transport model. The finer mesh results in fracture properties being averaged over a smaller grid block area and volume. This has the effect of increasing the effective porous medium permeability of the fracture blocks connected to the 1D well element, with the result of reduced drawdown at the well. This causes a smaller number of realizations with negative well heads as compared to the PSA Flow model. It should be noted that the drawdown due to the well decreases rapidly with increasing distance from the well nodes and has very little effect on transport occurring within the fracture and intact rock outside the immediate vicinity of the well.

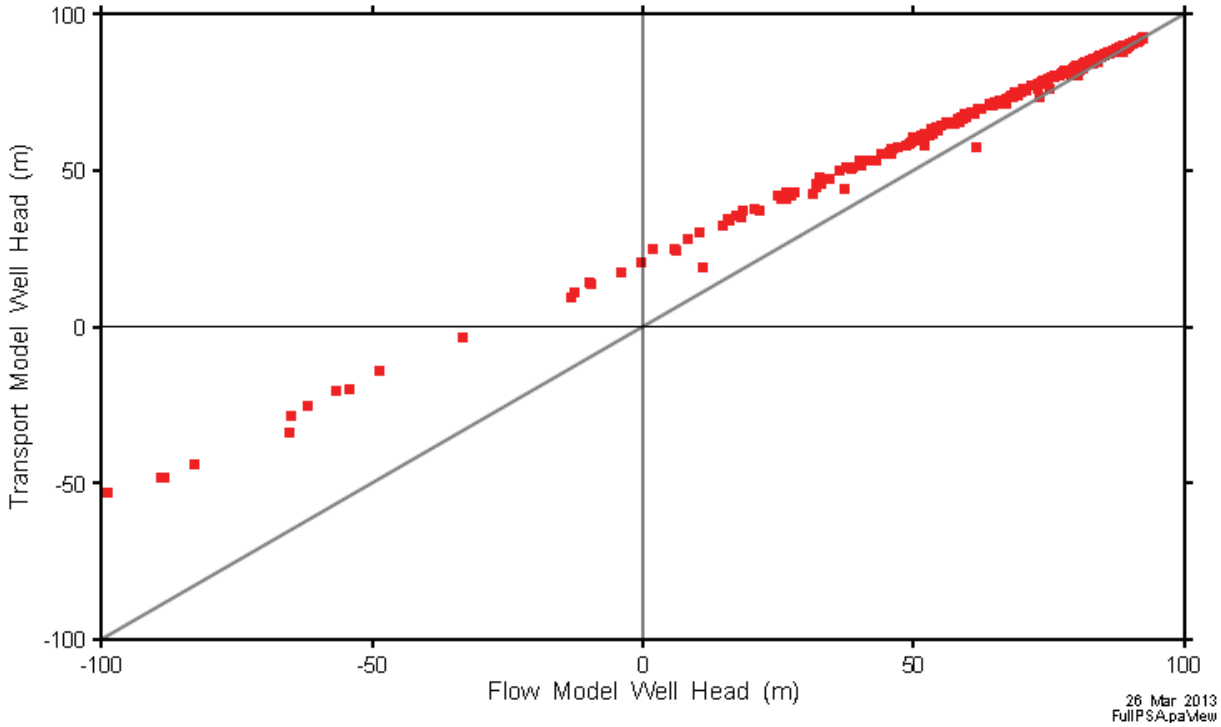

Figure 5.4: Well Head Comparison - PSA Transport vs PSA Flow

Transport results at the container and well for the failure cases are presented in Figure 5.5. With one obvious exception, results for Container, Room, and Well transport do not look anomalous. The case with oscillating results apparent in the Container and Room transport is associated with a flow convergence failure and negative well head. Reviewing the specific parameters for the realization has yet to provide any insight into the cause of the problem. There was also no apparent significant correlation of the surface oscillation cases with any parameters. Cases with any of the three failure modes (flow convergence, negative well head, surface oscillations) have been removed from all assessments presented in this section.

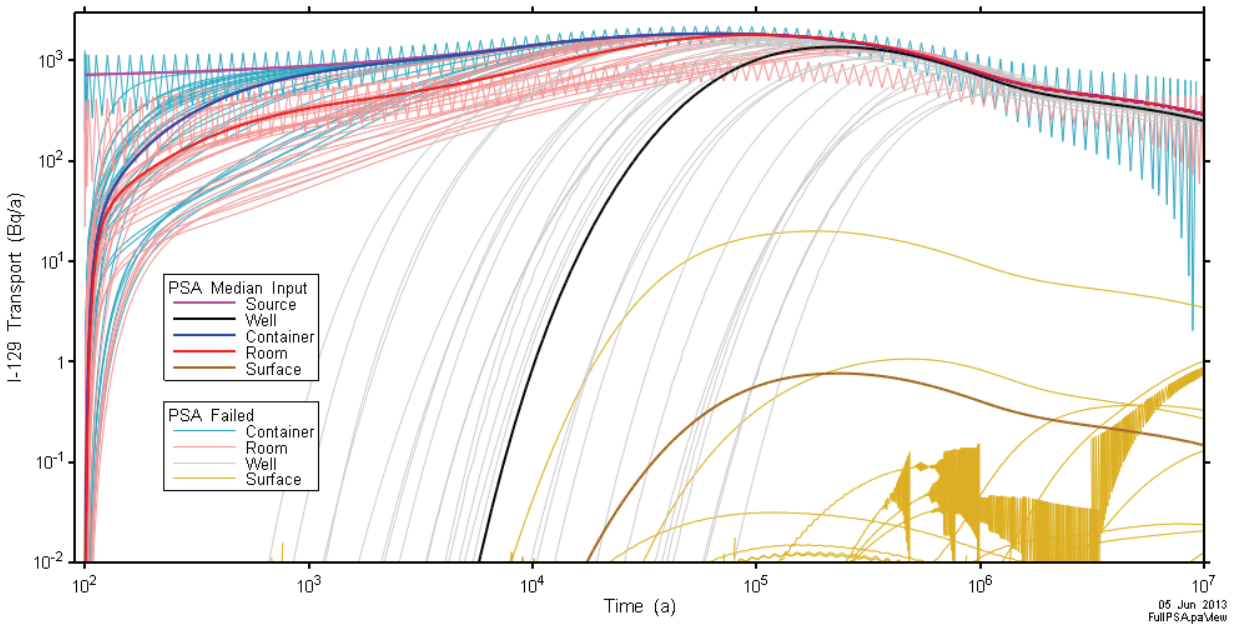

Figure 5.5: Full PSA – I-129 Transport - Flow convergence Failure, Negative Well Head, and Surface Oscillation Cases.

5.1.2 Graphical Assessment

Transport results for each metric with failed realizations removed are shown in Figure 5.6 through Figure 5.9.

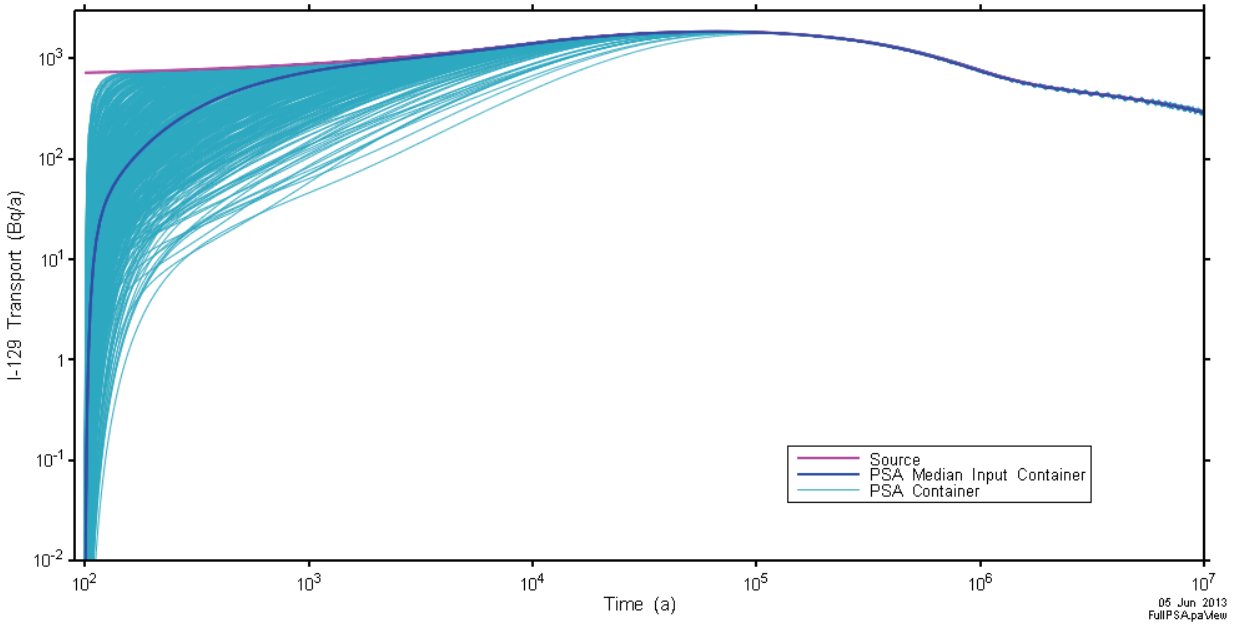

Figure 5.6: Full PSA – Container Transport

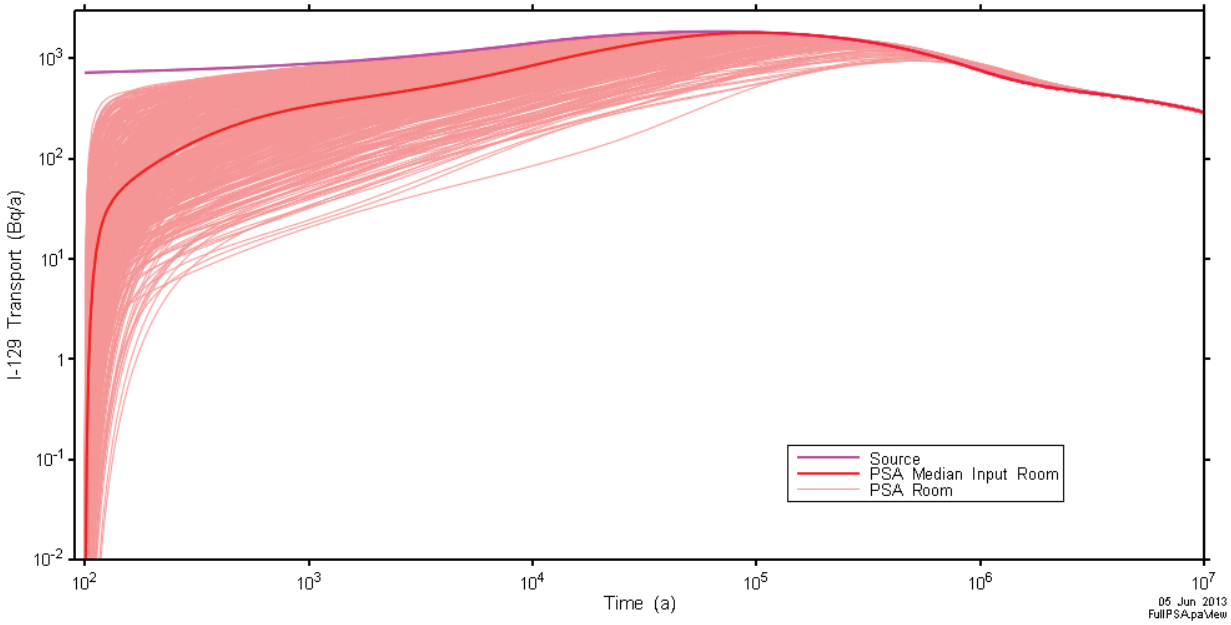

Figure 5.7: Full PSA – Room Transport

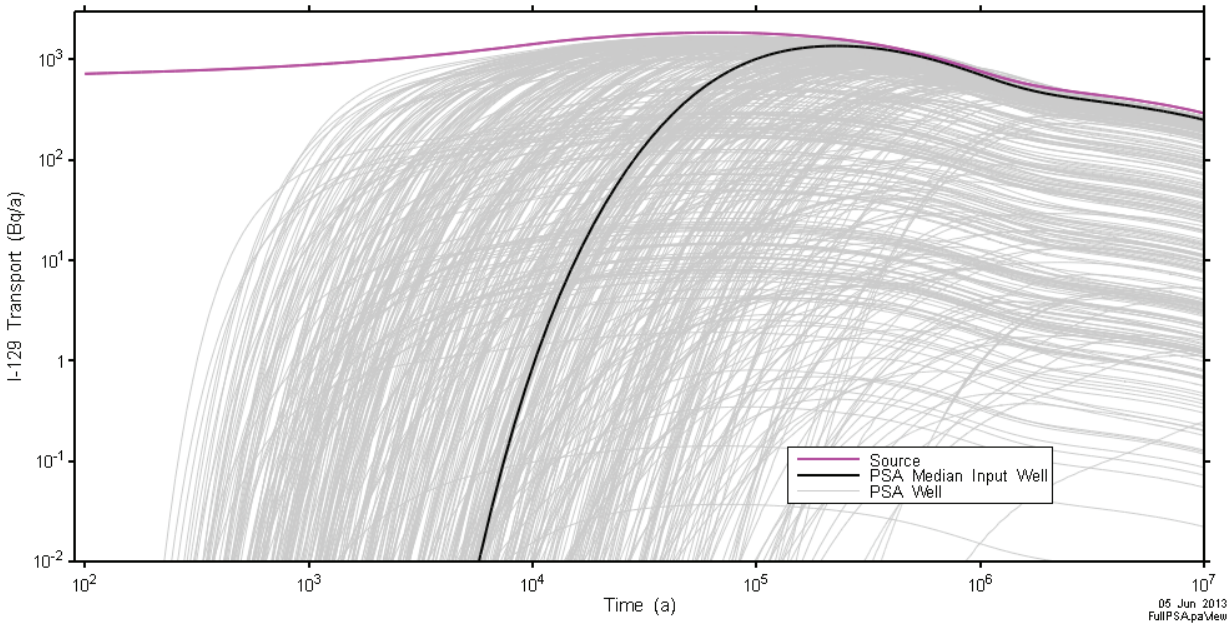

Figure 5.8: Full PSA – Well Transport

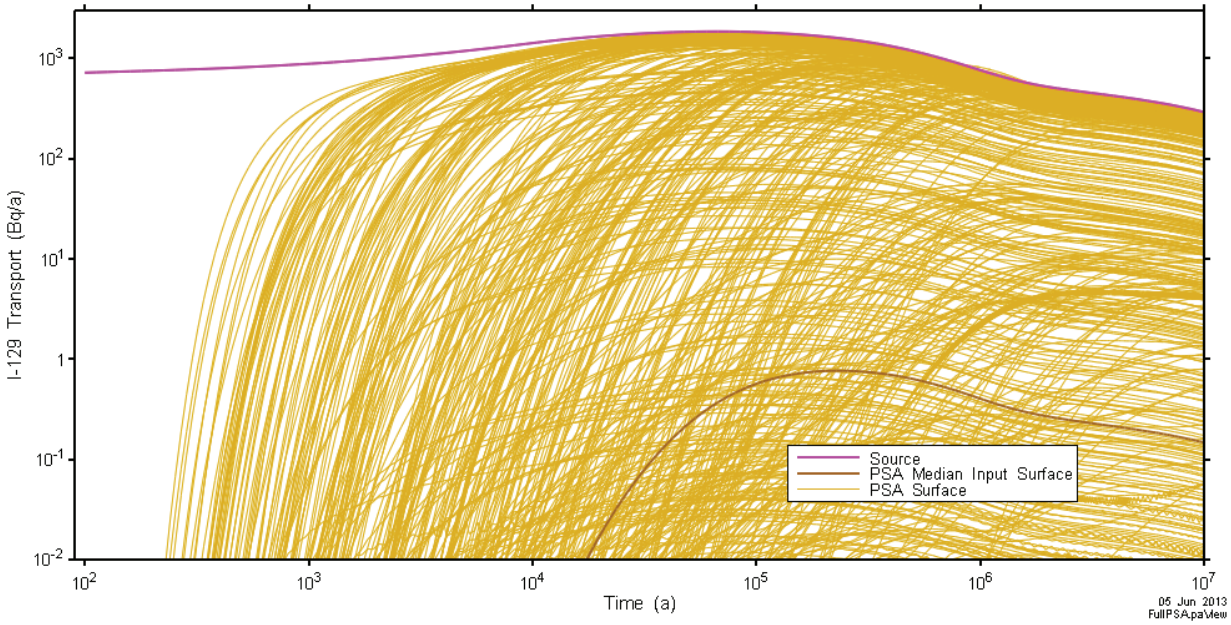

Figure 5.9: Full PSA – Surface Transport

It is clear from the horsetail plots that surface and well transport overlap. Presenting subsets of results based on well rate helps clarify the relationship. Figure 5.10 and Figure 5.11 shows combined results for the top 10% and bottom 10% well rate realizations respectively. The figures show that higher well rates results in generally higher rates of mass capture at the well and lower at surface.

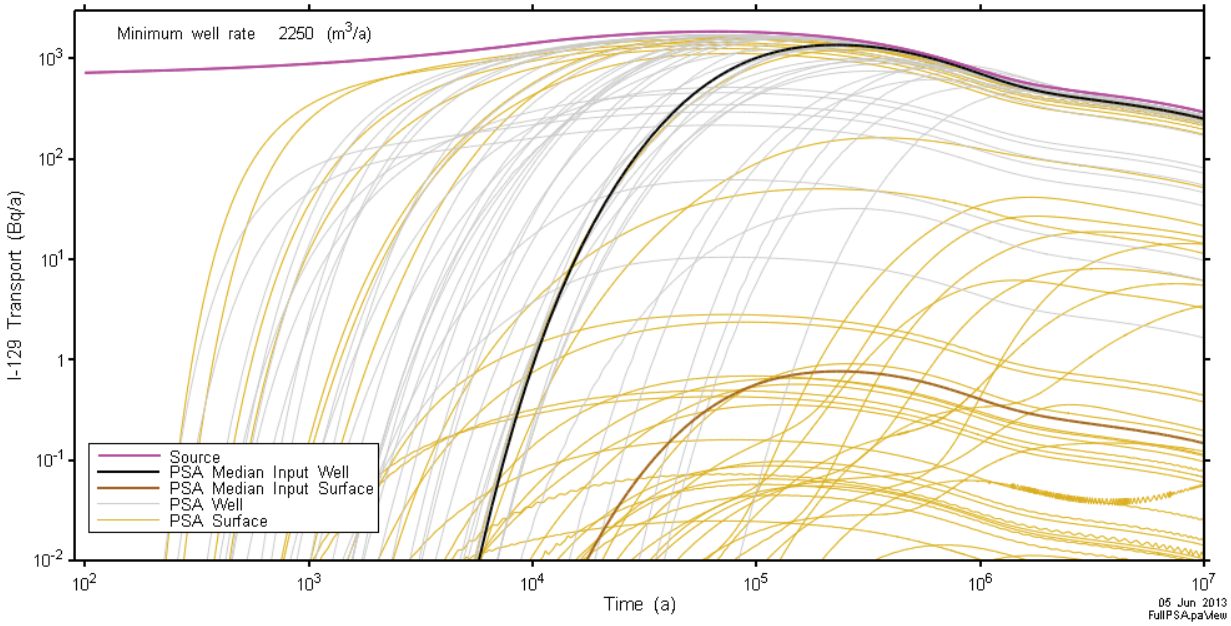

Figure 5.10: Full PSA – Surface and Well Transport for Realizations With Well Rate Greater Than 2250 m^3/a

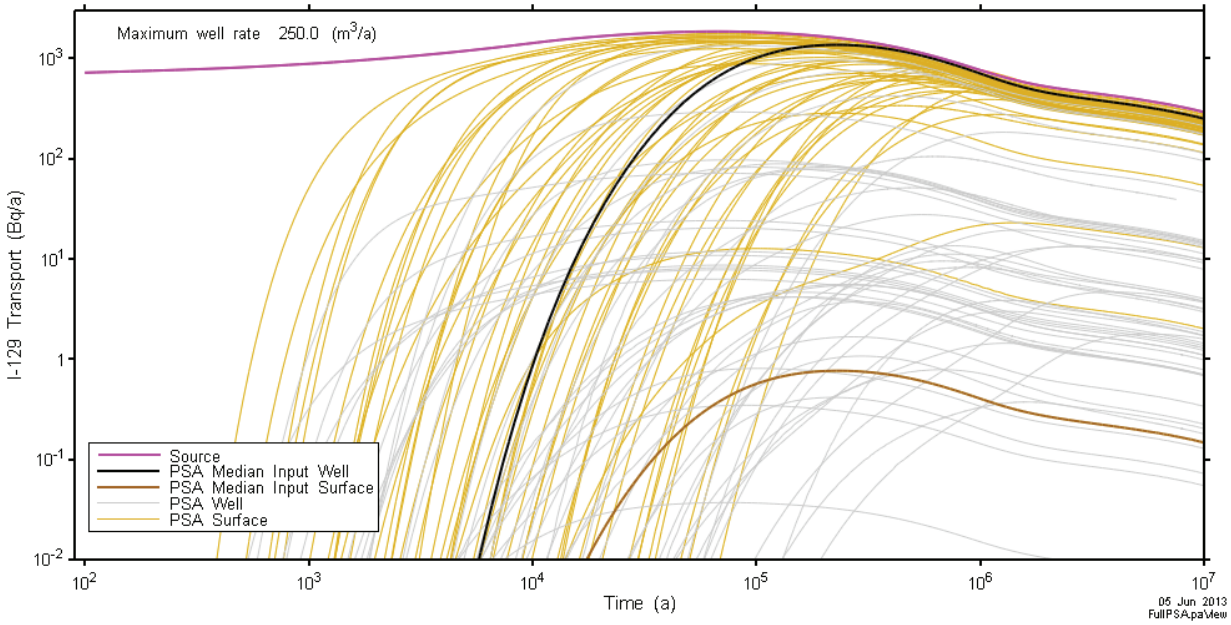

Figure 5.11: Full PSA – Surface and Well Transport for Realizations With Well Rate Less Than 250 m^3/a

Peak transport at the well will exceed that at surface in most cases, as shown by the probability distribution in Figure 5.12. The median value for peak well transport is approximately a factor of 15 larger than the median for peak surface transport.

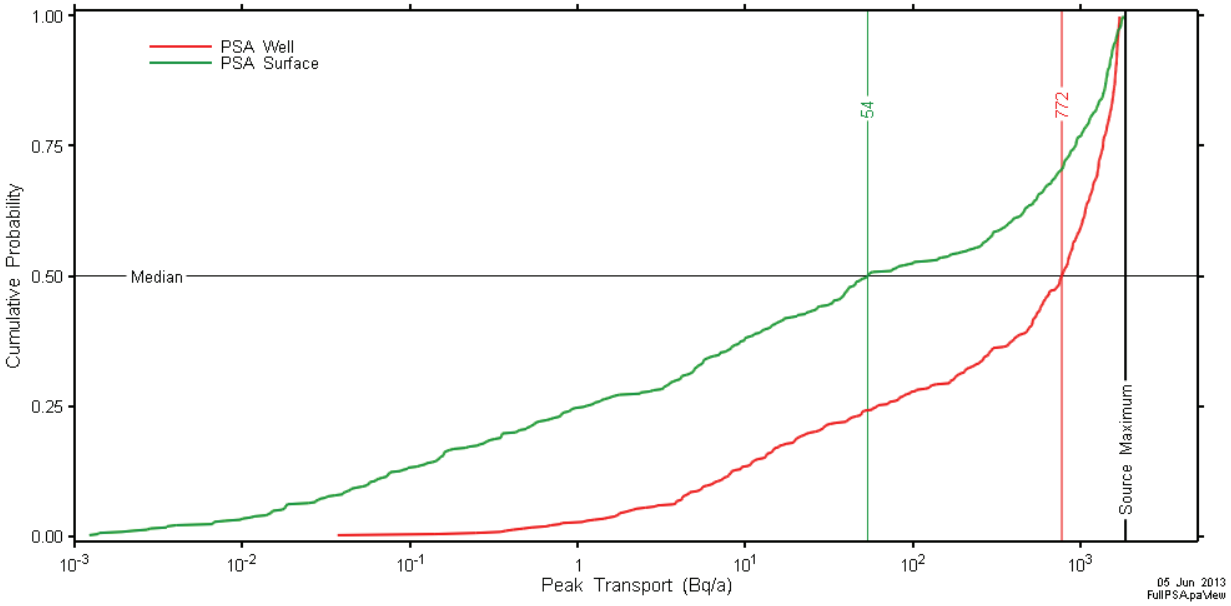

Figure 5.12: Full PSA – Surface and Well Transport Peak Value CDF

Although peak transport value at the well and surface show a wide distribution, the arrival times of the peak values are restricted to a limited range, as the source term peak time (67 ka) is delayed relative to the arrival time of meaningful transport levels. Consequently the surface and well peak time values do not fully capture the variability that is present within the results. If arrival time is defined as the time at which a specified (lower) transport rate is measured, then

the results show much greater variability and are a better representation of performance, as shown in Figure 5.13. “Well arrival” is defined as the time at which transport in the well exceeds 0.01 Bq/a, while “Surface arrival” is defined using a lower limit of 0.001 Bq/a. The difference in the thresholds reflects the generally lower values of transport at surface. All well transport results reached the 0.01 Bq/a threshold, while two surface transport results were below the 0.001 threshold. If a surface threshold of 0.01 Bq/a had been used, the results for 17 simulations would not be included.

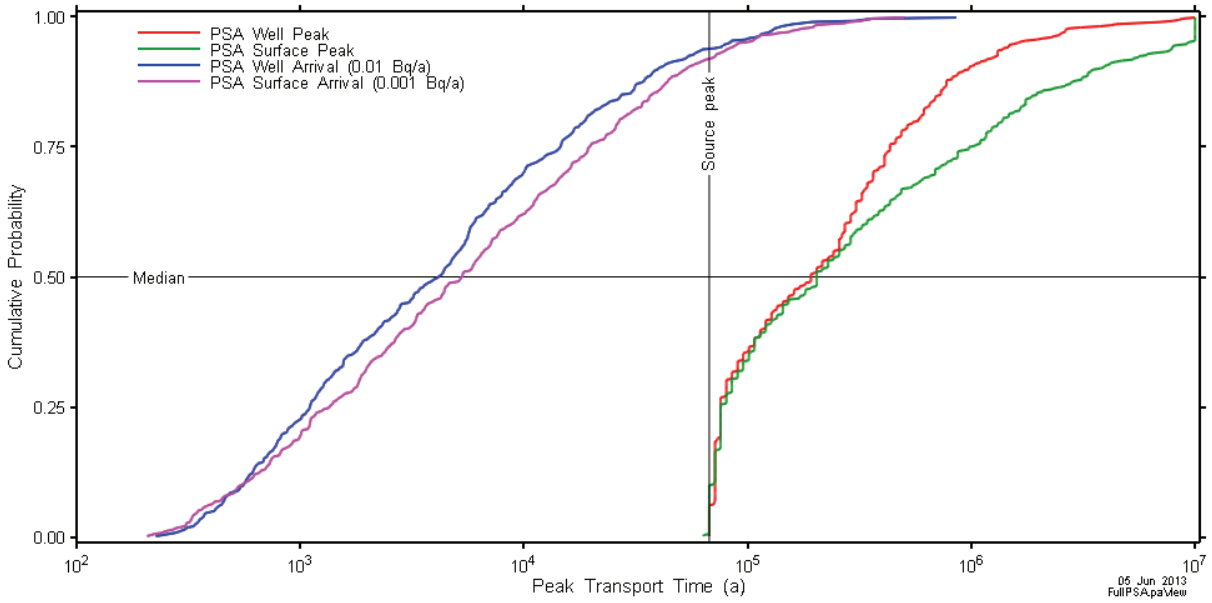

Figure 5.13: Full PSA – Surface and Well Transport Arrival Time and Peak Time CDF

5.1.3 Regression Analyses

Regression analyses were performed on samples with failed case results removed. Dependent variables analysed were: peak well value and arrival time of well transport at 0.01 Bq/a (Table 5.2), and peak surface transport value and arrival time of surface transport at 0.001 Bq/a (Table 5.3).

Table 5.2: Full PSA – Well Transport Ranked Stepwise Regression Results

Peak Transport			
Model significance (R^2)			**0.71315**
Variable	**R^2 Included**	**R^2 Deleted**	**Regression Coefficient**
INT*FRAC_K	0.31423	0.37752	-0.58069
ROCK*WellRate	0.63100	0.42725	0.53754
SHALL*FRAC_K_Mult	0.67425	0.66976	-0.20877
INT*K	0.70625	0.67982	0.18332
SHALL*K_Mult	0.71046	0.70928	-0.06244
ROCK*FRAC_Porosity	0.71315	0.71046	-0.05201

Arrival Time (0.01 Bq/a)			
Model significance (R^2)			**0.88234**
Variable	**R^2 Included**	**R^2 Deleted**	**Regression Coefficient**
INT*K	0.75594	0.14581	-0.86283
ROCK*Diffusion	0.80706	0.84182	-0.20349
ROCK*WellRate	0.83919	0.84636	-0.19240
INT*Porosity	0.85929	0.86213	0.14366
INT*FRAC_K	0.86687	0.87596	0.08077
SHALL*FRAC_K_Mult	0.87182	0.87820	0.06500
ROCK*Dispersivity	0.87540	0.87942	-0.05446
EDZ*IEDZ_K_Mult	0.87819	0.87976	-0.05150
EDZ*HDZ_K_Mult	0.88056	0.88019	-0.04674
EBS*De_Mult	0.88234	0.88056	0.04254

Table 5.3: Full PSA – Surface Transport Ranked Stepwise Regression Results

Peak Transport			
Model significance (R^2)			**0.68914**
Variable	**R^2 Included**	**R^2 Deleted**	**Regression Coefficient**
INT*FRAC_K	0.33292	0.31613	0.61417
ROCK*WellRate	0.49070	0.51932	-0.41613
INT*K	0.59289	0.58950	0.31712
SHALL*FRAC_K_Mult	0.64814	0.63507	0.23308
ROCK*Diffusion	0.66779	0.67070	0.13722
SHALL*K_Mult	0.67966	0.67924	0.10020
ROCK*Dispersivity	0.68452	0.68412	0.07128
ROCK*FRAC_Porosity	0.68914	0.68452	0.06827

Arrival Time (0.001 Bq/a)			
Model significance (R^2)			**0.89538**
Variable	**R^2 Included**	**R^2 Deleted**	**Regression Coefficient**
INT*K	0.74736	0.12350	-0.88325
INT*FRAC_K	0.80428	0.82794	-0.26215
ROCK*Diffusion	0.84638	0.85459	-0.20401
INT*Porosity	0.86626	0.87569	0.14162
ROCK*Dispersivity	0.88437	0.87952	-0.12705
ROCK*WellRate	0.88764	0.89256	0.05372
SHALL*FRAC_K_Mult	0.89056	0.89174	-0.06090
EDZ*IEDZ_K_Mult	0.89320	0.89281	-0.05136
EDZ*HDZ_K_Mult	0.89538	0.89320	-0.04703

The significance of the peak transport regression model fit is much less than that of the model for transport arrival time. Visually this is indicated in a comparison of scatter plot results shown in Figure 5.14 and Figure 5.15.

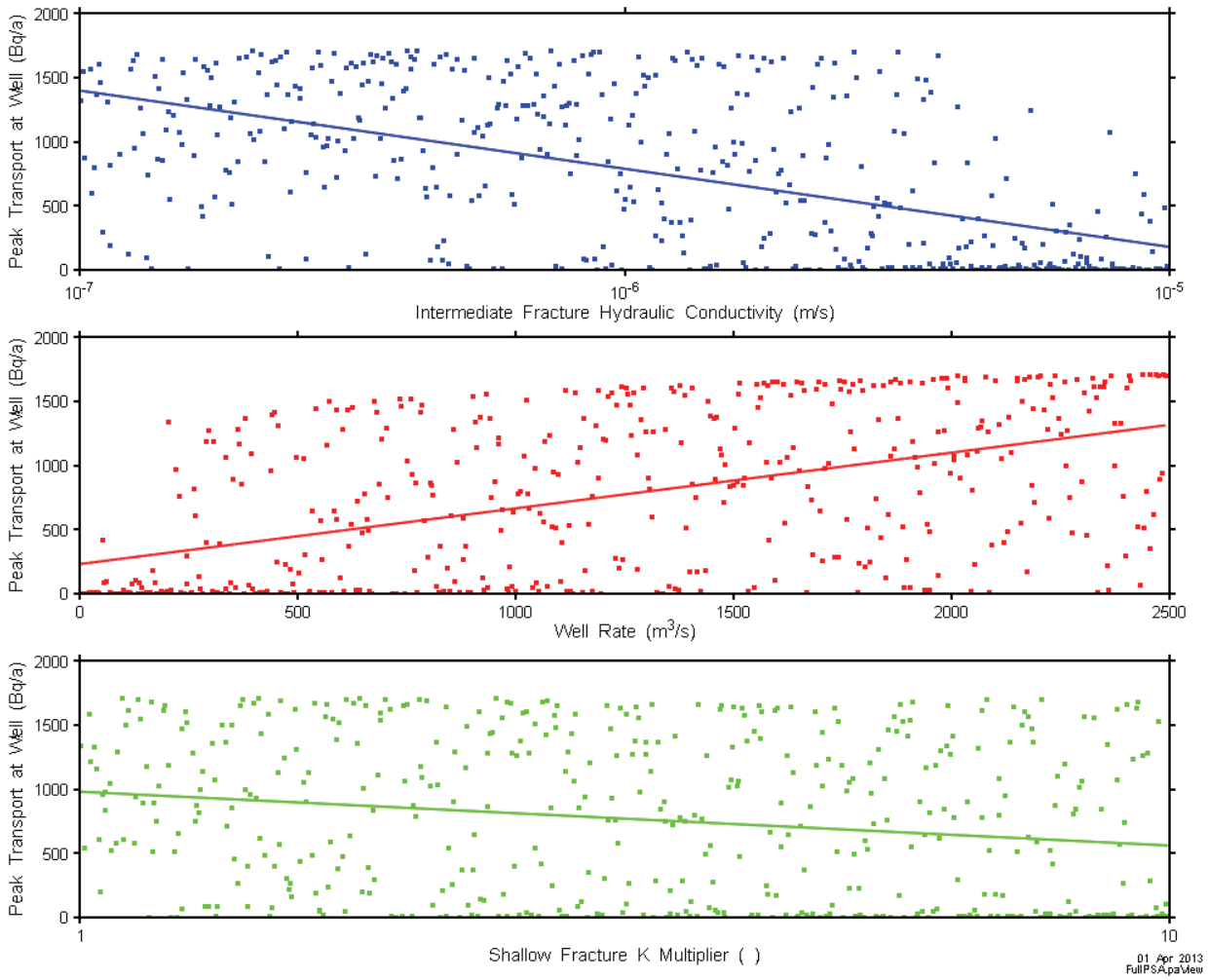

Figure 5.14: Full PSA – Scatter Plot – Peak Well Transport

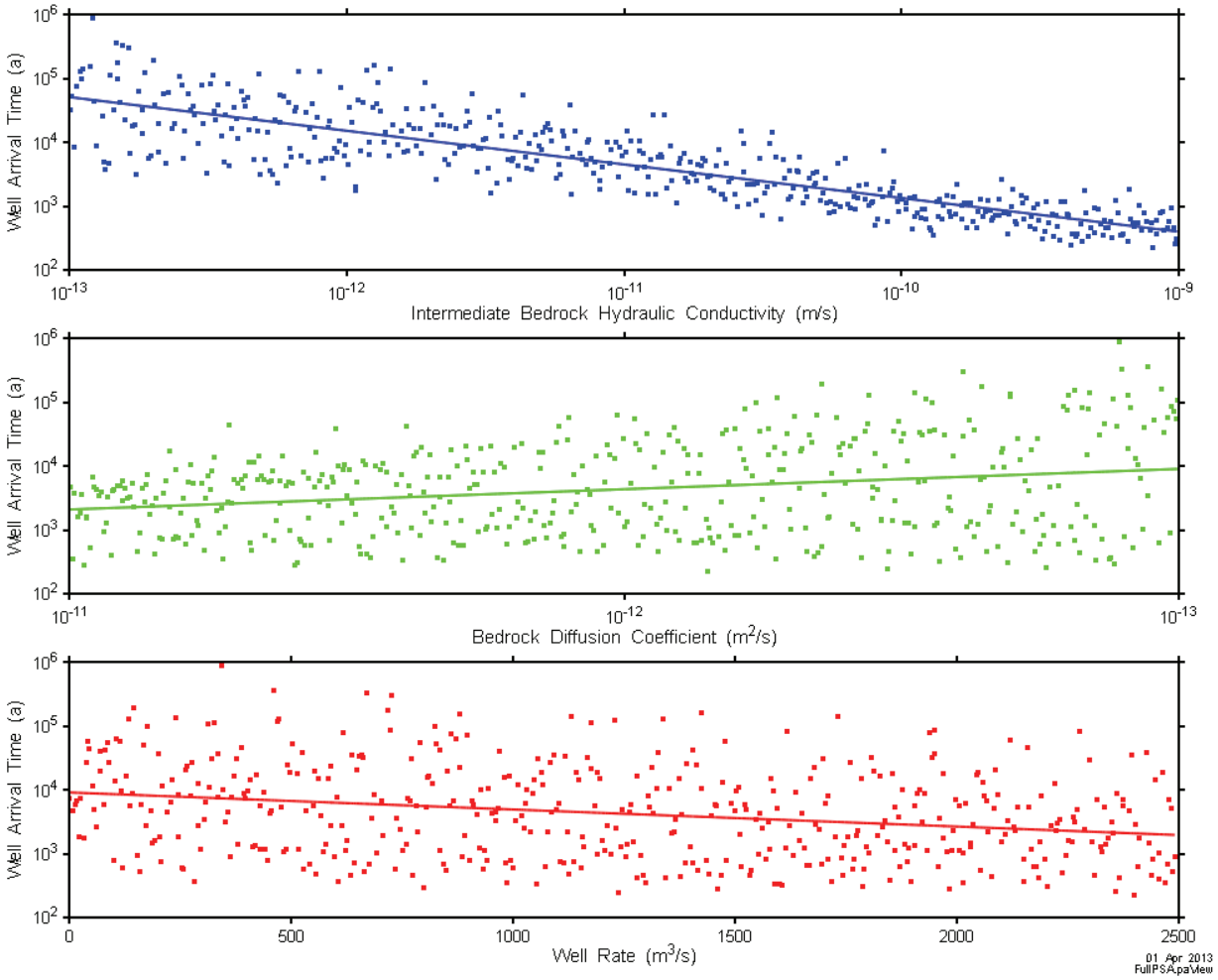

Figure 5.15: Full PSA – Scatter Plot – Well Transport Arrival (0.01 Bq/a) Time

The regression results indicate:

1. The most significant effect is the control on arrival time of well and surface transport by hydraulic conductivity of the bedrock.
2. Of lesser significance, the magnitude of peak transport is influenced by fault conductivity and well rate. Peak transport at the well is negatively correlated with fault conductivity while peak surface transport is positively correlated. High well rates increase transport to the well and low well rates increase transport to surface.
3. EDZ and EBS properties are largely irrelevant to the performance indicators.

5.1.4 CDF Stability

The PSA Transport model sampled 27 variables with 500 realizations, for a total number of realizations equal to approximately 19 times the number of sampled variables. An additional assessment was performed with 250 realizations as part of the cloud computing tests (see Section 6.2). Figure 5.16 and Figure 5.17 compare the metric CDFs for each assessment. It is clear that the cases are slightly different, although the general shape and statistics are similar, indicating that the 500 realizations are a reasonably accurate representation of system

behaviour. An additional simulation with 1000 realizations would help to confirm adequacy of sampling.

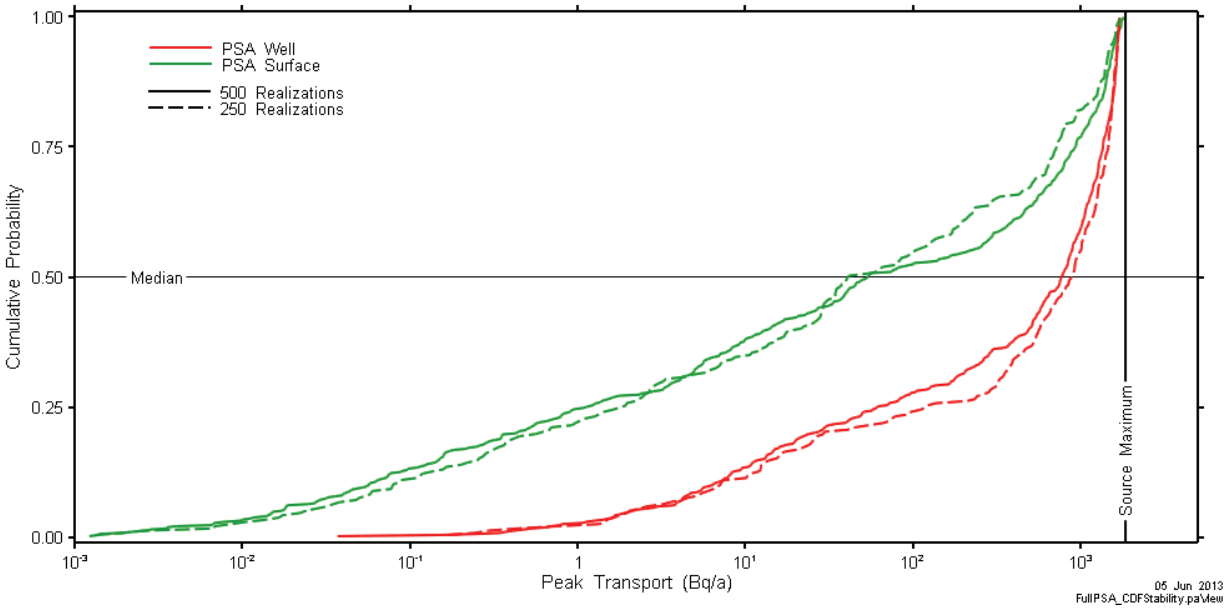

Figure 5.16: Full PSA – Surface and Well Transport Peak Value CDF Stability Comparison

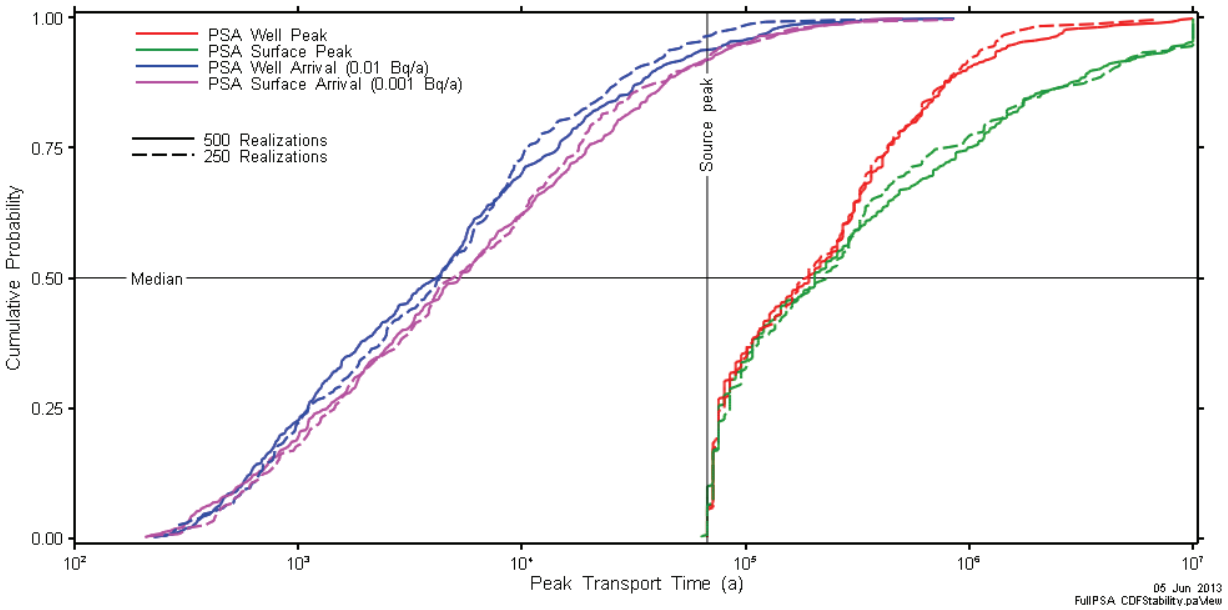

Figure 5.17: Full PSA – Surface and Well Transport Arrival Time and Peak Time CDF Stability Comparison

5.2 MEDIAN GEOSPHERE SIMULATIONS – ASSESSMENT OF EDZ AND EBS SIGNIFICANCE

The full assessment results presented in Section 5.1indicate that geosphere and well rate parameters dominate the system response. However, most of the transport specific parameters presented in Table 4.1 are related to parameterization of the room EBS and EDZ. To assess the relative impact of EDZ and EBS parameters, additional simulations were conducted with all geosphere values fixed at median. It is expected that results will show much less variability than the full transport results, but without geosphere variability it may be possible to determine, which, if any, EBS and EDZ parameters are most significant. This data may be helpful in value engineering studies on the engineered repository components, as well as providing a rationale for further repository characterization studies.

The assessment consisted of 250 realizations, simulated using a total of 31 cores on two server boards. Total elapsed real time was 3.4 days, with total processor time of 2247 processor hours. Individual realization execution time ranged from 3.69 hours to 24.19 hours. One case was terminated after the transport simulation had been executing for 24 hours.

There were two cases of flow convergence failure in the transport model (see Figure 5.18). These were removed from the analyses.

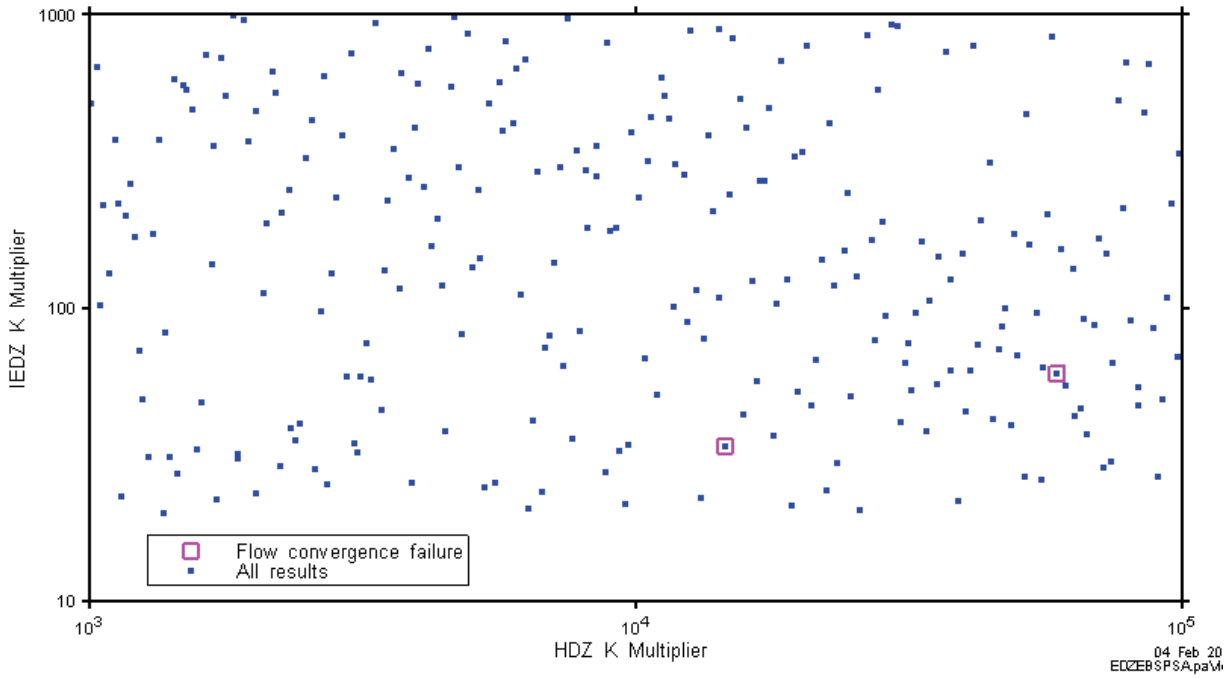

Figure 5.18: Full PSA– HDZ Multiplier vs Inner EDZ Multiplier Scatter Plot with Numeric Failure Cases

Transport results for each metric with flow convergence errors removed are shown in Figure 5.6. As expected, there is much less variation in results.

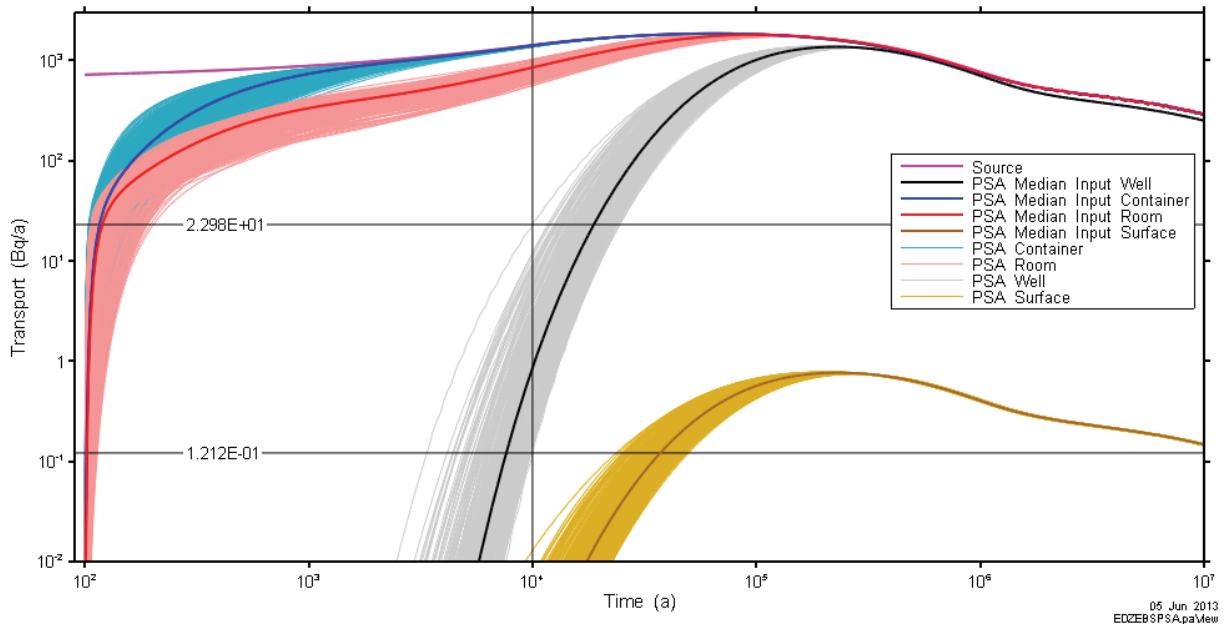

Figure 5.19: EDZ and EBS PSA –Transport Metrics

Metrics used in the Full PSA regression are not appropriate as there is essentially no variation in peak value and only small variations in arrival time. There is however, variation in well transport at early times, shown on Figure 5.19 at 10,000 years, with the CDF given in Figure 5.20.

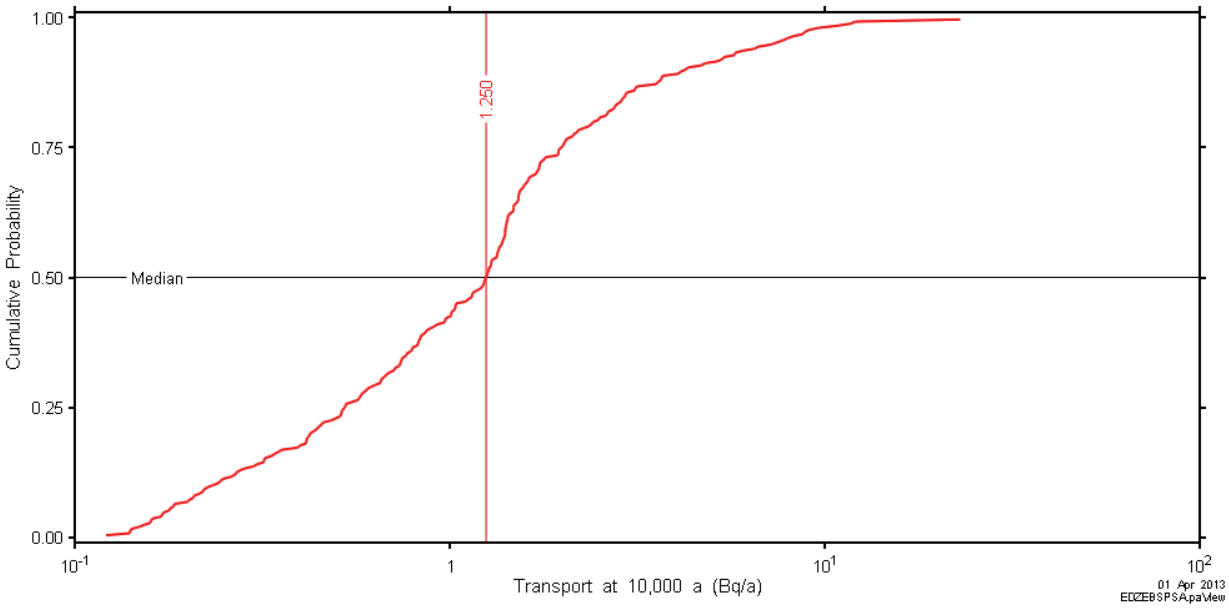

Figure 5.20: EDZ and EBS PSA – CDF of Well Transport at 10,000 a

Regression analysis of well transport at 10,000 years was performed on samples with failed flow convergence removed, and on variables with fixed geosphere values removed (Table 5.4).

Table 5.4: EDZ and EBS PSA – Well Transport at 10,000 a Ranked Stepwise Regression Results

	Model significance (R^2)		0.88093
Variable	**R^2 Included**	**R^2 Deleted**	**Regression Coefficient**
EDZ*HDZ_K_Mult	0.47750	0.30798	0.76338
EDZ*IEDZ_K_Mult	0.83157	0.52632	0.60536
EBS*De_Mult	0.86162	0.85091	-0.17437
EDZ*OEDZ_K_Mult	0.87054	0.87036	0.10414
EDZ*Dispersivity	0.87439	0.87706	0.06266
EBS*DBF K	0.87756	0.87751	-0.05916
EBS*CONC K	0.88093	0.87756	0.05836

In this case, EDZ variables are of greatest significance. The scatter plot in Figure 5.21 shows the relative significance of the three most significant variables.

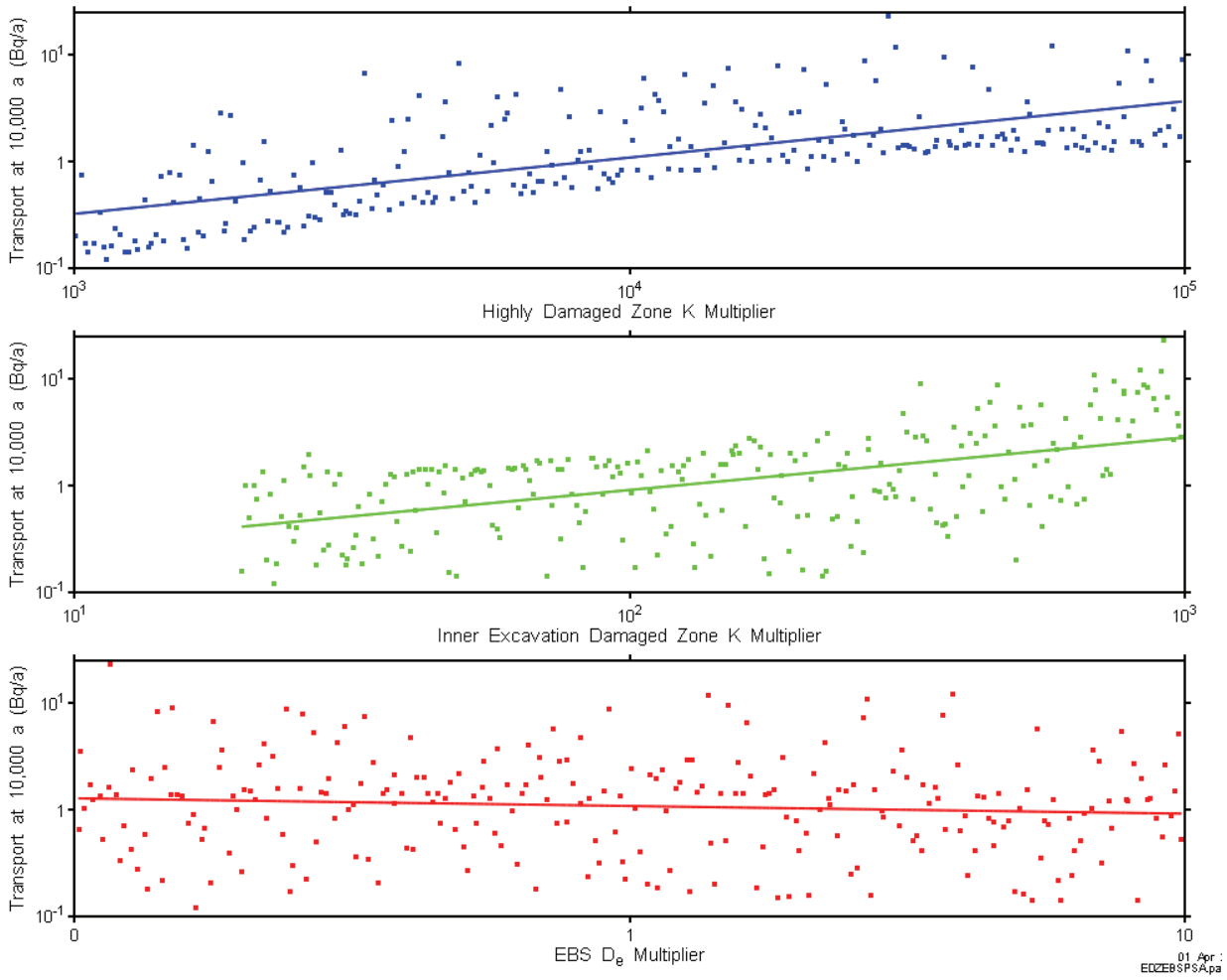

Figure 5.21: EDZ & EBS PSA – Scatter Plot – Well Transport at 10,000 a

5.3 ENHANCED EBS SIMULATIONS

A final set of simulations were performed with just room EBS variables sampled and all geosphere and EDZ variables fixed at median values. This allowed the assessment to focus only on engineered barriers. The distributions on all EBS values were modified by increasing upper limits by a factor of 10 and decreasing lower limits by the same amount, as summarized in Table 5.5.

Table 5.5: Enhanced EBS Model Parameter Distributions

Group	Parameter	Distribution
CB	Hydraulic Conductivity	Log-uniform, Min 1E-15, Max 1E-11
HBF	Hydraulic Conductivity	Log-uniform, Min 1E-15, Max 1E-09
CONC	Hydraulic Conductivity	Log-uniform, Min 1E-13, Max 1E-07
GF	Hydraulic Conductivity	Log-uniform, Min 1E-15, Max 1E-10
CB70	Hydraulic Conductivity	Log-uniform, Min 1E-15, Max 1E-11
DBF	Hydraulic Conductivity	Log-uniform, Min 1E-13, Max 1E-08
EBS	D_e Multiplier	Log-uniform, Min 0.01, max 100

The assessment consisted of 250 realizations, simulated using a total of 31 cores on two server boards. Total elapsed real time was 5.08 days, with total processor time of 3176 processor hours. Individual realization execution time ranged from 5.11 hours to 24.20 hours. In marked contrast to previous simulations, 48 cases, or nearly 20 percent, were terminated after the transport simulation had been executing for 24 hours.

There was one case with flow convergence failure, which was removed from the analyses. Transport results for each metric are shown in Figure 5.22. There is a further reduction in variation in results at the well (Figure 5.23), although room and container transport show greater variation. This is expected as these are most dependent on EBS characterization.

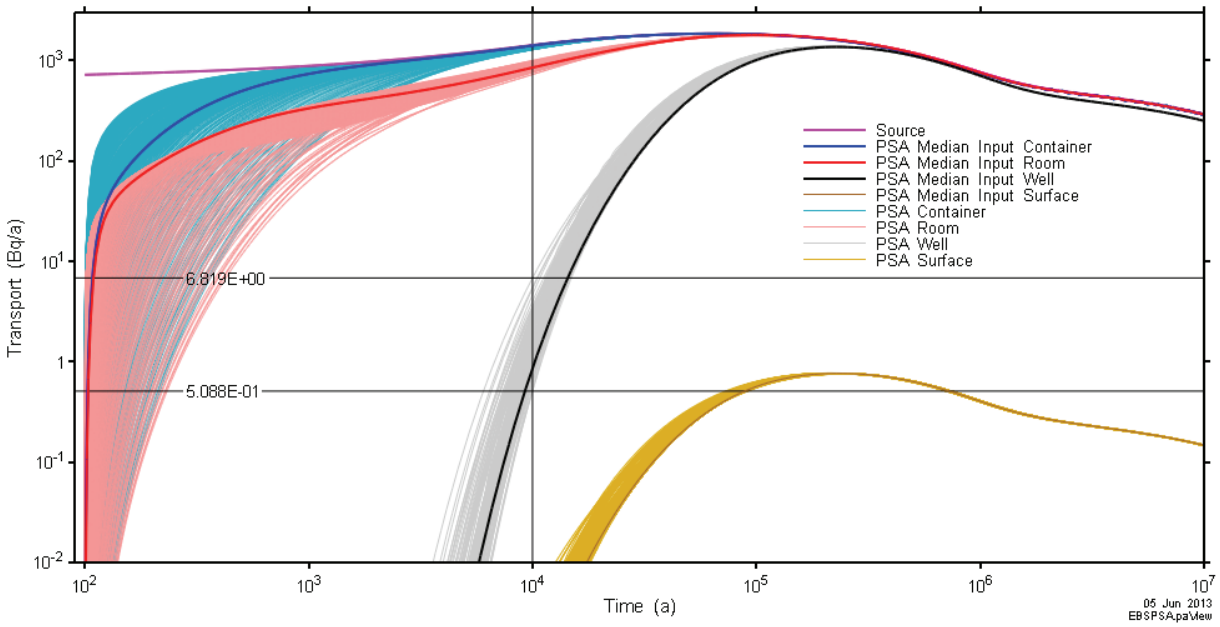

Figure 5.22: Enhanced EBS PSA –Transport Metrics

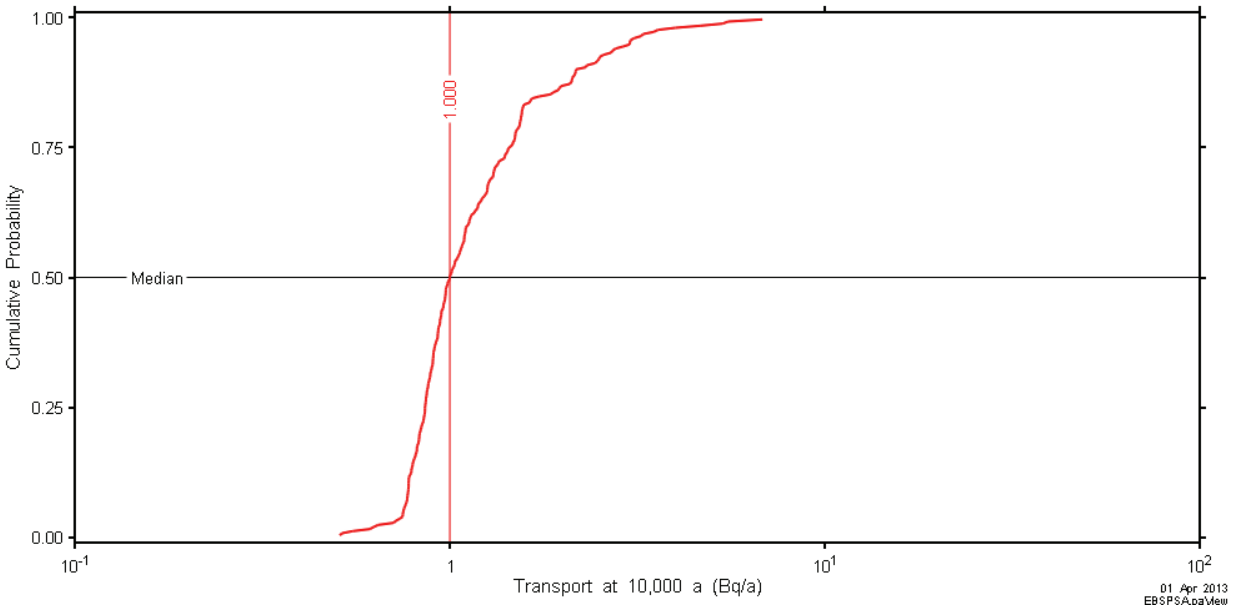

Figure 5.23: Enhanced EBS PSA – CDF of Well Transport at 10,000 a

Regression results show a poor fit between the metric and the independent variables, with only two variables showing even marginal correlation with results (Table 5.6 and Figure 5.24). The figure shows some structure to the EBS D_e multiplier, however it does not fit the linear model assumed by the regression procedure

Table 5.6: Enhanced EBS PSA – Well Transport at 10,000 a Ranked Stepwise Regression Results

Variable	Model significance (R^2) R^2 Included	R^2 Deleted	0.14336 Regression Coefficient
EBS*CONC K	0.08371	0.29756	0.29756
EBS*De_Mult	0.14336	0.24438	0.24438

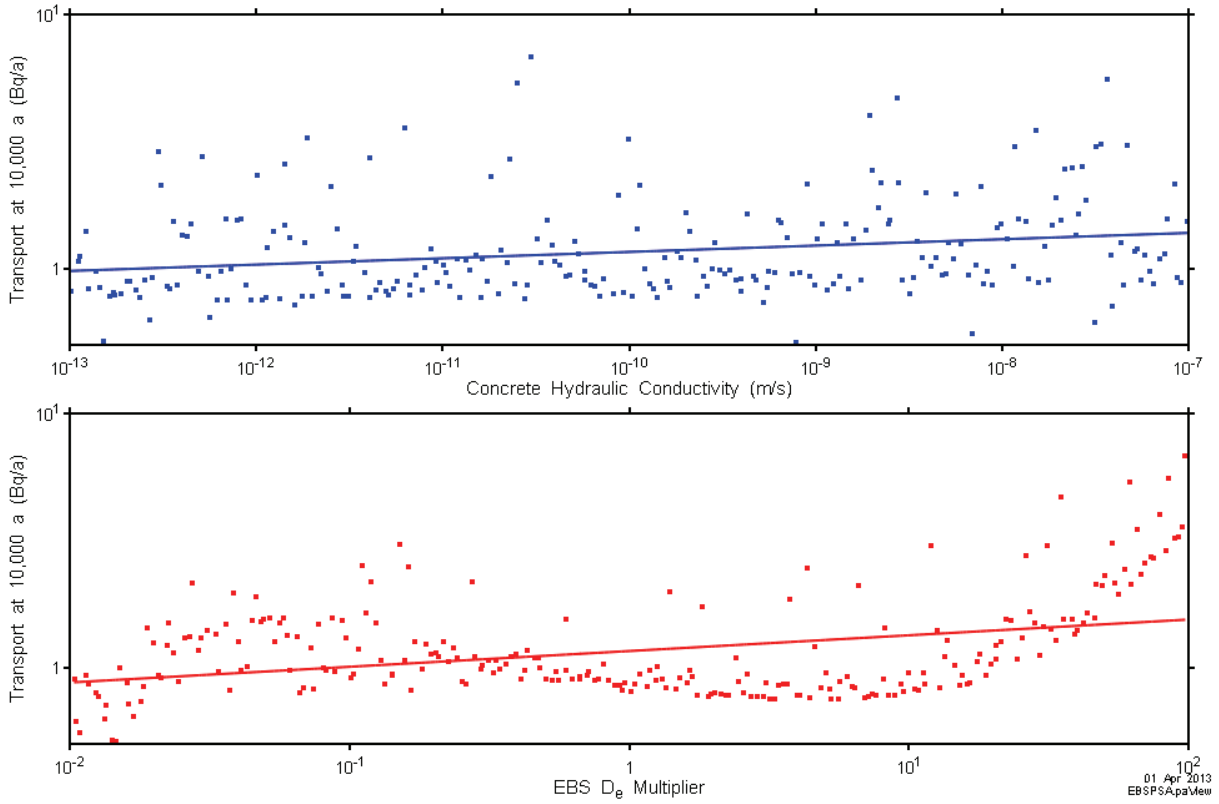

Figure 5.24: Enhanced EBS PSA – Scatter Plot – Well Transport at 10,000 a

6. CLOUD IMPLEMENTATION

Assessments described in previous chapters were simulated on a locally available dedicated cluster machine configured with five Xeon server boards, each with 48 GB of RAM and 16 hyper-threaded cores for a total of 80 available virtual cores. Other projects were also reliant on the hardware, so maximum usage for the 3D PSA simulations was 46 cores on three server boards. One goal of this project was to examine the feasibility of using third-party computer resources available over the internet, or more colloquially, “in the cloud”, to perform 3D PSA. After a review of available options, Amazon Elastic Compute Cloud (EC2) from Amazon Web Services (AWS) was selected for evaluation. The available 64-bit hardware with Windows Server operating system was similar to the local cluster configuration, which simplified porting.

6.1 APPROACH

After obtaining an account from AWS, the EC2 Management console is used to launch machine instances (Amazon Machine Instances, or AMI), each of which consist of a completely configured remote machine with a specified operating system. The instance is then further customized by installing required software. After configuration, the AMI is saved so that subsequent invocations include all the installed software. For 3D PSA, the Microsoft Windows Server 2008 R2 Base AMI was initially selected, with a 50 GB local drive. Amazon Elastic Block Storage (EBS) was used to create a virtual disc on which network drives could be created. Drive mappings were specified that mimic the network drive configuration on the local cluster machine. The following software was installed:

1. mView (including mViewX)
2. paCalc (including paView and paCalcX)
3. FRAC3DVS-OPG
4. MPICH2 version 1.4.1
5. Subversion – version control system used to transfer PSA configurations from local hardware to the remote instance.
6. Cisco VPN – virtual private network connection to allow remote mapping of local disk resources.

This configuration was then saved as a custom AMI, and the EBS saved as a volume.

The custom AMI is then invoked using a specified hardware profile. The AMI hardware profile most consistent with the local cluster is the “M2 High-Memory Quadruple Extra Large”, or m2.4xlarge, which consists of 4 cores (8 hyper-threaded cores) and 68.4 GB RAM. This profile was used for all assessments presented in this section. Multiple instances can be launched within a private local subnet that allows MPICH communication. This allows clusters of any arbitrary size to be created.

Amazon Elastic IP addresses are allocated for and attached to each instance to allow the instances to be accessed with the Windows Remote Desktop Connection application. This is the same approach used to set up and manage simulations on the local cluster. After initial configuration, the 3D PSA assessments can be simulated using the same procedures as on the local cluster.

6.2 RESULTS

The No-Well MLE assessment presented in Section 3.7.1was repeated with 125, 500, and 2500 realizations as initial test cases for the cloud implementation. Assessments were performed using four AMIs for a total of 32 available cores. Results were consistent with the local cluster, as shown previously in Figure 3.11. Model execution times for the AWS runs are compared

with the local cluster in Figure 6.1. The AWS hardware is a factor of approximately 1.5 times faster than the local cluster on a per core basis for the MLE assessments.

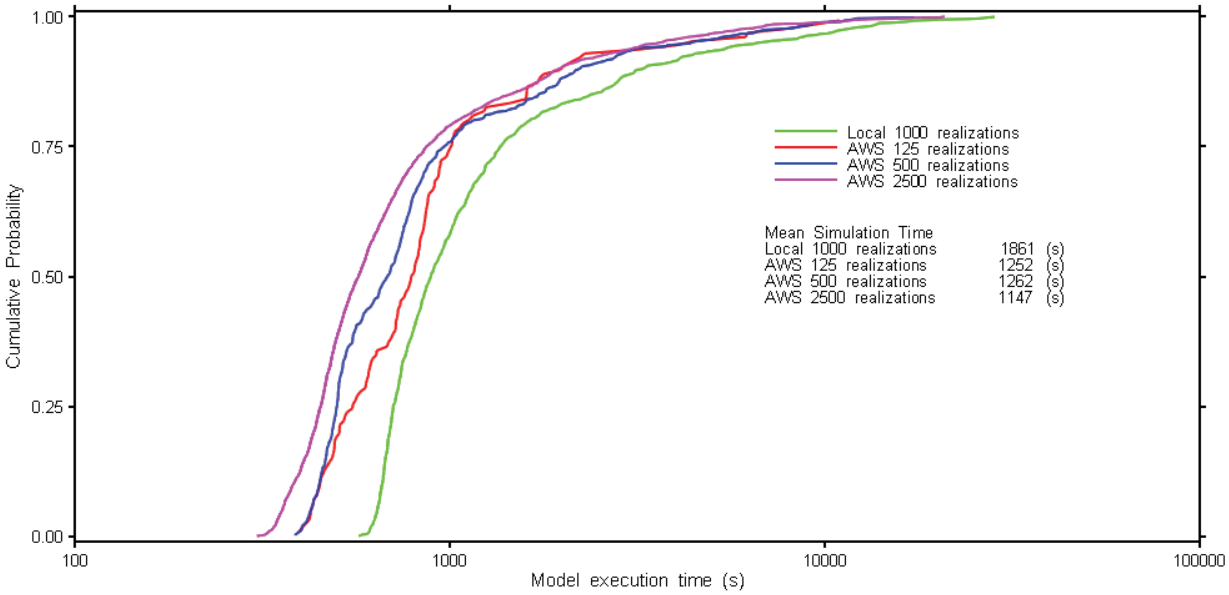

Figure 6.1: Flow MLE: Comparison of Local Cluster and AWS Model Execution Times

Total elapsed real times were 3.3 hours for 125 realizations, 7.3 hours for 500 realizations, and 27.2 hours for 2500 realizations. Associated total processor times were 43.4 hours, 175.3 hours, and 796.2 hours, respectively. It should be noted that elapsed times reflect the time taken for the last core to complete. This explains the non-linearity in total elapsed time: for 125 realizations the average core completed all assigned runs in 5020 seconds, whereas one core required 11878 seconds. The relative impact of this effect decreases with an increasing number of realizations. Total processor times scale nearly linearly with the number of realizations.

A single full transport assessment was conducted with 250 realizations. Results were consistent with the 500 realizations simulated on the local cluster as previously presented in Figure 5.16 and Figure 5.17. The AWS model execution time statistics are compared to the local cluster in Figure 6.2. For the transport runs, the AWS hardware is 1.9 times faster than the local cluster. There is no immediately apparent cause for the discrepancy between the relative speedup for MLE (x 1.6) and Transport (x 1.9) assessments. It may reflect differences in the specific hardware used when the AMI is instantiated.

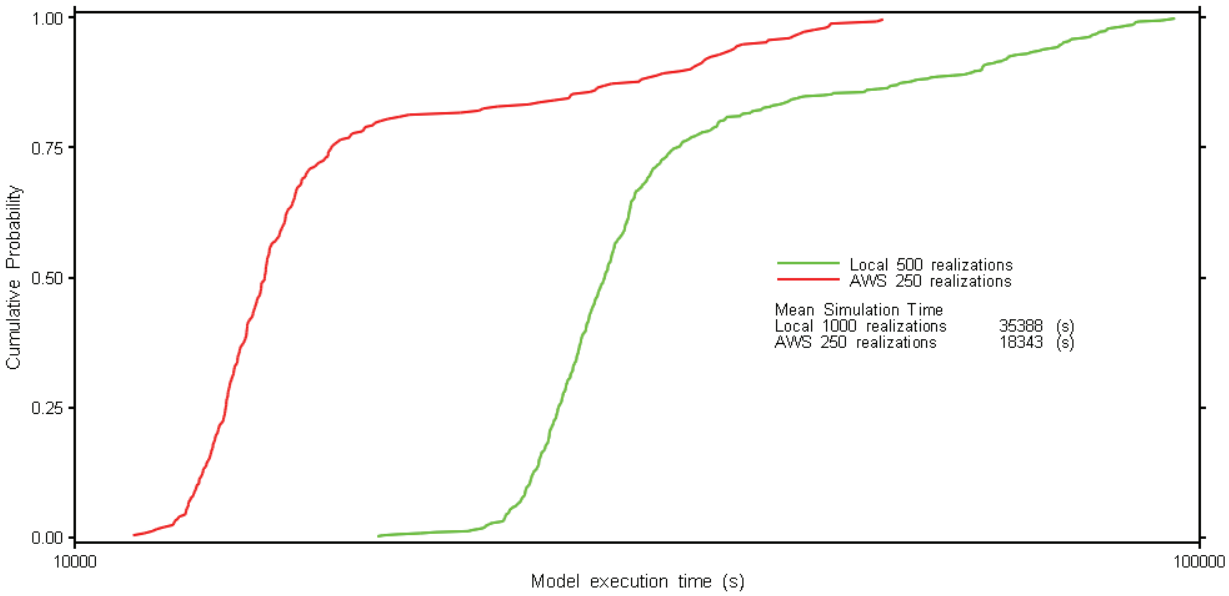

Figure 6.2: Transport: Comparison of Local Cluster and AWS Model Execution Times

Total elapsed real time was 46.3 hours, with total processor time of 1274 processor hours.

6.3 COST

The AWS test simulations were conducted using the basic pricing structure for on-demand instances which is a flat hourly rate per AMI. The m2.4xlarge AMI costs $US 2.28 per hour, for each complete or partial hour. All simulations were conducted using four instances, for an hourly cost of $US 9.12. Using the timings presented above, nominal costs are given in Table 6.1.

Table 6.1: AWS Assessment Costs

Run	Hours	Cost ($US)
MLE 125	4	$36.48
MLE 500	8	$72.96
MLE 2500	28	$255.36
Transport 250	47	$428.64

Actual billed costs are slightly higher as the billed time includes all instance hours from AMI creation to termination. AWS alerts were used to generate e-mails indicating when the runs were finished, however, actual termination was delayed in some cases until a computer could be accessed.

AWS offers different pricing structures for different utilization levels. For example, a “light utilization” reserved m2.4xlarge instance would cost $1412 up front with a reduced hourly rate of $1.16 per hour (or $5648 and $4.64 per hour for four instances). This would represent a reduced cost approach if, for example, ten 1000 realization transport assessments were

undertaken (estimated at $17145 for on-demand, $14371 for reserved). Careful planning of simulations could result in substantial savings.

As an additional note, AWS prices are continually declining as computing costs decrease and performance increases.

6.4 FURTHER IMPROVEMENTS

The AWS simulations were developed as proof-of-concept only, with no further effort made to optimize procedures for production usage. Specific improvements that could be made include automatic termination of instances and simplified setup procedures. Other available AMIs (cc2.8xlarge for example) may offer better performance at a reduced cost, however there are additional configuration details that must be tested.

7. EXPANSIONS AND LIMITATIONS

7.1 ADDITIONAL FEATURES

The 3D PSA methodology and results detailed in this report show that PSA with complex deterministic models can be performed in a robust manner. The analyses presented here are intended as proof-of-concept only, and could easily be extended to provide more coverage of 4CS system attributes. Specific enhancements include:

1. Multiple radionuclides – the current report describes a system with transport of a single radionuclide (I-129). Multiple radionuclides can be handled by running the multiple consecutive transport simulations for each realization. Decay chains can also be handled by FRAC3DVS. The 4CS simulations included U-238 to U-234 ingrowth. There are practical limits to the number of nuclides in the decay chain as time step size is limited by the half-life of the fastest decaying child. For example, it would be impractical to simulate the U-238 to Rn-222 chain. Memory requirements also increase for each species added. Additional variables would be required to describe D_e and sorption parameters for each material type/radionuclide combination.

2. Sampled main fracture position – the location of the main fracture is constant in the current system. However, sensitivity analyses conducted for NWMO (2012) showed that well transport time was sensitive to fracture location. This is consistent with the importance of bedrock hydraulic conductivity in the current analyses. Fracture position could be sampled and thus included in the analyses. There are some complications as the grid discretization would limit available fracture positions to discrete points rather than a continuously variable location.

3. Multiple release points – for the current analyses, the west well location and associated shortest MLE placement room node formed the basis for selecting a single release location and room. However, multiple transport models, placed at different locations could easily be incorporated, such as at the end of a placement room near the east well.

4. Additional surface release definition – a single surface discharge area is defined. In the 4CS simulations there were five separate discharge areas. Incorporating all discharge areas would involve expanding the model domain.

5. Container release and biosphere models – paCalc was originally designed as a framework for conducting safety assessments using simplified models, and supports the direct incorporation of additional models in the calculation framework. Models for source release and biosphere/dose could be incorporated directly within paCalc, or as external models, using the same approach as with FRAC3DVS.

6. Parameter correlations – paCalc can force parameter correlations with LHS sampling. This capability was not used in the assessments presented here. Correlating well pumping rate with intact bedrock conductivity is physically reasonable and would reduce or eliminate the number of realizations discarded due to negative well heads. Correlations may also be appropriate for other cases, such as porosity and diffusion coefficient.

Enhancements 1), 3), and 4) above would incur additional computational costs, scaling based on 1) number of nuclides, 3) number of release points, and 4) increase in number of nodes.

7.2 LIMITATIONS

The 4CS repository and geosphere are ideally suited for modelling with a PSA application. The normal evolution release scenario consists of a single container, and the flow field yields a relatively unambiguous location for such a release to maximize impact. It is conceivable that other topographic or geologic settings would be more variable, yielding more failure locations, and that alternative release scenarios, such as all container failure, would be less amenable to a simplified representation. The former could be dealt with by multiple release points (see item 3) above), while the latter would require additional model simplifications. Given that current results show the general irrelevance of the placement room EDZ and EBS system it is likely that suitable simplifications could be made.

Negative well heads were the most significant numerical problem noted in the assessments. Their frequency was reduced in the PSA Transport model due to finer discretization. Additional steps that could be taken include forcing a correlation of well rate with bedrock conductivity.

As a simulator, FRAC3DS-OPG has proven to be relatively robust. Although flow convergence can be an issue, especially with extreme parameter variations, the model executes in a consistent fashion with minimal critical numeric issues. Other models, such as TOUGH2 and variants, are not so well behaved, and tend to fail more frequently before any output is produced. Incorporating these models would require additional steps to predefine “failed output” files that would only be overwritten if the simulation was successful. These could be incorporated in the current framework, but would slightly increase complexity of the approach.

8. CONCLUSIONS AND RECOMMENDATIONS

The 3D PSA methodology described and implemented in this report demonstrates that useful PSA can be performed with complex numerical models. It has proven robust with no overall failures for the five assessments presented. It is flexible, and can be modified to address different or expanded assessment requirements. The stability of the various metric CDFs indicates that 500 to 1000 realizations are adequate to obtain statistically reliable results.

3D PSA provides a useful capability to augment and verify the current SYVAC-CC4 methodology. For a limited number of nuclides, the 3D PSA approach could replace the SYVAC-CC4 vault and geosphere models. Output in the form of transport CDFs for each nuclide and exposure route (well and surface) could form the input to a SYVAC-CC4 biosphere only model. Alternatively, release and dose models could be included directly in the 3D PSA workflow to provide end-to-end verification of CC4.

Additional conclusions can be drawn about the 4CS Reference Case system from the results of the assessments:

1. The flow system MLE analyses validate the well and defective container location selection performed for the 4CS. The flow system shows little variability in structure over a wide range of parameter values. It would be possible to augment the 4CS analysis with an eastern well location; however, this would only be significant for the upper range of possible bedrock conductivities.

2. The geosphere is by far the most important barrier system. Hydraulic conductivity of the bedrock is the dominant control of time of peak transport. This has been recognized in the NWMO (2012) with sensitivities performed on geosphere permeability.

3. The most significant variable related to magnitude of peak transport at the well and surface is hydraulic conductivity of the fault system, which affects the partitioning of transport between well and surface. Low values of fault conductivity lead to higher values of well transport, while higher values of fault conductivity lead to higher values of surface transport. This is largely due to increased conductivity decreasing the radius of influence, or capture radius, of the well. Sensitivity to fracture conductivity was not included in the 4CS assessment, although sensitivity to well rate was included. Well rate has a similar impact at slightly lower levels of significance.

4. The placement room EDZ and EBS had virtually no impact on system performance as indicated by the safety assessment metrics. With the median geosphere assessment, EDZ parameters proved slightly more important than EBS.

These points will not necessarily be valid for other DGR systems or scenarios.

Results of the cloud implementation provide further support for the 3D PSA approach as the requirement for dedicated and specialized local hardware is eliminated. However, computer costs are significant and usage would have to be carefully planned.

REFERENCES

Benedetti L., F. Claeys, I. Nopens and P.A. Vanrolleghem. 2011. Assessing the convergence of LHS Monte Carlo simulations of wastewater treatment models. Water Science and Technology 63:10, 2011.

Deshler, B., H. Kieffel, L. Merkhofer and S Mishra. 2005. Value of Information Analysis to Support Data Collection for Characterizing Radionuclide Transport at the Nevada Test Site. Managing Watersheds for Human and Natural Impacts: pp. 1-12.

Iman, R.L. and M.J. Shortencarier. 1984. "A Fortran 77 Program and User's Guide for the Generation of Latin Hypercube and Random Samples for Use with Computer Models, "NUREG/CR-3624, Technical Report SAND83-2365, Sandia National Laboratories, Albuquerque, NM.

Iman, R. L., J. M. Davenport, E. L. Frost, and M. J. Shortencarier. 1980. Stepwise Regression with PRESS and Rank Regression (Program User's Guide). SAND79-1472. Sandia National Laboratories, Albuquerque NM.

Nuclear Waste Management Organization (NWMO). 2012. Adaptive Phased Management Used Fuel Repository Conceptual Design and Postclosure Safety Assessment in Crystalline Rock, Pre-Project Report, NWMO TR-2012-16. Toronto, Canada.

WIPP Performance Assessment, 1995a, User's Manual for STEPWISE, Version 2.20. Document Version 1.0, WPO# 27768, Sandia National Laboratories, Carlsbad, NM.

WIPP Performance Assessment, 1995b, User's Manual for PCCSRC, Version 2.21. Document Version 1.0, WPO# 27773, Sandia National Laboratories, Carlsbad, NM.